University of Southern Queensland

Faculty of Health, Engineering & Sciences

A Verification of AprilTags for a Pharmacy Application

A dissertation submitted by

C. Moore

in fulfilment of the requirements of

ENG4112 Research Project

towards the degree of

Bachelor of Mechatronic Engineering (Honours) and Bachelor of Science (Mathematics)

Submitted: October, 2020

Abstract

AprilTags are an artificial tag that provides pose estimation. Commonly, it is used to determine global coordinates of a space so that robots can determine where they are within the area. In this project, however, the AprilTags were attached to a specific object needing to be moved. The scope was to verify the robustness and functionality of the tags in order to determine the plausability of them being used for a Pharmacy application.

The Pharmacy is a highly crucial part of the hospital system and the time of the Pharmacists is of the upmost importance. One of the tasks of a Pharmacist is to unload the boxes of medication from delivered orders and organise it into the dispensary. Robotic arms already exist to help with the retrieval and stocking in the dispensary. However, the process of sorting the delievered orders has not been automated and this is a time-consuming task for a Pharmacist or Pharmacist assistant. Hence, the thought towards verifying the functionality of AprilTags was to determine whether they could be used on medication packaging to potentially automate the process of unboxing.

The method undertaken to verify the tags took on a couple of stages. In each stage, an OpenMV H7 Camera was used for the detection process. This camera was attached to Haddington Dynamics' Dexter HDI robotic arm. An AprilTag was attached to the test object and tests were run to verify the tags ability to handle various distances between the camera and tag, the size of the tag, the angle of the camera, occlusion to the tag, and lighting.

The results of these tests were interesting. It appeared that there was only a limited range of distances, tag sizes, camera angles, and occlusion that could still result in a detection accuracy above 80%. The smallest tag that gave functional results was the 25mm tag. The optimal conditions for high accuracy was the camera being between 10 and 20 cm above the tag with a camera angle of 90 degrees, with controlled lighting and no more

than 17% occlusion.

From the results and analysis, the tags are a possibility for automating the unboxing of medication packages. Further testing needs to be conducted with the pose estimation to determine its accuracy. Other detection methods may need to be used alongside the AprilTags since this project's testing has demonstrated the limited range from where the tag can be detected.

University of Southern Queensland

Faculty of Health, Engineering & Sciences

ENG4111/2 *Research Project*

Limitations of Use

The Council of the University of Southern Queensland, its Faculty of Health, Engineering & Sciences, and the staff of the University of Southern Queensland, do not accept any responsibility for the truth, accuracy or completeness of material contained within or associated with this dissertation.

Persons using all or any part of this material do so at their own risk, and not at the risk of the Council of the University of Southern Queensland, its Faculty of Health, Engineering & Sciences or the staff of the University of Southern Queensland.

This dissertation reports an educational exercise and has no purpose or validity beyond this exercise. The sole purpose of the course pair entitled "Research Project" is to contribute to the overall education within the student's chosen degree program. This document, the associated hardware, software, drawings, and other material set out in the associated appendices should not be used for any other purpose: if they are so used, it is entirely at the risk of the user.

Dean

Faculty of Health, Engineering & Sciences

Certification of Dissertation

I certify that the ideas, designs and experimental work, results, analyses and conclusions set out in this dissertation are entirely my own effort, except where otherwise indicated and acknowledged.
I further certify that the work is original and has not been previously submitted for assessment in any other course or institution, except where specifically stated.

C. Moore

Acknowledgments

I would like to thank Dr Tobias Low for his advice and guidance throughout this project; Mr Ross Leamon and Mr Ben Leamon for the opportunity to complete this thesis through Downey Engineering and DCISIV Technologies.

I would also like to thank my family, church family, and friends who have supported me constantly throughout this arduous journey - I am ever so grateful for the prayers and encouragement you have given me.

Soli Deo gloria.

C. Moore

Contents

List of Figures

List of Tables

Chapter 1

Introduction

Engineers have been continually working on the development of robotics to assist in many different industries so that efficiency can increase. This happens particularly in tasks that are tedious, repetitive and time consuming. Alongside robotics, machine vision is increasingly used to give perception to the robots so that they may be more autonomous. Machine vision requires complicated algorithms to be able to identify, locate, and determine the real-world coordinates of objects.

The aim of this final year project is to bring together robotics, machine vision and fiducial tagging systems in order to assist in localising and detecting objects for real-world applications, specifically medication packaging for this project. The project scope includes evaluating literature to determine the most suitable fiducial tag, testing and verifying the results, as well as combining a low-cost camera with a low-cost robotic arm in order that objects can be detected and sorted. The robotic arm, camera, and tags are pre-existing technology but the goal is to combine the three systems into one system.

The study will entail testing of fiducial tags to determine their effectiveness and suitability for application in pharmacy. Many variables will be tested with the tags and initially just the camera to determine functionality and any limitations. Ultimately, the aim is to have a functioning robotic arm, being driven by the perception of the camera to sort medication packages. The result of this project will demonstrate whether such a system, as proposed here, could be viable in a hospital pharmacy dispensary.

1.1 Background to Thesis

This section will discuss the background to the thesis by explaining the motivation behind the thesis and the objectives.

1.1.1 Motivation

Robotics are beginning to be used more in health care settings. Within the hospital pharmacy, robotics are increasingly being considered as a potential solution in the dispensary (Rodriguez-Gonzalez et al. 2019). By incorporating robotics to help dispense medication, the human error is reduced and pharmacists can be more concerned with patient care rather than administration of stock and dispensing (Rodriguez-Gonzalez et al. 2019).The study conducted by Rodriguez-Gonzalez et al. (2019) was particularly focused on robots in the dispensary to improve efficiency and safety. The robot could determine the correct medication by scanning the barcode, which also allowed for automatic documentation of the dispensed medication. This documentation then kept the stock levels updated which helped the pharmacists to know what medication to order. This research was conducted in Europe but there is a slow uptake of robotic implementation even though there are many benefits to having such a system (Rodriguez-Gonzalez et al. 2019).

This is important research to help streamline the hospital pharmacy. However, there is still the issue of the unsorted medication orders that are received into the pharmacy. In preparation for this project, a pharmacist mentioned to the author of this paper that when they receive orders, the different medication does not come pre-sorted into their types but jumbled altogether in boxes. For this reason, much time is spent sorting the orders and then placing them into the dispensary. This is the motivation behind the project: to begin to develop a system that will help to streamline pharmacists' work so they can focus on the clinical care of the patients.

1.1.2 Objectives

The objectives of this project aimed to be achieved through experimentation and research are:

1. A verification of the functionality of artificial tagging through various tests determining how shape, size, camera angle, camera distance, lighting, tag size, and occlusion affect the function. AprilTags will be the artificial tag that will be implemented and tested.

2. The utilisation of the Open MV camera as a potential low-cost machine vision system to accurately detect the AprilTags. The low-cost device enables the potential for wider application use, particularly if it proves to be reliable and accurate.

3. The development of a combined machine vision and robotic arm system in order to autonomously detect and locate tags for autonomous sorting. The robotic arm that will be implemented is Dexter HDI developed by Haddington Dynamics.

4. The utilisation of the whole system to identify, locate, and accurately pick up different medication packages – ultimately the ability to sort a box of different medication packages into relevant categories.

1.2 Research Questions

The questions framing this research project were:

- What methods are there for object recognition already?
- What sorts of tags exist for object recognition?
- How do tags work?
- What methods for sorting objects already exist in the robotic world?
- How does depth affect tag recognition?
- How does occlusion affect tag recognition?
- How does the size of the tag affect detection?
- How does object shape affect tag detection?

Through the literature review and through testing and analysis, an answer has been found for each question. In the conclusion, the answers will be drawn together.

1.3 Hypotheses' to the Research Questions

The research questions that will be tested through the project are:

- How does depth affect tag recognition?
- How does occlusion affect tag recognition?
- How does the size of the tag affect detection?
- How does object shape affect tag detection?

The hypotheses' to these questions are:

- As the distance between the tag and camera increases, the detection accuracy will decrease.
- As the occlusion of the tag increases, the tag will be indetectable as the payload pattern will be covered which determines the ID and pose estimation of the tag.
- As the tag size decreases, the range of heights that will accurately detect the tag will decrease.
- It is predicted that cylinders will cause more distortion to the tag, particularly as the diameter decreases, which will cause reduced accuracy in detection.

1.4 Overview of the Dissertation

- Chapter 2 details the literature that has been reviewed and provides the background information to the project. It is here that Machine Vision and Artificial Tagging are discussed in detail.
- Chapter 3 outlines the methodology of the project, looking at the methodology of the whole project as well as more specifically the method of testing. It is here that the risks and ethics of the project are also discussed.
- Chapter 4 discusses the specifications of the hardware and software that has been used throughout the project. It also explains the reasoning behind the experimental design as well as the experimental setup.

- Chapter 5 describes further how the tests were conducted, and provides the naming conventions of the tests. The results of the experiments will also be reported.
- Chapter 6 analyses the results that were achieved in detail, examining and verifying the robustness of the tags.
- Chapter 7 concludes the dissertation, drawing together the answers found for the research questions and providing a summary of the objectives achieved. Future work will also be discussed in this last chapter.

Chapter 2

Literature Review

This section will contain a review of the literature regarding previous work done. The literature review will be broken down into the three main areas of the project: the robotic arm, machine vision, and artificial tagging.

2.1 Machine Vision

2.1.1 Machine Vision Theory

Machine vision is the field in engineering that deals with perception (Davies 2005). It studies how human vision works and tries to resemble it using machines and algorithms. Like any engineering discipline, it is based on mathematics and science as well as design (Davies 2005). It is a complex problem that researchers are seeking to solve and improve because machines, at this stage, cannot compete with the processing capability of the brain from the eyes due to the lack of parallel processing capabilities (Davies 2005). Much improvement has been made however, and many tasks today are utilising machine vision to automate systems. In particular, machine vision is being used to help solve industrial tasks that are very complex, and they are doing so robustly and reliably (Cognex n.d.).

Machine vision can be used for object detection and much research has gone into this area. Some of the theory behind object detection will now be discussed.

Simultaneous Localisation and Mapping (SLAM) are algorithms that are used to develop

a map of the environment that a robot is moving in by using machine vision (Cheein et al. 2010). These algorithms assist a robot in identifying where it is within the environment. It was first thought to be most useful for mobile robots but it is not limited to that application.

Pose estimation is a technique used in machine vision to identify humans within an image or video (TensorFlow 2020). The algorithms do not detect or recognise who the person is in the image, it only identifies specific body parts or joints. This technique has been further implemented in other applications where position and orientation is required to be known (Corke 2017). Pose estimation can be performed if a coordinate system is assigned to an object; using a vector, the position and orientation can be defined. For the pose to be fully described, there needs to be six dimensions: three describing the position and three describing the orientation. Position is also known as translation, and orientation known as rotation. The camera, whether fixed or attached to a robot, estimates the object's pose relative to its own position.

Hamming distance is the process used in machine vision for object recognition. It is a system of measurement that compares two strings of binary data, identifying errors between the strings (Raut 2018). The number of bit positions that are different is said to be the Hamming distance. It is performed by computing the 'exclusive or' operation on the two strings and then counting the number of ones in the resultant. The principle is the same when it comes to object recognition. The object in the camera frame is compared to templates in the system because these templates are just binary bit patterns (Davies 2005). The sum of the number of differences between the bits results in the Hamming Distance and sections where the Hamming distance is low indicates that the match between the detected object and template is acceptable.

When detecting objects, a metric known as false positive rate can also be considered. It occurs when a data point is labelled to be positive, but it is actually false (Koehrsen 2018). It is a measure that is often used in statistics and probability but it is also used in machine vision as it is a measurement that describes accuracy. When detecting a tag within an image, there is said to be a false positive rate when the camera incorrectly detects a tag being present, but in fact there is no tag in the image (Fiala 2005*a*). A similar metric is the false negative rate. This occurs when the camera misses a tag that is present in the image (Fiala 2005*a*). There is also the possibility of a camera detecting a tag but assigning the wrong ID to it (Fiala 2005*a*). When this occurs, it is known as the inter-marker confusion

rate.

2.1.2 Object Detection and Sorting

Methods of sorting require two main areas: object detection, and a pick and place system. Much research has been conducted in the field of object detection. Algorithms of all sorts have been developed to assist in the progress of this area. There are detection methods that use infrared light, feature-based techniques, edge detection, light levels, and many more (Colyer et al. 2018)(Sakhare et al. 2019). One common method of object detection is by colour. The machine vision system is programmed to locate a certain colour. Through image processing, the levels of Red, Green, Blue (RGB) or Hue, Saturation, Value (HSV) will be determined in an image and then matched against the desired colour until there is a match. Once there is a match, the system can state and locate which object has the particular colour. Further algorithms can then be used to calculate the pose of the object. This pose can then be given to the sorting system to move the object. Often the system used to move the object will be a robotic arm (Sanchez & Martinez 2000)(Mada Sanjaya et al. 2018)(Abbood et al. 2019).

One paper developed a system that uses a camera and a distance sensor mounted on the tool adapter of a robotic arm (Sanchez & Martinez 2000). In this system, it detects the object through the camera and distance sensor which is calibrated using the Tsai model. This calibration allows for accurate pose estimation. With this system however, the user is required to click on a live image for calibration and to define the locatation and orientation of the object before it can be picked up. This means that the process is not fully autonomous as it requires human input to locate the object.

Two of the papers reviewed used colour as the method for sorting. Sanjaya et al. (2018) used a fixed camera for object detection. The robotic arm was a basic constuction with servo motors and a gripper. The system used real-time image processing that detected colour and through the colour detection gave a coordinate. The system also used Artificial Neural Network (ANN) to build a library of data for the inverse kinematics of the robotic arm. When a new object was located, it was matched against the already trained data until it gets the new data of the angle of the motor. The ANN controlled the robotic arm to pick and place the objects. Abbood, Abdullah and Khalid's (2019) system also contained a fixed camera rather than a camera attached to the robotic arm like Sanchez

(year). The sorting method was based on the HVS mode algorithm which sorted objects by colour. This method also distinguished object shape, although the main focus was on using colour. Another algorithm, colour segmentation, was used to process and analyse the image to determine whether the value of redness in a pixel matched with the set criteria. Alongside the RGB, the HSV appearance model was also used. These methods and models combined allowed for accurate detection of colour.

Another potential method of detection is through the use of artificial tags, which will be the study of this project.

2.1.3 Open MV Camera

The OpenMV camera was developed as part of a project to create low-cost and extensible machine vision devices programmed in Python (OpenMV 2020*a*). The developers of the modules aim at becoming the 'Arduino of Machine Vision' (OpenMV 2020*a*). It incorporates a microcontroller board, like an Arduino, that is very powerful with a camera attached (Figure 2.1a). All the algorithm work has already been completed by the developers so it allows the product to be used by those who are not experts. The camera is able to detect faces, take pictures, has low power consumption, can record video, can control input/output pins as well as track blobs or markers. The OpenMV project has developed its own programming environment (Figure 2.1b). It features a text editor that has many example codes that can be modified or a program can be written completely by the user, utilising the pre-written libraries and functions. The software also has a viewer where it shows what the camera sees.

2.2 Artificial Tagging

Fiducial tagging systems are an artificial feature that are used in computer vision applications (Krogius et al. 2019). Some of these applications include augmented reality, object tracking, and SLAM applications. They are designed to be easily recognisable and distinguishable from one another (Olson 2011). Fiducials are similar to other barcode systems, however they use a much smaller payload and can be detected at low resolution. They are designed to be detected automatically and localised under many different conditions. Also, unlike other barcode systems like the QR code, fiducials provide information about

2.2 Artificial Tagging

(a) OpenMV Camera

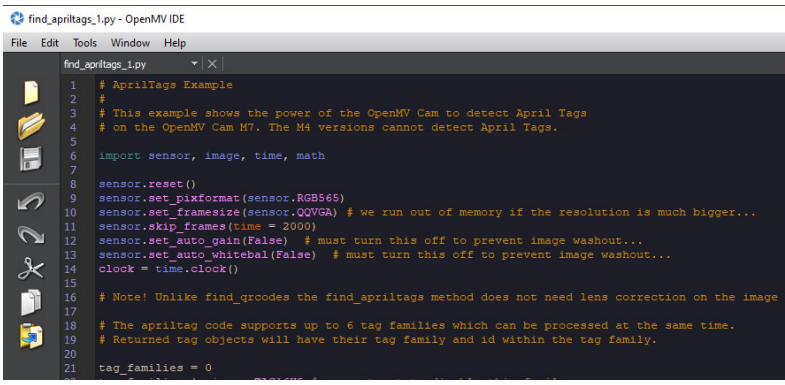

(b) OpenMV programming environment

Figure 2.1: OpenMV Camera and IDE

position and orientation relative to the camera. Fiala (2005a) also notes that barcode systems generally require a large portion of the image in order for the tag to be detected, and this limits the range to which they can be used. Ultimately, the different markers have different uses, so comparing them is not of much use as fiducial tags are the focus of this project due to their ability to estimate pose. Some fiducial tags include ARToolkit, ARTags and AprilTags.

ARToolkit was among the first of the fiducial markers to be developed (Fiala 2005*b*). The intended use of the tags were for augmented reality, but they have also been used for more general purpose applications such as human to computer interactions and landmarks for navigation (Olson 2011)(Fiala 2005*b*). The tags use a square layout with a black border so that they can be distinguished from other objects in the environment. In the centre is what is considered to be the payload, the information that allows for detection and differentiation from another tag. It is a greyscale image that is usually a symbol, like a Latin character, that is compared against a library of symbols (Fiala 2005*b*) (Olson 2011). The best correlation is reported to the user. This process has many disadvantages. Fiala (2005b) states the process of morphology that the ARToolkit uses as a weakness because it requires controlled lighting to accurately detect the image within the borders and distinguish the grayscale. Olson (2011) also comments that ARToolkit has many disadvantages such as the computational cost of correlating and decoding tags as well as the difficulty in generating templates that are 'orthogonal to each other'. The use of images as the payload also means that ARToolkit tags cannot handle occlusion and they

have a high inter-marker confusion rate (Olson 2011)(Fiala 2005*b*). ARToolkit markers also have a high false positive rate due to often detecting a tag when there is not one in the image. The positive in this system is that the payload can be more meaningful to the user because they consist of common and known images or symbols (Fiala 2005*b*). Since the development of ARToolkit, there has been further development of the marker into ARToolkit Plus and whilst there has been improvement in the marker, it still utilises some of the same processes as the predecessor and so still has many weaknesses.

ARTags were developed to improve upon ARToolkit. Unlike ARToolkit, which uses correlation to verify the tag, ARTag uses digital coding theory in order to achieve a very low false positive rate and inter-confusion rate (Fiala 2005*a*). The marker utilises an edge-based method to first detect the tag instead of the morphology approach that ARToolkit uses (Fiala 2005*b*). This helps for accurate detection even in poor lighting conditions. The tag consists of only black and white which adds to its robustness to varying lighting conditions (Fiala 2005*a*). By having only two stark shades, the camera can easily distinguish the difference between them, unlike the ARToolkit library which uses a greyscale. Each tag has a square black border around a 6x6 grid of squares in the middle with a combination of the two shades to form a pattern (Fiala 2005*a*). There are 1001 different combinations within the 6x6 grid, and if the border colour is changed to white, there are another 1001 tags (Fiala 2005*a*). So, in total, ARTags have a library of 2002 usable tags. Because of the use of two colours, the tag can easily be processed into binary which means that there is a very low probability of mistaking one tag for another. Fiala (2005a) records the probability of confusing markers to be less than 0.0039%. Even when the tag is partially occluded, the outline of the tag can still be detected (Fiala 2005*a*). The amount of coverage correlates to the accuracy of tag identification. Olson (2011) also stated the improvements that the ARTags include but explained that not all of their work is open-sourced – the detector algorithm is not available to the public. Olson (2011) mentioned that ARTags were the first to provide a coding system based on forward error correction, enabling easier generation, faster correlation, and greater orthogonality between tags. However, the work conducted by Olson (2011) and those at the University of Michigan demonstrates that the ARTag does not perform as well as their tag and coding system.

AprilTags were developed by the University of Michigan in order to improve upon the previous fiducial tagging systems. AprilTags continued with the theme of a black border

their predecessors used but were able to vary the size of the payload in the middle of the tag (Olson 2011). The style of payload is similar to ARTag and ARToolkit Plus with the grid pattern of black and white squares. Olson (2011) describes their methods for improving robustness of fiducial tags and demonstrates how they are consequently better. The paper proposes a 'graph-based image segmentation algorithm' which allows for more robust and precise detection of tags (Olson 2011). Figure 2.2 demonstrates the processing procedure. The beginning of this approach detects lines in the image through the use of gradients at each pixel. It is 'similar in basic approach to the ARTag detector' (Olson 2011). From there, the pixels are grouped together according to similarities in gradient direction and size. It was found that the method of determining gradients and clustering pixels was sensitive to noise in the image which, if present, could cause significant variations in the results (Olson 2011). To counteract this, a low pass filter, which does not removed any information, is used over the image. The line segments that are determined are then connected using a method of least-squares, which uses weighting dependent on the gradient size. Olson (2011) states that the segmentation algorithm is the slowest phase of the detection process. Once it is completed, a quad extraction method is used to find places where a quad is formed. The challenge here is to complete this whilst keeping the tags robust to occlusion and noise. ARTags also use a quad extraction method where the grouping of line segments into quads allows for a map to be created to 'sample the marker interior' (Fiala 2005*a*). From quad extraction, a homography matrix is computed so that the payload can then be decoded (Olson 2011). This is done by computing the coordinates relative to the tag of each bit in the image and then transforming them relative to the image using the homography matrix. These coordinates are then adjusted using spatially-varying thresholding so that it is robust to lighting (Olson 2011). Two spatially-varying models are built to handle the black and white pixels, as their intensities are different (Olson 2011). All of this is just the detection scheme; there is still the coding system which determines whether a tag is valid. The coding system seeks to maximise the number of codes that can be distinguished and the number of bit errors that can be corrected whilst minimising the false positive rate, inter-marker confusion rate, and the total number of bits per tag (Olson 2011). Because some of these things appear contradictory, there are trade-offs. The approach that Olson (2011) describes uses lexicodes, which is their new method, so that the user can determine the properties that best fit their needs. Using this system, they seek to make the tag robust in every 90-degree rotation, so that when it is rotated, there is still the same Hamming distance between other tags. In order to achieve this and ensure that the false positive rate remains low, the lexicode generation

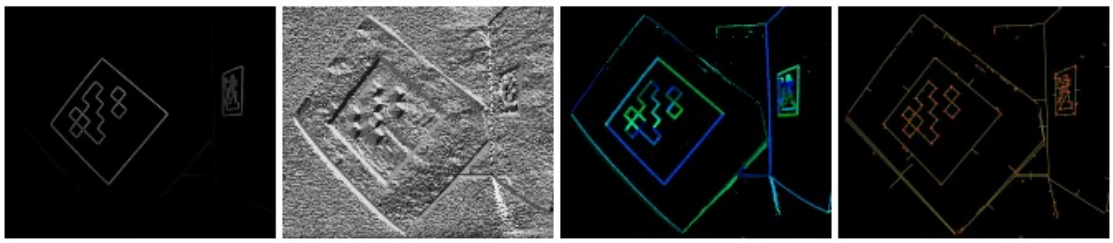

Figure 2.2: Processing of an AprilTag using the graph-based segmentation algorithm (Olson 2011)

algorithm is modified to remove codes with too simple geometric patterns (Olson 2011). In the error correction analysis, Olson (2011) shows the resulting false positive rate of the proposed AprilTags. Whilst it looks like ARTag has a better percentage of 0.0039%, it is stated that the coding scheme is stronger in AprilTags because they achieve a minimum Hamming distance between all pairs of tags as well as having a considerably larger number of distinct tags. The University of Michigan could not compare every test with ARTags as some of their information is not public (Olson 2011).

The University of Michigan has done further developmental work on the AprilTags. They improved the detection speed, but at the cost of the inability to detect occluded tags (Wang & Olson 2016). The result was that there were fewer false positives and a reduction in computation time. It was found, through users of the AprilTag, that the error induced from decoding partially-occluded tags was more than acceptable (Wang & Olson 2016). The University of Michigan deemed it a favourable trade-off to increase speed at the cost of occlusion detection (Wang & Olson 2016). Further research and development was conducted in 2019 where Krogius, Haggenmiller, and Olson identified three main problems with the layout of the tags: the border takes up a lot of usable area that could be used for the payload, the square shape does not make it efficient for objects of other shape, and the standard tag has a limited range over which it can be detected. The development of the tag addressed these issues whilst seeking to keep the same results in detection speed and accuracy. They sought to create a system that could have a flexible layout as well as increasing the range that the tag could be detected from (Krogius et al. 2019). The paper detailing this work shows the improvements that are achieved through these developments. Figure 2.3 demonstrates some of the different tag families and layouts.

These papers are important papers in reviewing artificial tags. They describe the functioning of the tags and the type that is best. From these research papers it can be seen

that it is crucial for tags to be robust and to have low false positive and negative rates as this means that the probability of correctly detecting a tag is greater. It is also important that the Hamming distance, the measure of error between bits, is low in order to achieve precise detection. The conclusion drawn from these studies is that AprilTags are the best choice to implement for this research as they out perform ARToolkit and ARTag markers as well as being completely open-sourced.

2.3 Multi-axis robotic arm

Dexter HDI is a desktop robotic arm which was developed by Haddington Dynamics as seen in Figure 2.4. The company's philosophy is to make 'automation accessible' (Haddington Dynamics 2020*b*). Unlike other robotic arms, the Dexter robotic arm is low cost making it more attainable for use with equal, if not higher, precision. The robot utilises a FPGA supercomputer which allows for incredibly precise movements from all joints, even though they are nominally imprecise on other robotic arms. The supercomputer helps to achieve 0.8 to 1.6 million points of precision. Alongside the supercomputer, Dexter uses encoder technology. This technology adds to the precision of the movement in each joint. It consists of light being shone onto a disk with many holes in it that indicate position. The pattern is detected by the sensor in the joint and because Dexter uses the analog value, it is able to detect many 'thousand positions per hole' (Haddington Dynamics 2020*b*). Because of the use of encoders, it also means that the motors do not need to be inside the joint. The design of this robot reduces the necessity for such rigidity and power that industrial robots require because the motors and gearboxes are used more as counterweights rather than being lifted (Haddington Dynamics 2020*b*). For a desktop robot that is lightweight in comparison to other desktop robotic arms, Dexter HDI has an equal payload of 3kg and can reach up to 700mm in the standard build.

Haddington Dynamics specify that the robot has seven axes. The base joint, which can rotate the whole arm, can turn 365-degrees. The next joint up resembles the shoulder; it has 270-degrees of freedom. The elbow joint also has a 270-degree range. There are two wrist joints; the first only has a 180 degree range but the second has a full 360-degree rotation. The last two joints work the gripper. The gripper is able to rotate around and open to 300-degrees.

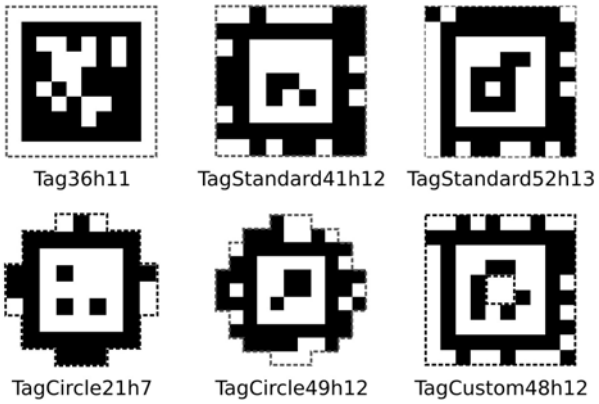

Figure 2.3: Various AprilTag families (April Robotic Laboratory 2010)

Figure 2.4: Dexter HDI robotic arm by Haddington Dyanmics (2020)

2.4 Review of Literature

From the research conducted, there was an application found where a robotic arm, camera system, and AprilTags have been used together. In an industrial setting of manufacturing, like cars and aircrafts, the process is becoming more automated and robotic arms are often being used to complete the work (Nissler et al. 2016). There are difficulties in the standard setup of the production line that make the pose estimation unreliable. For this reason, Nissler et al. (2016) sought to investigate the use of AprilTags to gain a better estimate of the pose of objects. The research used robotic arms and a camera system; however, the robotic arm was an industrial arm and the camera system was a 'state-of-the-art' camera in comparison to the low-cost robotic arm and camera that is to be used in this project (Nissler et al. 2016). Whilst this source is helpful, it does demonstrate that there is a gap in low-cost systems and a space to use this sort of technology in less industrial settings. Additionally, there seems to be a gap in physical tests with the AprilTags documented by the University of Michigan for detecting objects rather than just globalising the environment coordinates. Consequently, it is suggested that this would be helpful research to verify the conclusions made about AprilTags and provide information for uses in other real-world application. Examination of extant research data indicates that there has been no research conducted with a robotic arm, camera, and AprilTags in the pharmaceutical world, demonstrating another potential gap in research.

Chapter 3

Methodology

The project as a whole contains five phases in order to achieve the project objectives. These are as follows.

1. The Start-up phase contains the literature review and study of the relevant theory behind the project. The planning of the testing methodology, the development of test objects, and the examination and decision on type of artificial tag will be completed in this phase.

2. The Programming phase consists of writing the necessary code for the project. This includes scaffolding code for the robotic arm and for the camera. The programs will likely be altered through the whole project as adjustments are needed.

3. The Testing phase includes all of the experiments to be conducted within the project. This phase will experiment with different sized objects and shapes as well as varing the size of tag. The final test will be to combine the whole system to sort medication packaging firstly into shapes, and ultimately into medication types.

4. The Data analysis phase will compare the data collected from the testing phase. The analysis will consist of determining accuracy of detection, pick-up and placement of the objects. Time will also be a considered factor. Phases 4 and 5 will occur concurrently as tests are completed.

5. The Write-up phase contains the preparation and finalisation of the dissertation that will detail all the findings from the experimentation and analysis.

3.1 Testing Methodology

It is planned for there to be four stages of testing to be conducted. Each stage will test potential limitations to the use of artificial tags. Within each stage, there are smaller tests that will be conducted to change a number of variables. The first three experiments will use the camera only. Stage four will incorporate both the camera and robotic arm. Stages will only be advanced after the previous stage has been completed satisfactorily.

1. Stage 1: Manual Testing
    1 Cube Tests
        - Variables that will be tested:
            i. Size of tag
            ii. Distance between tag and camera
            iii. Camera angle
    2 Cylinder Tests
        - Variables that will be tested:
            i. Size of tag
            ii. Distance between tag and camera
            iii. Size of cylinder
    3 Occlusion Tests
    4 Lighting Tests
2. Stage 2: Semi-automated Testing
    1 Cube Tests
        - Variables that will be tested:
            i. Camera angle
            ii. Distance between tag and camera
    2 Cylinder Tests
        - Variables that will be tested:
            i. Camera angle
    3 Occlusion Tests
    4 Lighting Tests

3. Stage 3: Autonomous Testing

    1 Medication Packaging

    - Variables that will be tested:

        i. Types of packaging

        ii. Position of tag on object

        iii. Distance between tag and camera

4. Using Dexter to pick and place

    1 Cubes

    2 Cylinders

    3 Medication packaging

These tests have been designed in order to identify any limitations in using artificial tags. By testing the accuracy of detection upon variance of tag size, it will provide useful information as to other potential applications. If the tag is only accurate for larger objects, then it may only be useful to identify the environment around the object. Testing different camera angles will help to determine another aspect of robustness as it will determine if a specific angle is required to gain interpretation of the tag. Distance from tag is similar to the angle; the question revolving this test is whether there is a limit in detection range. By testing occlusion, this will identify whether an object can still be located even if the tag is obstructed.

To some extent, these aspects have been tested by the developers of the AprilTag. However, the tests are not clearly documented in their papers and the results that are discussed are more surrounding the specific algorithms used rather than the practical uses of the tag. They were more concerned with improving upon previous fiducial systems, and then later upon their own. The point of this research and testing then is to confirm whether what they say is true and then implement the tagging system on a particular real-world application: pharmacy.

The combination of the camera and the robotic arm also will make the system more versatile. Again, this is not new as cameras have been used in tangem with robotic arms for many years, but with the incorporated use of AprilTags, it will be a viable solution for the pharmacy application provided it is successful, particularly because the whole system will be low cost.

There was not a threshold for detection accuracy given in the literature so for the purpose of this study the tags will be considered accurate in the relevant testing conditions if the detection accuracy is greater than 80%.

3.2 Risk Assessment

This section contains the identification, evaluation, and reduction measures of the risk within the project.

Identification of Risk

The risk involved in this project is minimal; however, it still needs to be considered. The highest potential risk is that of injury from the robotic arm. It is possible for injury to occur if the user gets in the way of the moving robotic arm. Another occurence of injury could occur when the user is trying to prevent the robotic arm from moving outside of its limits. If this happens, it is possible that fingers could become squished or other muscle injury may occur as the robot is lifted off the desktop to prevent it from breaking. Other potential risk includes damage to the equipment, mainly the robotic arm. There is potential for damage if the arm moves too fast, attempts to move outside of its boundaries or if it tips over. The potential risk of damage to the camera is if it falls off the robotic arm and breaks. There is also the risk associated with the power source. The robotic arm requires 40 to 100 Watts of power but even with the low power rating and low voltage, there is still the risk of electrocution as the robot is plugged into a power outlet.

3.2.1 Evaluation of Risk

Any system which is programmed but still in development has a level of risk associated with it because it is subject to human error and experimentation. With this system, there is mostly pre-written code available for use which has been tested and approved by the developing companies. This significantly reduces the risk associated. However, there will still be some risk, mainly with Dexter HDI, as code is modified to suit the environment it is in and the task that it is performing. For this reason, it is critical to evaluate the level of risk associated with each potential risk. Table B.1 and Table B.2 in Appendix B

demonstrate the risk levels and evaluation of risk.

3.2.2 Management of Risk

In order to reduce hazard levels, measures will be put in place to assist in preventing the hazards from occurring. This will include keeping a clear workspace, having unobstructed access to the power source of the robotic arm and standing out of the robot's reach whilst it is running. A more detailed description of the management measures to reduce the level of risk is also shown in Table B.2.

3.3 Ethics

The nature of the project does not require much consideration of ethics as no testing will be conducted with human or animal participants. The safety towards the researcher has been considered in the risk assessment where measures have been put in place to ensure the tests are good and safe. All equipment used is open-sourced so that the technology can be accessed by hobbyists or researchers and the information can be further developed and shared with the world.

Chapter 4

Specifications and Experimental Setup

This chapter describes the specifications of the hardware and software that was used, and the experimental setup of the tests conducted. It also explains the options that were available for artificial tags and justifies the choices that were made.

4.1 Hardware Specifications

The hardware used in this project was the OpenMV H7 Camera and the Dexter HDI robotic arm.

4.1.1 OpenMV Specifications

The OpenMV project was developed to be a "small, affordable, and expandable machine vision module" (Agyeman 2020). It is a microcontroller board that allows for easy implementation of machine vision in real-world problems (OpenMV 2020*c*). The camera that was used for this project was the OpenMV Cam H7. The product page gives the complete list of specifications for the camera (OpenMV 2020*c*). Some of the specifications will be listed here.

The processor that it uses is the STM32H743VI ARM Cortex M7 processor. Some of the

key features of this processor are:

- 480Hz running speed
- 1MB SRAM
- 2MB of flash
- 3.3V output on I/O pins and 5V tolerance

The processor also has many I/O interfaces such as:

- USB interface to the computer that runs at 12Mb/s
- A micro SD card socket
- A SPI bus that allows for streaming data
- An I2C bus, CAN Bus and an Asynchronous bus
- Analog-to-Digital and Digital-to-Analog converters

The H7 camera has a removable camera module system which helps to achieve the goal of being expandable. This removable system allows for interfacing with different sensors. The OV7725 image sensor is the standard sensor that the OpenMV H7 Camera is sold with. It has the capability of capturing 640x480 8-bit Grayscale images or 640x480 16-bit RGB565 images at 75 frames per second. This is if the camera resolution is above 320x240. The speed doubles to 150 FPS if the resolution is lower. The image sensor has a 2.8mm lens that fixes onto a standard M12 mount. This lens is interchangeable for other specialised lenses. The camera can connect to the computer being used to program it, a single board computer like the RaspberryPi, or a microcontroller like the Arduino. It does this over UART, I2C Bus, SPI Bus, CAN Bus, USB port or over Wifi using a Wifi Shield. The SPI Bus has the fastest transmission rate at 80 Mb/s. The connection between USB and the camera runs at 12 Mb/s. Further specifications are included in Appendix D.

The cost of the OpenMV H7 is $65 USD.

4.1.2 Dexter HDI Specifications

As previously mentioned in the Literature Review, Dexter HDI is a desktop robotic arm which was developed by Haddington Dynamics that has "a set of industrial features while being a fraction of the cost of other robots" (Haddington Dynamics 2020*b*). Dexter HDI has a weight of 6kg which makes it considerably lighter than other desktop robotic arms (Haddington Dynamics 2020*b*). It is constructed with 3D printed carbon fibre (Haddington Dynamics 2020*d*). The standard reach of the robot is 700mm but can be customised up to 4m depending on the requirements of the user. With this standard setup, Dexter can lift half its weight – 3kg – and more if it is counter-balanced.

There are seven defined joints that govern the movement of the robot (Haddington Dynamics 2020*b*):

- J1 – the base – 365 degrees
- J2 – pivot – 270 degrees
- J3 – shoulder – 270 degrees
- J4 – differential – 180 degrees
- J5 – differential – 360 degrees
- J6/J7 – gripper – 300 degrees

The joint J1 rotates around the z axis which runs vertically. This joint changes the direction of the entire robotic arm. Joint 2 raises and lowers the whole arm. The third joint is labelled as the shoulder, but it acts more like the elbow. It is the joint that allows the robot to pick up things close to the base or at the awkward, elevated angles in the air. Joints 4 and 5 resemble the wrist but with less restrictions. Joint 4 allows the end effector to be moved up or down, having limits of 90 degrees downward and 90 degrees upward. This gives the pitch of the end effector. Joint 5 provides 360 degrees rotation of the end effector to give the yaw. Joints 6 and 7 control the gripper itself.

Dexter HDI is highly precise. Even though it is 3D printed with material that causes imprecision, the encoder technology that Haddington Dynamics developed for the robot increases the precision. This allows joints to be significantly more precise than they

normally would be. The encoders have a stepping precision of five micrometres and a repeatability precision of 25 micrometres – that is its ability to repeat a task accurately. This is also a result of the use of the FPGA supercomputer that works with the encoder technology. It allows responsive feedback between the encoder and motor in about 200 nanoseconds (Newton 2020). It achieves 0.8-1.6 million points of precision to each joint of the robot. This design also does not need high amounts of power but can be connected via a standard outlet. Dexter HDI does not have a control box as it can be directly run by the script written in its programming environment.

The price of a standard Dexter HDI robotic arm is $11 000 USD which is $21 000 less than the starting price of a UR3e robotic arm (Haddington Dynamics 2020*b*).

4.2 Software Specifications

This section details the software that was used in the project.

4.2.1 OpenMV IDE

Along with the camera, the OpenMV project has its own programming environment. The environment contains a text editor that allows for scripts to be written in high level Python. The underlining operating system is MicroPython (OpenMV 2020*c*). The developers chose Python over C or C++ due to its ability to handle the "complex outputs of machine vision" more easily (OpenMV 2020*c*). The software also contains a debugging terminal so that any errors in the scripts can be identified (OpenMV 2020*b*). Also, importantly, it has a frame buffer viewer where the image from the camera can be seen (OpenMV 2020*b*). Underneath the frame buffer viewer is a histogram display that is linked with the frame buffer viewer (OpenMV 2020*b*). The histograms change in real-time with the image the camera is seeing. It is affected by colour and lighting, among other factors, at the time the script is running.

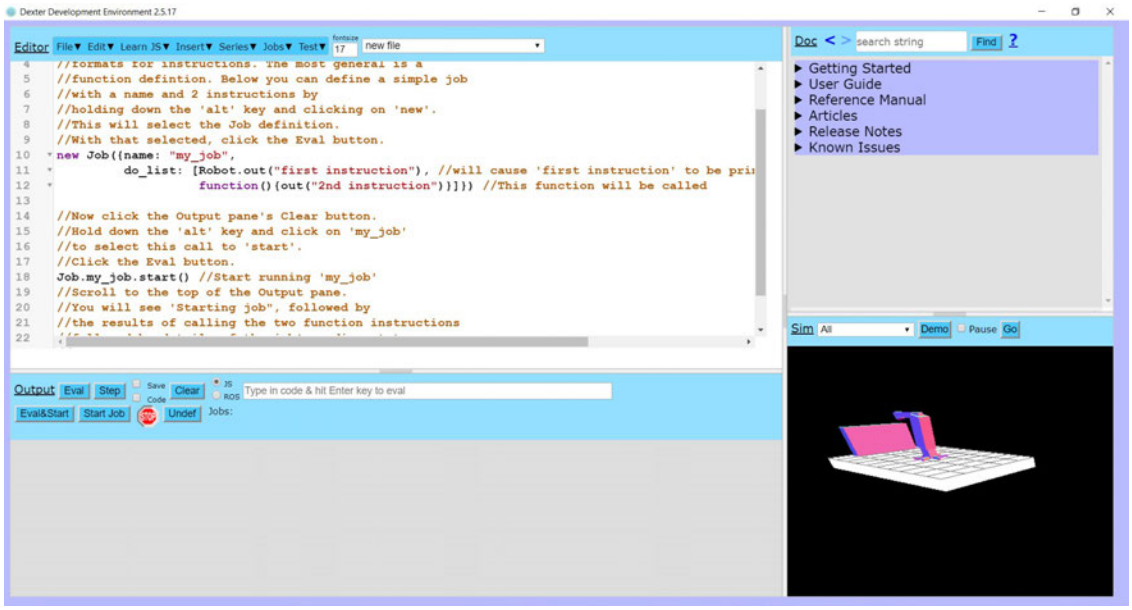

Figure 4.1: Dexter Development Environment

4.2.2 Dexter Development Environment

Dexter Development Environment (DDE) was the software developed entirely for the Dexter robot arm. Whilst it has some instructions specifically created to control Dexter, the environment is based on JavaScript (Haddington Dynamics 2020*a*). When the user opens DDE they will see four panes: the editor, the output, the documentation, and the misc. pane. Figure 4.1 displays this. The editor pane is in the top left of the screen; it is the largest of the panes. It is here that scripts are inserted through the drop-down menus or typed by the user (Haddington Dynamics 2020*c*). DDE has some specific functions like "new job" that control the robot. Within these functions, there are commands that specify how the arm is to move. The output pane gives the user information when the scripts are running: how far through it is, what job is running, errors, etc. The documentation pane (located in the top right) locates all the necessary information on the programming environment and on Dexter itself, as well as articles and release notes. In the documentation pane, key words can be searched and the software will return all the places where the word or phrase appears in the documentation. The misc. pane includes various other pieces of content. Most notably is the simulation of Dexter that allows the user to test programs without having a physical Dexter.

4.3 Experimental Setup

In this section, the choice of AprilTags and testing objects is explained as well as the experimental setup.

4.3.1 Artificial Tags

Artificial Tags are identifiers that are used to provide information in a digital way. Specifically, for this research, fiducial tags are the focus. Fiducial tags are a branch of artificial tags. As described in Chapter 2, fiducial tags provide information on an object's pose: its position and orientation. They are often also used for global coordinates. It has already been discussed that in this research, three main types of tags were investigated: ARToolkit, ARTags, and AprilTags. ARToolkit was one of the first fiducial tags to be developed (Fiala 2005*b*). They sought to use these markers in augmented reality. The research suggests, however, that there were many disadvantages to this system. Some of the disadvantages included the need for controlled lighting, a high computational cost when attempting to detect and decode the tag, and difficulty in generating tags that were detectably different (Fiala 2005*b*)(Olson 2011). The main advantage to this system is that the tag payload was meaningful because it used common images and symbols (Fiala 2005*b*). ARTags were developed from ARToolkit. The developers sought to improve the detection accuracy so that there would be less confusion between tags (Fiala 2005*a*). ARTags changed the payload from known symbols in greyscale to using a grid of black and white squares (Fiala 2005*a*). This allowed for better accuracy in tag detection because it could be processed into binary. It also meant that tags could be detected in poor lighting. The disadvantage to this system is that it is not all open-sourced and so cannot be accessed by the public (Olson 2011).

AprilTags were a further development from the previous two systems. They are similar to ARTags by using the two tones with the grid pattern of squares for the payload (Olson 2011). However, they use a different method of detection which adds to their ability to detect tags with higher accuracy (Olson 2011). There is more flexibility in AprilTags so that the user can choose the properties that best suit their needs, and the developers have done a lot of work to ensure that when a tag is rotated in each direction there is the same Hamming distance between all other tags within the family (Olson 2011). Further work

was conducted so that the detection rate was even greater. This was at the expense of detecting occluded tags (Wang & Olson 2016). They have also developed tags for different shapes and layouts. Within AprilTags, there are many different families which allow for different requirements.

As was discussed in Chapter 2, AprilTags appear to be the most robust of the fiducial tags since it has built upon predecessors. AprilTags have observed the problems associated with ARToolkit and ARTags and have sought ways to improve upon the design. This, according to the research, has led to a more functional tag all round. AprilTags are also open-sourced. For these reasons, AprilTags were chosen to be the fiducial tag to be tested in this project. The other design decision that was made was the selection of tag family. Each family had a different number of tags within it. The payloads were also different sizes. The OpenMV camera was used and the programming environment for it provided some example code for AprilTags. In the OpenMV IDE, it also had an AprilTag generator. This suggested that tag family 36H11 was most suitable with 587 different tags. For this reason, TAG36H11 was chosen to be used.

4.3.2 Testing objects

The aim of the project was to verify the robustness and usefulness of AprilTags, particularly in a pharmacy application. In order to verify the tags, it was planned that several different objects would be tested to understand how they would affect the tags. It was decided that the shapes would be cubes, cylinders, and medication packaging. There was no need to test the tags on more complex shapes as medication packaging is usually rectangular or cylindrical. The added complexity to testing with medication packaging was the shape of the bottle neck and the already existing information on the labels of the packages. Once the object shapes had been decided, the material of the object had to be decided upon. Initially the thought was to 3D print the objects, but this seemed like a waste of time and resources for such simple shapes. The other options were to make the objects out of balsa wood, dowel, or source pre-existing objects in the required shapes. It was determined that the square and round dowel were both too small, as ideally the objects need to be of similar sizing to medication packaging. Sourcing balsa wood in the required size that did not require too much extra work to shape the wood also proved difficult. So, it was decided to use pre-existing objects that are cubic and cylindrical.

Figure 4.2: Lego brick cube that was used

.

The cube was constructed out of Lego to be a 64mm x 64mm x 57.6mm. Figure 4.2 displays how many Lego bricks these dimensions equate to. Food tins were used for the cylinders. Three different sizes were chosen so that different curves could be tested. The sizes were 5.5cm diameter, 8cm diameter, and a 10cm diameter. These are all sizes similar to medication packaging sizes.

4.3.3 Setup

As mentioned in the section above on AprilTags, the tag family 36H11 was chosen to be used. As a singular object was tested on, only one tag was needed. Tag ID 0 was selected and was printed out at different sizes by a basic home printer. The sizes of the tags printed were 61mm x 61mm, 40mm x 40mm, 25mm x 25mm, 10mm x 10mm, and 5mm x 5mm. The tags are pre-set to 61mm. The tag was attached and centred on the object being tested by Blu Tack.

The setups were quite similar for the intial and semi-autonomous stages. In both stages the camera was zip-tied to the side of the suction end effector. This is depicted in Figure 4.3. Dexter HDI was set up on a desktop with the end effector pointing towards

the user. This was the home position. The room the testing was conducted in was lit by both artificial and natural lighting. The natural lighting caused difficulties in controlling the lighting.

The objects used during Stage 1 and Stage 2 were:

- Stage 1.1, 1.3, 1.4, 2.1, 2.3, and 2.4 used a cube of size 64mm x 64mm x 57.6mm which was constructed out of Lego bricks.
- Stage 1.2 and 2.2 used various sized cylinders; three were tested: 100 mm diameter, 80 mm diameter, and 55 mm diameter.

The 100mm cylinder was a medium sized Milo tin. The 80mm diameter was a bottle of wet wipes, and the 55mm diameter cylinder was a small tin of coconut milk. This is recorded for reference and repeatability purposes.

For Stage 1, the 'path and play' script was loaded into DDE and run on Dexter. This allowed the user to manually manipulate the robot to the desired location. By holding in the button on the side of J4, the arm was moved to each point. The object was adjusted to be directly underneath the camera. The distances between the tag and camera were approximate values, measured by a standard 30cm ruler. The idea of Stage 1 was to give a foundation for understanding the robustness of the tags. Figure 4.3 demonstrates the layout of the setup.

In Stages 1.1 through 1.4 - testing numbers as defined in Chapter 3 - the object was placed directly under the camera and the user ran the OpenMV AprilTag program for ten seconds, timed by a stopwatch. The output written into the Serial Terminal was then saved as a text file after each trial. There were ten trials in each test. The variables were tested as stated in the Methodology.

The advancement in Stage 2 involved using the dialog box in DDE to control the exact positioning of Dexter, and therefore, the camera. Figure 4.4 shows the dialog box. Dexter was first moved to its neutral position which is at the coordinates (0, 0.5, 0.075), all measured in metres. It was then moved up to 0.1 in the z direction to inspect whether it would be 10cm above the tag once the camera was rotated. J4 and J6 were both then rotated 90 degrees relative to its position. This positioned the camera to be pointing directly down on the benchtop. The object was placed underneath the camera and the

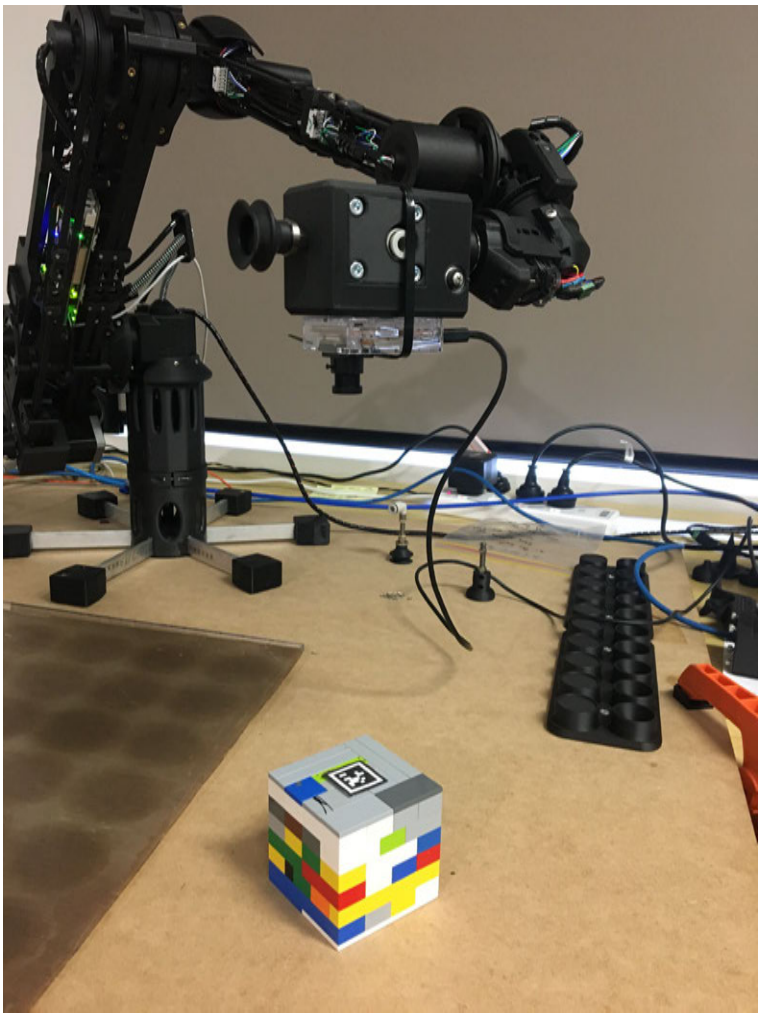

Figure 4.3: Stage 1 Setup with cube using Path and Play

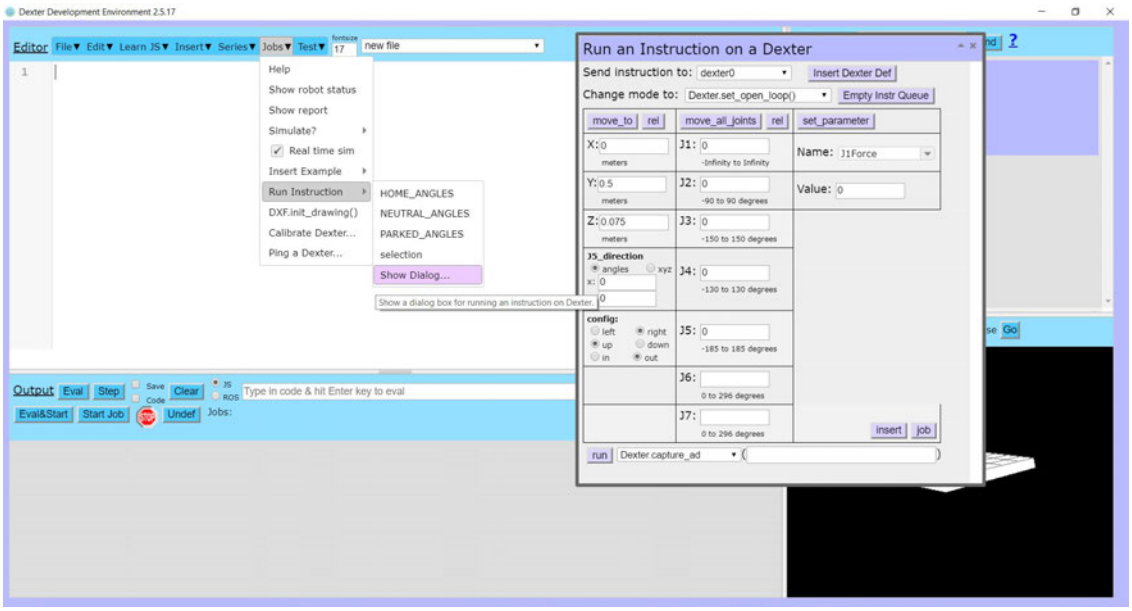

Figure 4.4: DDE's dialog box used to control the position of the arm

Table 4.1: Generalised coordinates and angles for positioning.

Angle Tested	**x**	**y**	**z**	**J1**	**J4**	**J6**
30 degrees	0	0.5	x+0.01	20 degrees	90 degrees	30 degrees
45 degrees	0	0.5	x+0.01	0 degrees	90 degrees	45 degrees
90 degrees	0	0.5	x+0.01	0 degrees	90 degrees	90 degrees

distance between the end of the lens and the tag was measured. It was found to be 9cm, so Dexter's position was reset to home and then moved to (0, 0.5, 0.11) and J4 and J6 were rotated again to have the camera pointing downwards, above the object. This resulted in the camera being 10cm above the tag. So, the adjustment of 0.01m was then able to be made on each coordinate that was tested.

Table 4.1 displays the generalised coordinates and angles that were used to control the positioning of Dexter HDI. The coordinates are measured in metres and the angles are in degrees. The value 'x' is the distance above the tag that is desired in metres. To achieve the correct position, the coordinates were run first in the dialog box. After this, the angles were inputted and the robot was moved relative to the position that Dexter was already in.

In Stages 2.1 - 2.4, there were three locations for the object depending on the angle that was being tested.

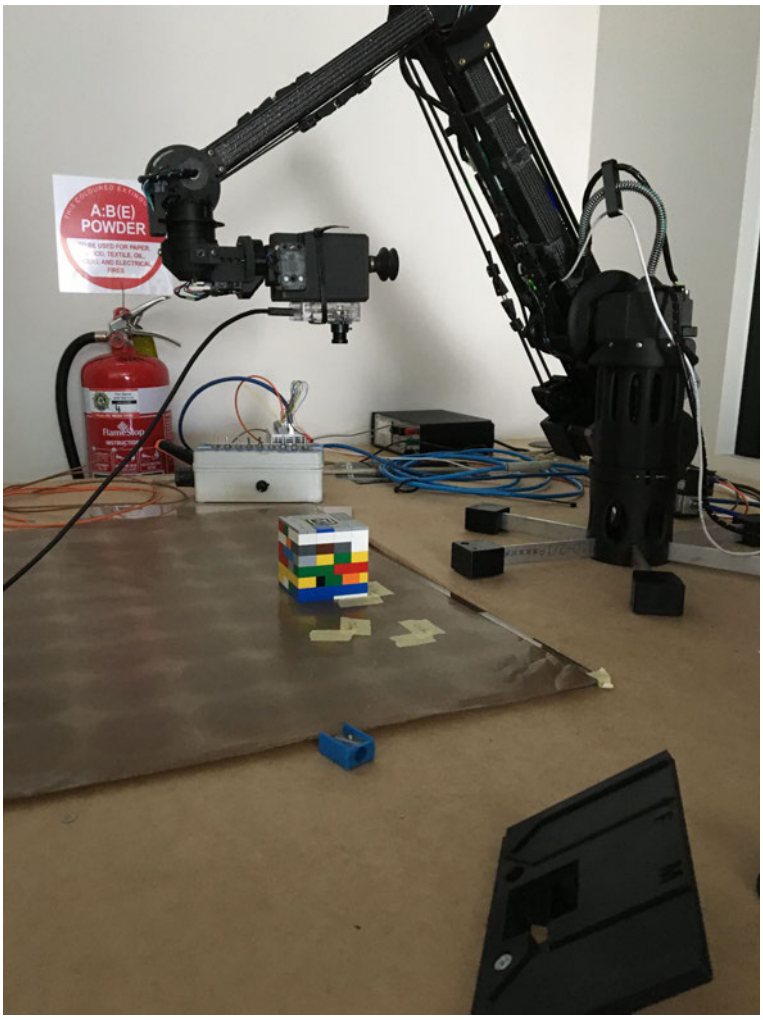

Figure 4.5: Stage 2 setup showing a test with the cube and 90 degree camera angle

- 3cm off the x, 12.5 off the y with the camera set to 30 degrees
- 6cm off the x, 10cm off the y with the camera set to 45 degrees
- 0 cm off the x, 10cm off the y with the camera set to 90 degrees

The measurements were taken from the middle of the front foot of the robotic arm to the first edge or corner of the object. The y axis was pointing towards the user when the user was facing the robot, and the x axis was to their right. The variables tested were as listed in the Methodology. Figure 4.5 displays the set up of Stage 2 with the markings for object positioning.

4.4 Chapter Summary

In this chapter, the specifications for the hardware and software have been discussed and listed. The choices of AprilTags and testing objects were explained as well as the explanation of the setup of testing.

Chapter 5

Testing and Results

This chapter outlines the specific tests that were undertaken to verify the usability of AprilTags and the results of the tests. Through the verification process, it will assist in determining whether AprilTags could be used to locate medication packaging so that the sorting process could be automated.

5.1 Data collection

The data was collected through OpenMV IDE where the detections were written to the serial terminal. Figure 5.1 displays the serial terminal display.

5.2 Stage 1 Testing and Results

The purpose of Stage 1 was to gain a 'big picture' understanding of the AprilTags. The tests constructed were designed to begin to answer some of the research questions.

- How does depth affect tag recognition?
- How does occlusion affect tag recognition?
- How does the size of the tag affect detection?
- How does object shape affect tag detection?

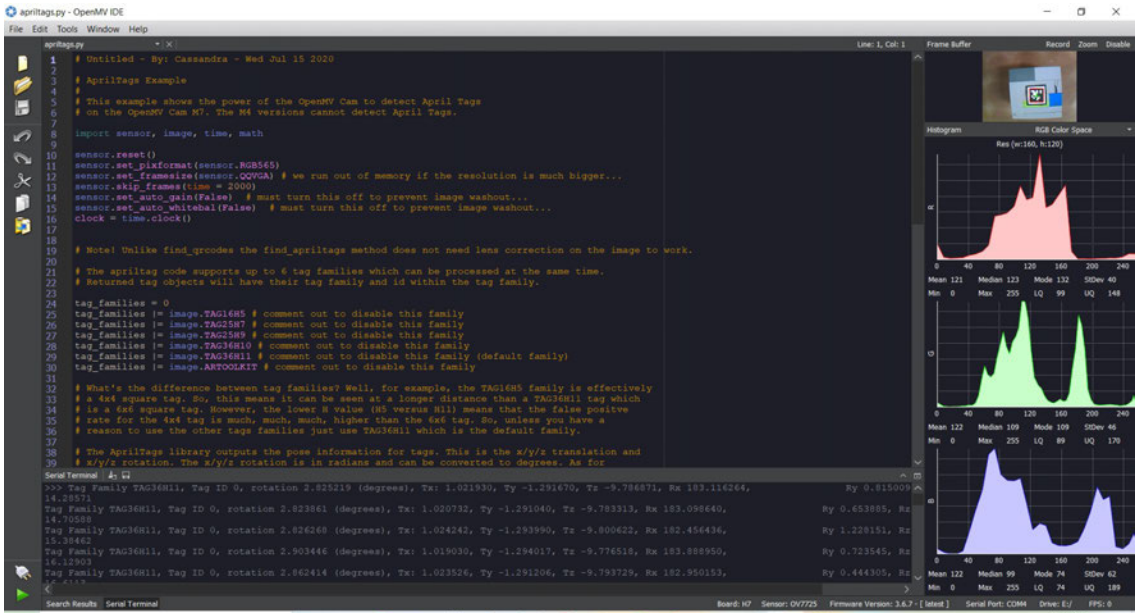

Figure 5.1: Data output in serial terminal and the frame buffer viewer image

5.2.1 Stage 1.1.i and Stage 1.1.ii

The tests conducted during 1.1.i and 1.1.ii were testing the affects of distance between the camera and the tag, and the affects of tag size. The other variables were set as follows:

- Object: Cube
- Camera angle: 90 degrees
- Occlusion: none
- Lighting: Controlled as possible

Table 5.1 displays the breakdown of tests. The testing was conducted on a sunny day with the lighting in the testing room to be generally consistent with both artificial and natural lighting.

Test 1

The distances tested are listed in Table 5.1. It was observed during this test that the camera did not detect a tag in the image very often. As the Serial Terminal was outputting data in real-time, the user could see that the detections were limited.

Table 5.1: Stage 1.1.i and 1.1.ii: Testing changes in height and tag size

Test name	**Tag Size**	**Height**
Test 1.1	5mm	3cm
Test 1.2	5mm	5cm
Test 2.1	10mm	5cm
Test 2.2	10mm	10cm
Test 3.1	25mm	10cm
Test 3.2	25mm	20cm
Test 3.3	25mm	30cm
Test 4.1	40mm	10cm
Test 4.2	40mm	20cm
Test 4.3	40mm	30cm
Test 4.4	40mm	50cm
Test 4.5	40mm	70cm
Test 5.1	61mm	10cm
Test 5.2	61mm	20cm
Test 5.3	61mm	30cm
Test 5.4	61mm	50cm
Test 5.5	61mm	70cm

Test 2

The distances tested for Test 2 are listed in Table 5.1. It was observed during this test that at the height of 5cm some detections were recorded and at 10cm very few were recroded.

Test 3

Test 3 used a 25mm tag. The distances are listed in Table 5.1. It was observed during this test that detections were made at 10cm and 20cm. At 30cm there appeared to be many less detections. The output was mostly the clock reading.

Test 4

Test 4 tested five distances as shown in Table 5.1. When the camera was set to 10cm, it appeared to detect the tag well. When the camera was set to 20cm, it still detected the tag well. Detections were still made at 30cm. At 50cm and 70cm, the Serial Terminal contained a few detections and lots of clock outputs.

Test 5

Test 5 used a 61mm tag and tested the distances as displayed in Table 5.1. While testing 10cm above the tag, the camera dropped slightly and so had to be adjusted on Trial 9 of the 10cm test. The detections across the ten trials were sporadic. At 20cm, the user noticed some different tag families entering the data. At 30cm, there was a mix of correct detections and incorrect detections. At 50cm and 70cm the correct detections were few with some incorrect detection as well as only clock outputs.

5.2.2 Stage 1.1.iii

The test conducted during 1.1.iii tested the affects of camera angle. The other variables were set as follows:

- Object: Cube

Table 5.2: Stage 1.1.iii: Testing changes in camera angle

Test name	Angle
Test 6.1	80 degrees
Test 6.2	115 degrees
Test 6.3	130 degrees

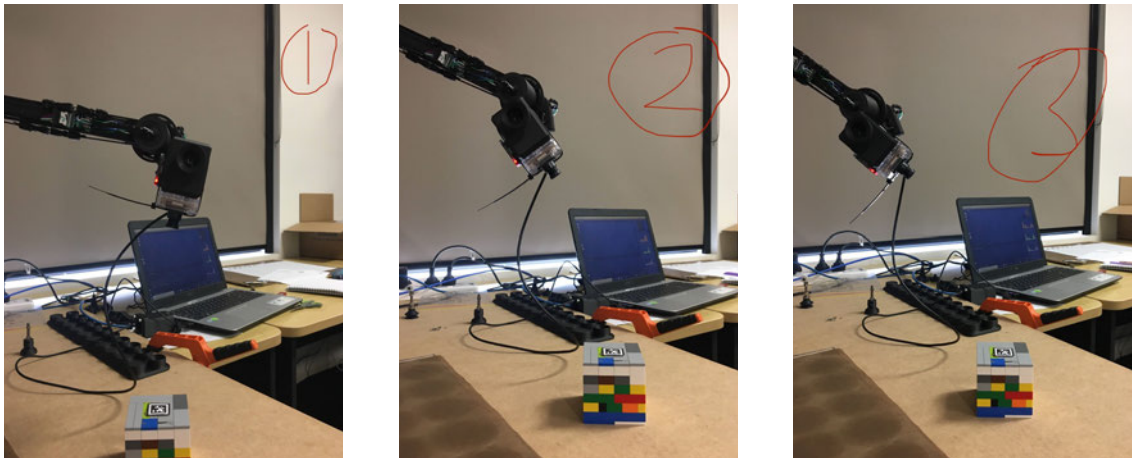

(a) 80 degree angle (b) 115 degree angle (c) 130 degree angle

Figure 5.2: Stage 1.1.iii: Testing various camera angles

- Distance above tag: 20cm
- Tag size: 25mm
- Occlusion: none
- Lighting: Controlled as possible

Table 5.2 displays the breakdown of tests. The testing was conducted on a sunny day with the lighting in the testing room to be generally consistent with both artificial and natural lighting.

Test 6

As shown in Table 5.2, there were three angles tested. The angles were measured from the centre of J4 in an anticlockwise direction. Figure 5.2 demonstrate the positions of the arm and camera.

5.2.3 Stage 1.2.i , Stage 1.2.ii, and Stage 1.2.iii

The tests conducted during 1.2.i, 1.2.ii, and 1.2.iii used various sized cylinders. Alongside the various sized cylinders, the affects of distance between the camera and the tag, and the affects of tag size were also being tested. The other variables were set as follows:

- Camera angle: 90 degrees
- Occlusion: none
- Lighting: Controlled as possible

Table 5.3 displays the breakdown of tests. The day that Stage 1.2.i through to Stage 1.2.iii was tested was an overcast day. The blind that was directly near the setup up of the robot was lifted as it was quite dark in the room with only the artifical light. This led to the light often changing as clouds moved outside.

Test 1

The cylinder size, tag size, and the various camera heights are listed in Table 5.3. During the trials when the camera was set to 10cm above the tag, the lighting did vary. It was also noted during the trials at 50cm that the detections were hit and miss. Generally though, across the trials, some correct detections were observed. It was also observed that the image from the camera did not appear distorted.

Test 2

Through Test 2 no abnormal observations were recorded. There were some correct detections that were observed. There were also some other detections and some misdetections. The image that could be seen through OpenMV IDE did not appear distorted.

Test 3

For Test 3, observations were fitting the trends that had already been seen. Besides the lighting varying throughout the testing, nothing else appeared different. No distortion

Table 5.3: Stage 1.2.i, Stage 1.2.ii, and Stage 1.2.iii

Test name	Cylinder Size	Tag Size	Height
Test 1.1	10cm dia	61mm	10cm
Test 1.2	10cm dia	61mm	20cm
Test 1.3	10cm dia	61mm	30cm
Test 1.4	10cm dia	61mm	50cm
Test 1.5	10cm dia	61mm	70cm
Test 2.1	10cm dia	40mm	10cm
Test 2.2	10cm dia	40mm	20cm
Test 2.3	10cm dia	40mm	30cm
Test 2.4	10cm dia	40mm	50cm
Test 3.1	10cm dia	25mm	10cm
Test 3.2	10cm dia	25mm	20cm
Test 3.3	10cm dia	25mm	30cm
Test 4.1	10cm dia	10mm	10cm
Test 5.1	10cm dia	5mm	10cm
Test 6.1	8cm dia	61mm	10cm
Test 6.2	8cm dia	61mm	20cm
Test 7.1	5.5cm dia	61mm	10cm
Test 7.2	5.5cm dia	61mm	20cm

was seen in the image.

Test 4

No abnormalities were seen during Test 4 besides some misdetections and incorrect detections. The image in the frame buffer viewer did not appear distorted.

Test 5

The data that was observed during Test 5 was minimal correct detections and many misdetections.

Test 6

Test 6 used an 8cm diameter cylinder and tested the 61mm tag. No distortion was observed in the frame buffer viewer and the detections appeared to follow the previous tests.

Test 7

Test 7 used a 5.5cm diameter cylinder and tested with the 61mm tag. There was no distortion that was observed in the image on OpenMV IDE. The detections appeared correct except for the occasional misdetection or other detection.

5.2.4 Stage 1.3

Occlusion was tested by using another bit of paper to cover up portions of the tag. Table 5.4 displays the portions of occlusion tested. The tag, camera height, and camera angle were fixed for the occlusion tests. These values were:

- Tag size: 25mm
- Camera height: 20cm

Table 5.4: Stage 1.3: Testing occlusion

Test name	Portion of Occlusion
Test 1.1	1/12
Test 1.2	1/6
Test 1.3	1/4
Test 1.4	1/2

- Camera angle: 90 degrees

Stage 1.3 was conducted on the same day as Stage 1.2. This meant that the light varied for the occlusion tests as well - it was particularly noticed to change frequently.

It was observed that when one border was covered (1/12 occlusion) there were many correct detections. When two borders were covered (1/6) there were correct detections observed too. During the 1/4 occlusion test, the robot arm had dropped so it was corrected back to a similar position to the previous location. It was also observed through the tests that when the light was bright, there were many correct detections.

5.2.5 Stage 1.4

Lighting was tested with a torch, and with a coverage around the object. Table 5.5 displays the lighting tested. The tag, camera height, and angle were fixed for the lighting tests.

- Object: Cube
- Tag Size: 25mm
- Camera height: 20cm
- Camera angle: 90 degrees
- Occlusion: none

The coverage was simply a piece of paper to try and create a shadow on the tag. The testing was conducted on an overcast day, the same as Stage 1.2 and Stage 1.3. It was observed that there were a mix of correct, incorrect, and misdetections.

Table 5.5: Stage 1.4: Testing lighting

Test name	Type of lighting
Test 1.1	torch
Test 1.2	shadowed lighting

The purpose of these initial tests was to understand the accuracy of tag detection and to determine which variables were the most significant.

5.3 Stage 2 Testing and Results

The second stage of tests were controlled and repeatable as an advancement on from manual manipulation of the robot. The purpose was to gain more specific, reliable data. Stage 2 further verifies the effects of distance from the tag, angle of the camera, occlusion of tag, and lighting building on from the results obtained in Stage 1. Size of tag was not tested in this stage as sufficient results were achieved in Stage 1 and since the direction of the research is towards the use of tags on medication packaging, there was not much point testing a large tag that would not fit on packages along with the information already there. For this reason, a 25mm tag was used across tests.

5.3.1 Stage 2.1.i and Stage 2.1.ii

The tests conducted during 2.1.i and 2.1.ii were testing the affects of distance between the camera and the tag, and the affects of camera angle. The other variables were set as follows:

- Object: Cube
- Tag Size: 25mm
- Occlusion: none
- Lighting: Controlled as possible

Table 5.6 displays the breakdown of tests.

Table 5.6: Stage 1.1.i and 1.1.ii: Testing changes in height and camera angle

Test name	Height	Angle
Test 1.1	10cm	30 degrees
Test 1.2	10cm	45 degrees
Test 1.3	10cm	90 degrees
Test 2.1	15cm	30 degrees
Test 2.2	15cm	45 degrees
Test 2.3	15cm	90 degrees
Test 3.1	20cm	30 degrees
Test 3.2	20cm	45 degrees
Test 3.3	20cm	90 degrees
Test 4.1	25cm	30 degrees
Test 4.2	25cm	45 degrees
Test 4.3	25cm	90 degrees
Test 5.1	30cm	30 degrees
Test 5.2	30cm	45 degrees
Test 5.3	30cm	90 degrees

Table 5.7: Stage 2.2.i: Testing camera angle on cylinder

Test name	Camera Angle
Test 1.1	30 degrees
Test 1.2	45 degrees
Test 1.3	90 degrees

It was observed that at the lower heights the tag was detected correctly quite often. It was found that as the distance between the camera and the tag increased correct detections were observed less. During Test 5.1, the object was not in frame due to its positioning. The object was not moved to be in frame so that there was continuity between the tests.

During these tests the lighting consisted of the artificial lighting and some natural lighting from the windows at the other end of the room. This meant that the lighting was mostly constant throughout the testing.

5.3.2 Stage 2.2.i

The tests conducted during 2.2.i tested the affects of camera angle when the tag was on a cylinder. The other variables were set as follows:

- Object: Cylinder, 8cm diameter
- Tag Size: 25mm
- Camera height: 15cm
- Occlusion: none
- Lighting: Controlled as possible

Table 5.7 lists the conducted tests.

It was found that at all angles tested, correct detections were outputted as well as some misdetections and incorrect detections.

Table 5.8: Stage 2.3: Testing occlusion

Test name	Portion of Occlusion
Test 1.1	1/12
Test 1.2	1/6
Test 1.3	1/4
Test 1.4	1/2

5.3.3 Stage 2.3

The tests conducted during 2.3 tested the affects of occlusion. The other variables were set as follows:

- Object: Cube
- Tag Size: 25mm
- Camera height: 15cm
- Camera angle: 90 degrees
- Lighting: Controlled as possible

Table 5.8 lists the tests conducted.

It was found that when the occlusion was small, there were correct detections. When the payload was partially covered the serial terminal outputted the clock.

5.3.4 Stage 2.4

The tests conducted during 2.4 tested the affects of lighting on tag recognition. The other variables were set as follows:

- Object: Cube
- Tag Size: 25mm
- Camera height: 15cm

Table 5.9: Stage 2.4: Testing lighting

Test name	Type of lighting
Test 1.1	Poor lighting
Test 1.2	Torch light
Test 1.3	Strobe lighting

- Camera angle: 90 degrees
- Occlusion: none

Table 5.9 lists the tests conducted. Poor lighting was defined as no artificial lighting as well as the blinds closest to the camera being shut. The blinds at the other end of the room were rolled up, so this let a little bit of natural light into the room. Figure **??** demonstrates the level of light for poor lighting. The torch light was held so that it shone directly on the tag. A colleague was asked to assist by holding the torch. By using a phone torch, the strobe lighting was achieved. It was set to 8Hz with a 50% duty cycle. The colleague was asked again to hold the light direcly pointing on the tag.

It was found with the strobe lighting that the detections were patchy. From observation it appeared to correctly detect the tag on every second output. It was observed both poor lighting and with torch light that there were many correct detections.

The purpose of these tests was to gain more reliable data that could be compared and analysed to verify the usefulness of AprilTags. The analysis will be conducted in the next chapter.

5.4 Layout of Data

Due to the large amount of raw data, it will not be presented here or in the Appendices. Figure 5.3 displays the construction of the spreadsheets containing the data. This was achieved through loading the text files into Excel and then the data being transformed by splitting the columns by the delimter “space”.

Tag Family	Tag ID	Rotation (d	Tx	Ty	Tz	Rx	Ry	Rz	Clock
TAG36H11,	0	3.119974	-6.814802,	-0.636018,	-18.525466,	174.316730,	43.209310,	3.119974	
TAG25H9,	5	73.422747	-3.916123,	-0.494297,	-10.274531,	25.119367,	313.359952,	73.422747	20.83333
TAG36H11,	0	2.773381	-6.795278,	-0.635449,	-18.472508,	174.086676,	43.399138,	2.773381	21.50538
TAG36H11,	0	6.087362	-6.828093,	-0.650429,	-18.566723,	185.244513,	42.932544,	6.087362	20.13423
TAG36H11,	0	3.391286	-6.754663,	-0.633524,	-18.372602,	176.026869,	45.699916,	3.391286	
TAG25H9,	5	72.739944	-3.932624,	-0.495179,	-10.317105,	27.020414,	313.588524,	72.739944	19.32367
TAG36H11,	0	6.66822	-6.778334,	-0.646182,	-18.431761,	187.331572,	44.288898,	6.66822	19.84127
TAG36H11,	0	2.894842	-6.803936,	-0.634396,	-18.493790,	173.192825,	43.841643,	2.894842	19.93355
TAG36H11,	0	2.279782	-6.742279,	-0.629867,	-18.337418,	172.308435,	44.842219,	2.279782	20.28986
TAG36H11,	0	5.044946	-6.799420,	-0.642035,	-18.486219,	181.792345,	43.803816,	5.044946	
TAG25H9,	5	72.140923	-3.858658,	-0.492365,	-10.122690,	26.536357,	312.205863,	72.140923	20.77922
TAG36H11,	0	5.399863	-6.764180,	-0.643202,	-18.404340,	183.279943,	44.996867,	5.399863	20.83333
TAG36H11,	0	4.122686	-6.773263,	-0.638534,	-18.425970,	178.727255,	44.882097,	4.122686	20.61856
TAG36H11,	0	4.043439	-6.836223,	-0.643060,	-18.587376,	178.081131,	42.849765,	4.043439	
TAG25H9,	5	74.902787	-3.998567,	-0.495697,	-10.523454,	25.229404,	315.908623,	74.902787	20.22059
TAG36H11,	0	3.546498	-6.795815,	-0.637113,	-18.477488,	176.372662,	44.132113,	3.546498	
TAG25H9,	5	73.990021	-3.998732,	-0.491258,	-10.527233,	27.711987,	315.897489,	73.990021	20.33898
TAG36H11,	0	4.114778	-6.768550,	-0.640064,	-18.407036,	178.929243,	44.608397,	4.114778	20.15504
TAG36H11,	0	3.118074	-6.819768,	-0.637829,	-18.544392,	174.278784,	42.928329,	3.118074	20.11494
TAG36H11,	0	4.972741	-6.815626,	-0.641605,	-18.521894,	180.989265,	43.467007,	4.972741	
TAG25H9,	5	73.486934	-3.926065,	-0.494591,	-10.289360,	24.972794,	313.598418,	73.486934	20.0
TAG36H11,	0	4.224214	-6.755335,	-0.638329,	-18.375647,	179.594064,	44.758534,	4.224214	20.15113
TAG36H11,	0	6.972345	-6.558967,	-0.627594,	-17.862761,	186.311932,	50.553379,	6.972345	20.35928

Figure 5.3: Excerpt of the data to demonstrate spreadsheet formatting

5.5 Chapter Summary

In this chapter, a more detailed explanation was given of how the tests were conducted. It discussed how the tests were structured and what the purpose of the tests were. The observations and results were also presented for analysis in the next chapter.

Chapter 6

Analysis

This chapter discusses the results obtained through the tests conducted and analyses the accuracy of detection. A threshold of 80% accuracy was set in Chapter 3 as the benchmark to verify the robustness of a tag. The project as a whole will also be analysed in this chapter.

6.1 Method of Analysis

As discussed in Chapter 5, the output files from OpenMV IDE were imported into Excel so that the data could be filtered and anaylsed. Each test contained ten trials which meant a large number of data points. The data points in each trial was recorded and across a test were summed together. The spreadsheet was filtered for TAG36H11, ID 0. The number of correct detections were recorded and summed together. The percentage accuracy was calculated by dividing the number of correct detections by the total number of data points. Figure 6.1 depicts the process of calcutating the detection accuracy across a few tests. As an example, the first entry is for the test on a cube when the tag size was 61mm and the distance between the camera and the tag was 10cm. The numbers on the left are the total number of data points in each trial and the numbers on the right are the number of correct detections in each trial. The yellow highlighted boxes provide the summation of the trials and the green highlighted box presents the detection accuracy as a percentage.

61mm_10			61mm_20			61mm_30			61mm_50			61mm_70	
217	213		115	115		114	114		118	1		131	0
99	92		114	111		115	115		145	120		137	0
123	119		123	122		112	112		141	122		118	0
125	119		124	118		117	116		131	130		135	0
124	111		117	117		117	116		140	135		128	1
121	111		127	122		123	116		135	135		125	1
123	64		195	120		114	112		156	146		135	0
122	34		125	122		115	114		158	97		135	0
152	0		162	115		132	123		158	94		127	0
127	64		141	117		125	123		165	34		145	0
1333	927		1343	1179		1184	1161		1447	1014		1316	2
69.54239			87.78853			98.05743			70.07602			0.151976	
40mm_10			40mm_20			40mm_30			40mm_50			40mm_70	
125	123		111	111		112	54		153	0		141	0
128	126		119	111		127	72		138	0		139	0
133	128		115	111		152	133		142	0		138	0
136	131		123	120		116	115		143	0		119	0
133	130		113	112		110	108		145	0		130	0
136	130		124	123		131	124		140	0		136	0
133	133		116	115		147	142		166	0		142	0
144	142		128	125		120	119		170	0		147	0
140	140		131	127		117	116		143	0		139	0
149	147		125	123		150	127		130	0		153	0
1357	1330		1205	1178		1282	1110		1470	0		1384	0
98.01032			97.75934			86.58346			0			0	

Figure 6.1: Example of the calculation for percentage accuracy

From these percentage values, graphs have been plotted to present the data. These graphs will now be discussed.

6.2 Tag recognition with changes in Depth

Presented in Figure 6.2 is the graph that addresses the question of the affects of depth as well as the additional variable of camera angle. These results test only one tag size: 25mm. Data discussed further down will explain the affects of tag size. Along the x axis are the increasing distances between the tag and the camera that were tested. These depths were measured in centimetres. The results of the data presented here were from Stage 2 where Dexter was moved to specific coordinates. The y axis displays accuracy of detection as a percentage. Each line represents a different angle that was tested.

The three different angles appear to each have different trends. At an angle of 30 degrees and a height of 10cm, the detection accuracy was 66.3%. When the camera was raised 5cm, the detection accuracy significantly dropped off, resulting in no correct detections. This remained consistent as the camera increased in height. As briefly mentioned in the previous chapter, the object was not in frame when the camera height was at 30cm. The object was not moved to be in frame so that there was consistency with the object location. However, considering that no detections were recorded from heights 15cm through 25cm, it is highly unlikely that any would have been detected at 30cm with the object in frame. At an angle of 45 degrees and a height of 10cm, the detection accuracy was 99.5%. When the height was raised to 15cm, the detection accuracy decreased slightly to 98.7%. As the camera was raised by another 5cm, the detection accuracy dropped to 0% and remained so for the rest of the 45 degree tests. The 90 degree test results were slightly more unexpected. When the camera was set to 10cm, only 76.4% of the detections were accurate and correct. As the camera was moved to 15cm above the tag, the accuracy increased to 99.2%. At 20cm above the tag, the accuracy decreased to 87.6% before decreasing to 0% at 25cm and 30cm.

As can be seen from Figure 6.2 the results are not linear. It can also be seen that each line has a different trend but they all do reach 0% accuracy. This demonstrates that the range for accurate detection is limited. There also appear to be some irregularities in the accuracy of the 90 degree line. It would be expected that at 10cm with a direct view on

the tag, the accuracy would be higher than when the camera is viewing the tag on an angle. However, here the data has resulted in an anomaly where the detection accuracy at 90 degrees, 10cm is less than the accuracy at 45 degrees, 10cm. This could be the result of lighting. There were no anomalies recorded in the lighting but there may have been some slight changes that affected the detection accuracy. Another possibility could be due to the printing of the tag and its low resolution. However, this does not seem likely as the 45 degree did not result in any difficulties with detecting the tag. Therefore, it is a bit unclear as to why the detection accuracy has resulted at 76.4%.

Comparing the accuracies to the threshold set in the Methodology, 30 degrees is not a suitable angle to use in accurately detecting the AprilTag. It is suitable to use a 45 degree angle in the range of 10-15cm above the tag as the accuracies are greater than 80%. However, it is not suitable in distances above 15cm. When the camera is set to look directly down on the tag, the data demonstrates that it is highly accurate in the range from 15cm to 20cm. Potential retesting could be done at the height of 10cm to observe whether the accuracy improves so that there is a greater detection range.

From analysing the graph, it can be seen that changes in depth does have an affect on tag recognition. The data demonstrates that as the distance between the tag and camera increases, the detection accuracy decreases. This is what was expected as stated in the hypothesis. It, however, does not decrease in a linear fashion. Having more data points inbetween would give a greater understanding of the trend of the data but from what is presented, the range for accurate detections is limited. The data also demonstrates that tag detection is affected by angle. The closer the angle gets to the horizontal (as suggested by the 30 degree angle), the less accurate the detections become.

6.3 Tag recognition with changes in occlusion

There were two tests conducted to test occlusion. The first was a preliminary testing of occlusion in Stage 1.3. The camera was set to approximately 20cm above the tag and the object was placed directly underneath. The second test was a controlled test in Stage 2.3 where the camera was moved to position by the dialog box in DDE. The height of the camera in this test was 15cm. Figure 6.3 shows the graph from Stage 1 and Figure 6.5 displays the graph from Stage 2. The axes for both figures are the 'Portion of Tag covered'

on the x axis as a decimal, and the 'Accuracy of Detection' as a percentage on the y axis.

The graph demonstrates that when there is no coverage, 8% coverage or 17% coverage, the detection accuracy is high, at 95.8%, 96.7%, and 95.3% respectively. Once the occlusion increased, to 25% and then 50%, no correct detections were recorded at all. These were all at a constant height. The lighting was inconsistent on the day that Stage 1.3 was tested as it was an overcast day. The sun fluxuated between coming out for a few minutes and cloud cover returning and so this may have affected the accuracy of detections.

The tag consisted of 12x12 squares, either black or white, where the payload was 8x8 sqaures. This left space for two borders: one white and one black. Figure 6.4 depicts this. The test with 8% coverage resembles the covering of one column of sqaures: one side of the black border. With this coverage, the payload was not affected. The coverage of 17% contained two columns: one black, one white. The payload was unaffected by this as well. However, when 25% of the tag was covered, which includes one column of the payload, and 50% of the tag, which covers four columns of the payload, results in no detections.

As can be seen in Figure 6.3, the relationship between coverage and detection accuracy is not linear. The first three points are very similar in accuracy, with a range of 1.4% difference, and then there is a steep decline to 0% accuracy when the payload is slightly covered. This suggests that the tag cannot handle occlusion if even a small part of the payload is covered. The literature review did state that the newer versions of AprilTags removed the ability to handle occlusion due to the amount of errors that were produced and the slower computation time. Therefore, this data does agree with that statement in the literature. However, it does not assist for the application. If AprilTags were put on medication packaging and it comes into the Pharmacy in unsorted boxes, the tags could be partially occluded and if the occlusion includes the payload, then the camera would not be able to detect the location of the object resulting in no pick up by the robotic arm.

In terms of the irregularities, there is only slight variances between the detection accuracies of no coverage, 8% coverage, and 17% coverage. However, it is odd as to why the accuracy would be greater when the tag is partially occluded as compared to no occlusion at all. As mentioned earlier, the lighting during testing did vary as clouds outside moved. It could have been that the sun was out when testing 8% occlusion and so the lighting was brighter allowing for greater illumination of the tag. The accuracy of 17% occlusion does make sense, though, as it is lower than both no coverage and 8% coverage, as would be

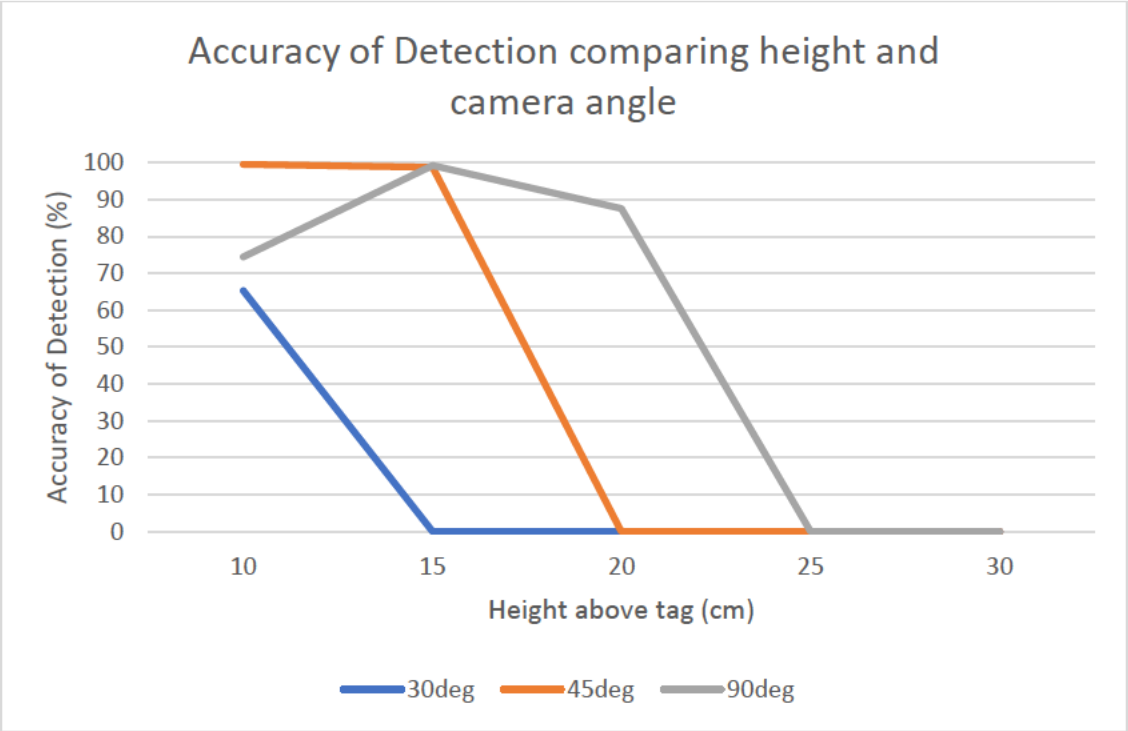

Figure 6.2: Angle and Height comparison

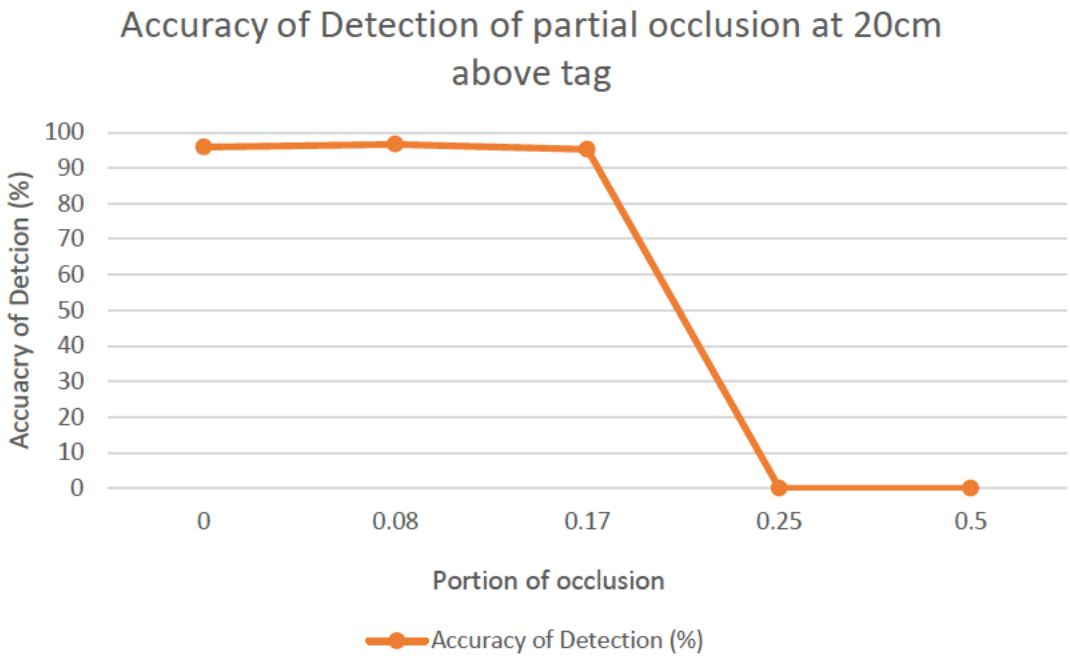

Figure 6.3: Partial Occlusion at a height of 20cm

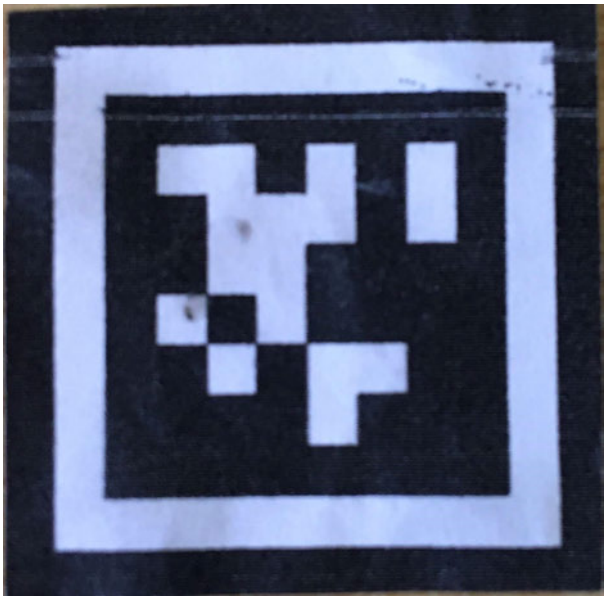

Figure 6.4: TAG36H11, ID 0, 12x12 tag

expected if more was hidden.

Comparing the accuracies to the threshold of 80% detection accuracy set in the Methodology, occlusion of greater than 25% is not suitable. In order to use AprilTags in the prescribed application, another sorting method might need to be used alongside the tags to locate the objects and the code might need to be altered to assist in the detection process.

Figure 6.5 displays the graph of the data from Stage 2.3. This test conducted was an advancement upon the last through controlling the position of the robotic arm through the programming software, DDE. The height of 15cm was chosen because from the data in Stage 2.1, it was the optimal height for accuracy. The graph demonstrates that when there was no coverage, the detection accuracy was 99.2%. The detection accuracy dropped to 88.9% when there was 8% occlusion. At 17% occlusion, the accuracy increased to 99.9%.

As seen in Figure 6.5, there is no trend that fits the data and there appear to be a few anomalies. Similarly to the test conducted in Stage 1.3, the anomalies lie with the detections between 0% and 17% coverage. The accuracy is high for no coverage, as would be expected. At 99.2%, this demonstrates that only a few misdetections occured. When the occlusion was increased to 8%, the detection accuracy dropped which is expected when occlusion is present. However, the accuracy is less than the accuracy that was seen

in Stage 1.3 with the same coverage. In Stage 1.3, the camera was higher than in Stage 2.3 which suggests that some other factor have contributed to the lower accuracy. When analysing the accuracy at 17% occlusion, the percentage increased to almost 100%. This appears counterintuitive considering with lesser occlusion the detection accuracy was 11% less. The percentage is also greater than what was found in Stage 1.3. Again, lighting could have been a factor. Nothing was recorded in the way of different lighting but there might have been some slight variations. Another factor could be in the camera; it might have had some variance in its detection algorithms as it was run but this does not seem likely. Otherwise, it is unknown why there are such dramatic differences in the results.

The data at 25% coverage and at 50% coverage supports the data from Figure 6.3 as they both record no accurate detections across the trials. This can suggest the conclusion that any occlusion of the payload cannot be handled by the tags.

This data, up to 17%, is still above the target accuracy set in the Methodology, as it was in Stage 1.3. This secondary data confirms the results found in the first stage. It data demonstrates that occlusion does affect the detection of the tag. Occlusion limits the accuracy of detection as the payload begins to be covered but while a border is covered, the accuracy is still high. The hypothesis stated that as occlusion increased, the tag would become indetectable as the payload determined the ID of the tag. The data analysed aligns with this hypothesis.

6.4 Tag recognition with changes in tag size

Presented in Figure 6.6 is the results of Stage 1.1. It was a study of tag size and height above the tag. This gave a greater understanding of the importance of tag size as it provided the range of each tag size tested. On the x axis is the distances between the camera and tag that were tested in centimeters. The y axis is the accuracy of detection as a percentage.

Testing began with the 61mm tag. At 10cm above the tag, the detection accuracy was 69.5%. As the height increased to 20cm, so did the detection accuracy. It increased to 88.8%. At 30cm above the tag, the detection accuracy was 98.1%. The camera was then lifted to 50cm where the detection accuracy resulted in 70.1% accuracy. At 70cm above the tag, only 0.15% of detections were correct. The tag was then reduced to be 40mm.

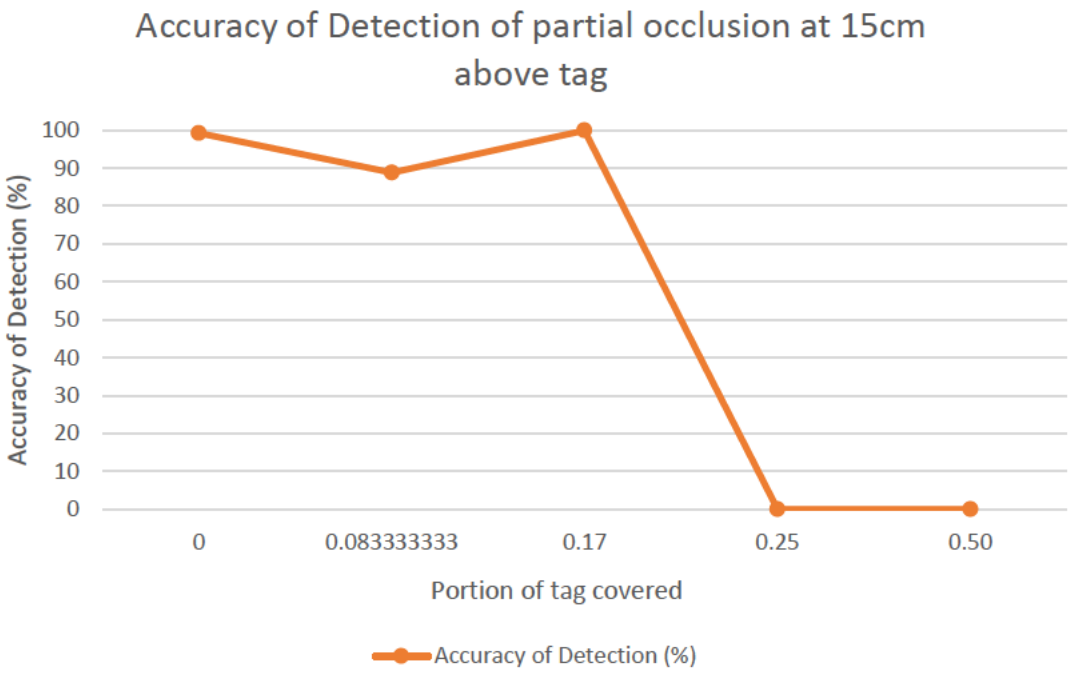

Figure 6.5: Partial Occlusion at a height of 15cm

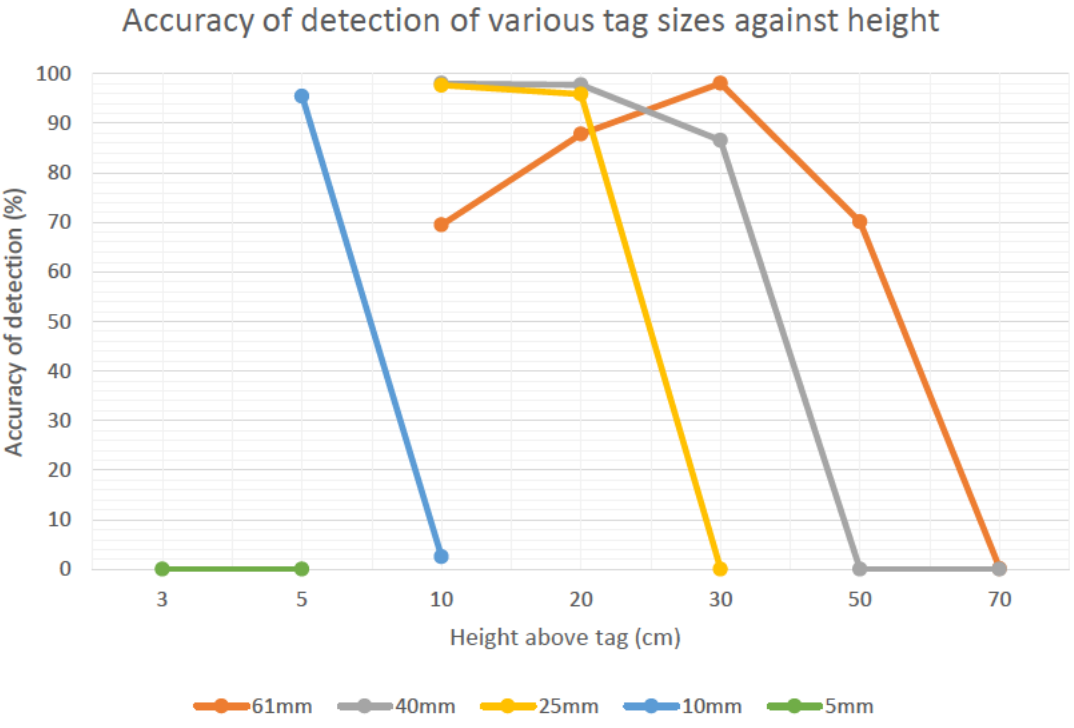

Figure 6.6: Various Tag Sizes and Heights

At 10cm above the tag, 98.0% of the detections were accurate. When the camera was 20cm above the tag, the accuracy decreased slightly to 97.8%. It decreased further still at 30cm to have an accuracy of 86.6%. The accuracy dropped to 0% accuracy when the camera was raised to 50cm and then remained so at 70cm above the tag. The tag size was further reduced to 25mm. At 10cm above the tag, the accuracy was 97.7%. It decreased to 95.9% at 20cm above the tag and then resulted in no correct detections at 30cm above the tag. When the 10mm tag was tested, there was a 2.5% accuracy when the camera was set to 10cm above the tag. Because of this low detection accuracy, the distance between the camera and the tag was decreased to 5cm. The accuracy achieved here was 95.5%. Due to the fact that the 10mm tag had a high accuracy at 5cm, this was the starting depth for the 5mm. However, no detections were recorded. Therefore, the distance was decreased further to 3cm. No detections were recorded at this height either, however.

As can be seen from Figure 6.6 the results are nonlinear within a test and across tests. There is no common pattern as the tag sizes decrease and the heights increase. The results of the 61mm tag are unexpected in the sense that the initial height of 10cm has the least accuracy besides when the camera is at 70cm. The hypothesis stated in Chapter 1 was that detection accuracy would decrease as the height increased. However, here the accuracy increases before it decreases at 50cm. This is also unusual as it was the largest tag tested. It would be expected with the large tag that the accuracy would be close to perfect at 10cm, and steadily decrease as the distance became larger. The 40mm tag behaved more as expected with the accuracy decreasing each time with a height increment. The 25mm and 10mm tag also behaved in a similar fashion. Each time the range became smaller as the tag decreased. The 5mm tag behaved differently again with no detections at either height that was tested. This demonstrates that there is no congruency in the results across the tag sizes. Again, some of the reasoning for differences could have been lighting. The heights for each tag size were slightly different but not so much that it would cause drastic differences. But still, this is something that should be accounted for. The reason the heights were slightly different across tag sizes was because of the 'Path and Play' program that was used as planned. A reason the smaller tags may have had a smaller detection range could be due to the printing quality. As the tags decreased in size, the printer may not have handled printing to the same amount of resolution and detail.

Comparing the results to the threshold, it can be seen that the 5mm tag is not suitable at

all. The 10mm tag is above the threshold when the distance between the camera and tag is 5cm. The 25mm tag is above the threshold for accuracy when the range was between 10cm and 20cm. The 40mm tag had the greatest range for accurate detections above 80% which was 10cm to 30cm. The 61mm tag could only be used inbetween the range of 20 and 30cm from the data given. The tag sizes that are above the threshold may not be useful though for the range that they are accurate for. Ideally, a tag of 25mm or less would be used on medication packaging due to the packaging needing other necessary information on it as well. If the detection range is only 10cm or less, this is not useful for object location and positioning because the arm has to be very close before it detects anything. For this reason, some other detection method might need to be used in conjunction with the tags. If the tags could be printed at a higher resolution, the range might increase which would be of more benefit.

Although the data appears a bit random in places, it can still be seen that tag size does have an affect on the detection accuracy. This affect is closely linked with the height of the camera from the tag. The relationship seen is as the tag size decreases, so does the range which was predicted in the hypothesis in Chapter 1.

6.5 Tag recognition with changes in object shape

The research question was quite broad, but there are not too many shapes when it comes to medication packaging: usually boxes and bottles. For this reason, different sized cylinders were tested to determine whether there are any affects to tag recognition. The idea was to examine whether different diameters, and thus curves, had any affect on the accuracy of detection. Figure 6.7 displays the results of testing with various cylinder sizes. Along the x axis is the three cylinder diameters that were tested. The y axis displays the detection accuracy as a percentage. The legend denotes the two heights that were tested: 10cm above the tag, and 20cm above the tag.

Across these tests, a 61mm tag was used as it was expected that it would experience the most distortion, particularly as the cylinder reduced in size. When the camera was set to 10cm, the detection accuracy on the 5.5cm cylinder was 98.8%. At the same height, the 8cm cylinder had a higher accuracy of 99.2%. The accuracy decreased to 90.5% as the cylinder increased to 10cm in diameter. When the camera was raised to 20cm, the

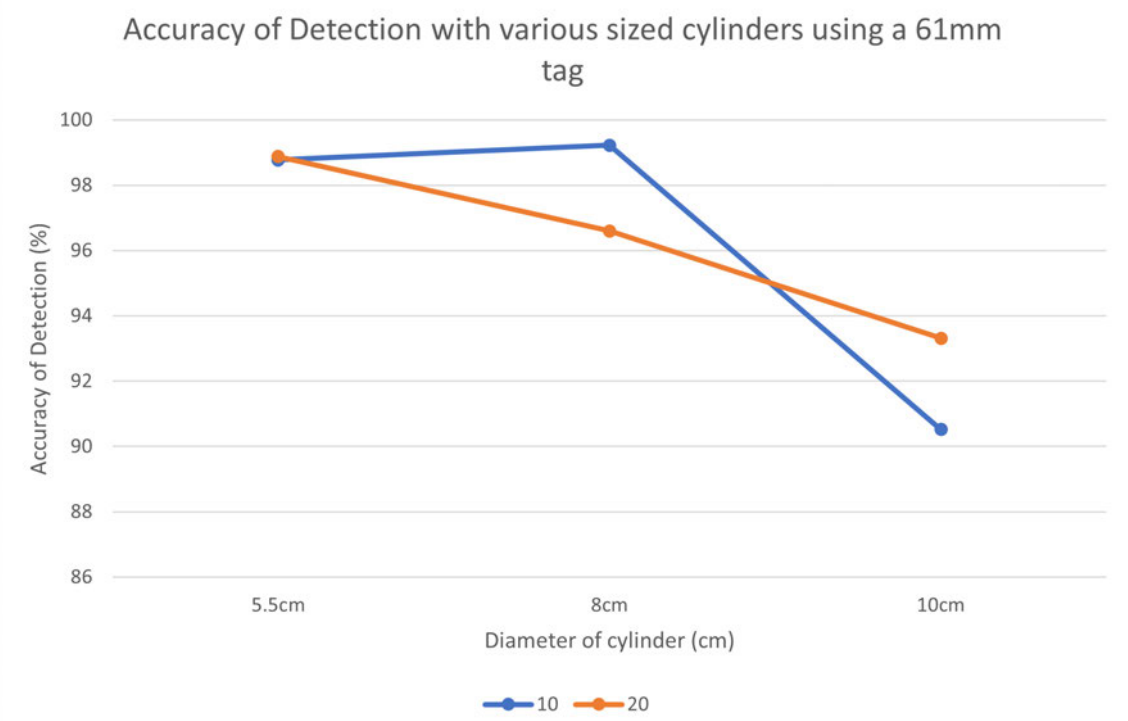

Figure 6.7: Affects of different sized cylinders on tag recognition

detection accuracy on the 5.5cm cylinder slightly increased to 98.9%. The accuracy of detection when testing the 8cm cylinder decreased to 96.6%. When the 10cm cylinder was used, the accuracy increased from the previous accuracy to 93.3%.

As can be seen in Figure 6.7 the results are varied. The accuracies achieved at 10cm above the tag are not linear and appear somewhat unusual. It makes sense that the accuracy increases from the 5.5cm cylinder to the 8cm cylinder as the 8cm surface is slightly flatter than the 5.5cm surface. However, the difference is not too large. The anomaly appears to be with the 10cm cylinder. The accuracy dropped to 90.5%. It was expected that as the curve of the surface flattened, the accuracy would increase. However, this result demonstrates that it did not. These tests were conducted on the day when it was overcast and so the lighting kept changing. This may have affected the result. The data achieved at 20cm above the tag appears much more linear. Although, the line is trending in the opposite direction to the 10cm height line and from what was predicted. The accuracy of the 5.5cm cylinder at 20cm is slightly greater than the accuracy at 10cm, although, it is only by 0.2% so is hardly significant. The accuracy of the 8cm cylinder dropped 2.6%. This makes sense with the change in height but it does not make sense with the curve of the surface being flatter than the 5.5cm cylinder. The accuracy decreased again for the 10cm cylinder in comparision to the accuracy of the 8cm cylinder, but it increased in

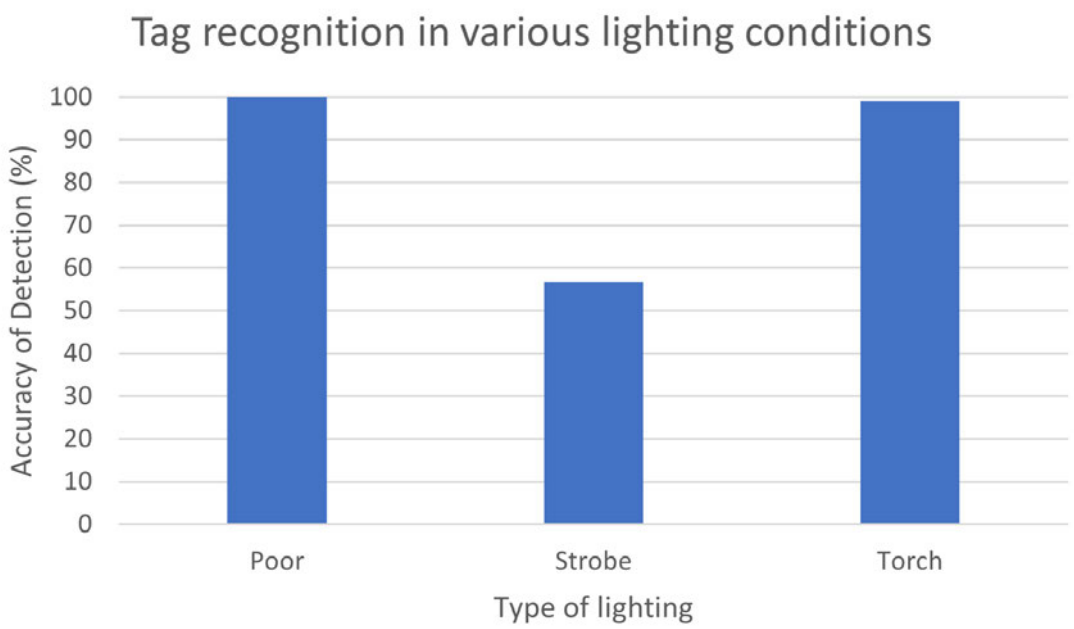

Figure 6.8: Affects of lighting on tag recognition

comparison to the camera being set 10cm above the tag. In the big picture though, the differences are not too great and all the accuracies are above 80%.

Therefore, although there are some unexpected results, a curved surface does not seem to affect the tag detection. This data suggests that the premise of the hypothesis that tag recognition would decrease as the diameter became smaller is not supported.

6.6 Other Findings

Lighting was not a specific question at the beginning of the project but it was tested to determine whether lighting did cause an affect, and so affect the other results. The results from Stage 2.4 will be considered here. Three lighting conditions were tested: poor lighting, strobe lighting, and torch lighting. These conditions are presented along the x axis of Figure 6.8. The y axis is still the detection accuracy as a percentage. The setup of the lighting conditions were defined in Chapter 5.

In poor lighting, the accuracy of detection was 100%. This is the first 100% accuracy in the entire study. The strobe lighting attained a 56.8% accuracy, and the torch light achieved a 99.1% accuracy. The camera was set to 15cm above the tag for each of these tests.

It is interesting to note that the consistent lighting conditions achieved a high accuracy. Even with lighting being poor, there was enough consistent light that helped to achieve high detection accuracy and the same can be said with the torch light: the lighting was consistently bright and so the detection accuracy was high. However, when the light varied, the detection accuracy decreased significantly. The result was little more than a detection every second data point as observed in Chapter 5. This may explain some of the unexpected results discussed earlier. When the lighting suddenly changed, the detection accuracy decreased, whereas when the lighting was consistent, the accuracy was high. Further testing, in a more controlled environment would need to be conducted to confirm this.

6.7 Problems Encountered

Through the study, some problems were encountered. First, the pose estimation calculated by the camera returned the results that appeared very strange. It became known that the results were in pixels. It was not intuitive, however, as to how to convert the results into millimetres. There was a program written by the OpenMV team that used tag size to convert the distances into millimetres except the results did not correspond to the actual distance to the tag. There appeared to be a scale factor but it was very random. This was a hindering factor to coordinating the robot arm and the camera. To move forward with combining the systems, the translation values would need to converted and assured that the values were consistent.

This leads to the second problem encountered. The values that were recorded in OpenMV for the translation were not consistent in Stage 1. Appendix C displays an excerpt of trials from one test. This was one test where the object and camera were not moved and the trials were run consecutively. But as the data shows, across the trials the translation in the x, y, and z changed with each trial. This might suggest that the camera is not accurate in calculating where the centre of the tag is located. If this is the case, there will be difficulties in controlling Dexter HDI by the camera. It was found though, that there was an improvement in the consistency of translation points in Stage 2 when the robotic arm was moved to specific coordinates. This is something that could be further investigated.

For these reasons, and due to limited time detection accuracy became the main focus of this project.

As already discussed numerous times, the inability to control the lighting also caused difficulties as did printing the tags with a home printer. Another potential factor may have been the resolution of the lens on the camera. OpenMV have many other lens that may improve the quality of detection.

6.8 Analysis of results achieved against Project Objectives

The first project objective was:

- A verification of the functionality of artificial tagging through various tests determining how shape, size, camera angle, camera distance, lighting, tag size, and occlusion affect the function. AprilTags will be the artificial tag that will be implemented and tested.

The main study of the project was to verify the function of AprilTags. The analysis that has just been conducted has demonstrated the process of verification of the tags through the results of camera distance, camera angle, shape and size, lighting, tag size, and occlusion. The data verified that within some ranges, the AprilTags are robust. In general, for tags equal to or greater than 25mm, the robust range is 10-20cm. Outside of this, the tags are much less functional. It was found that the size of the tag did have quite an impact on the range in which the tag could be detected. This was found particularly as the size decreased. The data demonstrated that the tags were not robust to occlusion. Detection was accurate when the borders were covered but once any portion of the payload was occluded, the accuracy would drop to 0%. The tags did seem to be robust to object shape as the detection accuracy was well above 80%, although further testing would confirm this statement because there were some anomalies in the trend of the data. The tags were not robust to all angles, in particular as the camera came closer to the horizontal and the height increased. The tags were not robust to strobe light. The changes in lighting caused the detection accuracy to drop from near 100% in consistent lighting to 56%.

From this, the conclusion can be drawn that a 25mm tag is robust when the camera is

10cm to 20cm above the tag, at an angle of 90 degree with consistent lighting and no more than 17% occlusion. This could be on a flat or curved surface.

The second objective was:

- The utilisation of the OpenMV camera as a potential low-cost machine vision system to accurately detect the AprilTags. The low-cost device enables the potential for wider application use, particularly if it proves to be reliable and accurate.

This objective is linked to the previous objective in the sense that it can only be deemed as successful if the tags were detected accurately and therefore, verify the funcitonality of the tags. It can be said that the OpenMV camera was utilised to detect AprilTags through all the testing. As with the conclusion of the first objective, a 25mm tag was accurately detected when the camera was 10-20cm above the tag at an angle of 90 degrees with consistent lighting and minimal occlusion. In this sense, the OpenMV camera was a suitable low-cost machine vision system to accuratley detect the AprilTags. At other times though, when the detection accuracy was low, it is hard to say whether it was due to the resolution of the tag or the resolution of the camera. Through this project, the OpenMV H7 camera is not unsuitable for the task. Potentially, a different lens and/or higher resolution printing could prove for the camera to be sufficient.

The third objective was:

- The development of a combined machine vision and robotic arm system in order to autonomously detect and locate tags for autonomous sorting. The robotic arm that will be implemented is Dexter HDI developed by Haddington Dynamics.

This objective was partially achieved. The camera and robotic arm were combined together but it was only the preliminary stages of the technologies being used together as the robotic arm was not controlled by the camera. They were combined together in the sense that the camera was attached to the robotic arm and the position of the robotic arm had to be manipulated to change the position of the camera. The process had begun in detecting and locating the tags for the purpose of autonomous sorting, however, as discussed in the previous sections there were some issues with the locating of the objects. The intent of Stage 3 was to solve the dynamic detection problem rather than use the

static detection as was used in Stages 1 and 2. However, as stated in the Methodology, stages would only be advanced upon the satisfactory completion of the previous stage. So, due to limited time Stage 3 was not begun.

The fourth objective was:

- The utilisation of the whole system to identify, locate, and accurately pick up different medication packages, ultimately being able to sort a box of different medication packages into relevant categories.

This objective was not achieved during the project due to limited time and the amount of tests undertaken in Stages 1 and 2. The testing completed in these stages had the direction of sorting medication packaging, but the autonomous sorting process was not attained.

6.9 Evaluation of the project

At the beginning of the project a few research gaps were identified. These were:

- The need for low-cost robotic arm and machine vision systems that can be used in non-industrial settings.
- The lack of physical tests and results on AprilTags
- The use of a robotic arm, camera, and AprilTags in the pharmaceutical setting

In evaluating the project, some of these gaps have been addressed or have begun to be addressed. The progress that has been made particularly is providing results from physical tests on the AprilTags. As has been discussed in this chapter, data was collected to test and verify the robustness and functionality of the tags. Even though some of the results did not align with the statements made in the AprilTag papers, the data helps to address the gap. The other area where progress has been made is in the low-cost system area. Whilst more testing still needs to be conducted, there is potential in the combination of Dexter HDI and OpenMV as a low-cost system for a less industrial setting. The results achieved have not deemed the equipment unsuitable for this purpose. The last research

gap is the least narrowed. The intent and focus of the study was to drive it in the direction of the hospital pharmacy but no specific work was conducted to narrow this gap. Some conclusions, though, have been drawn due to the focus being here.

In terms of the progress made within the test, there was progress made from using 'Path and Play' script to controlling Dexter with the dialog box. This was an advancement from manually controlling Dexter to controlling Dexter through the DDE environment with specific coordinates and angles being used.

There are many components of the project that could have been done better. Firstly, the tags could have been printed at a higher quality. This would have resulted in a clearer viewing of the tags' payload and so this may have assisted in increasing the detection accuracy. Secondly, the use a Lux metre would have helped so that the changes in lighting could be recorded for better test evaluation. Thirdly, the initial testing could have been more controlled by using the dialog box in Stage 1, and then programming the robot to automate it in Stage 2, to head in the direction of dynamically detecting the tag in Stage 3.

But overall, the results attained through this study are still reliable and helpful to head in the direction of automating the boxes in the Pharmacy that contain orders of medication.

6.10 Chapter Summary

In this chapter, the analysis of Stages 1 and 2 were conducted. The problems encountered and the analysis of the work completed was compared to the Project Objectives. The overall project was also evaluated by considering what progress has been made in decreasing the research gap and by considering what could have been done better.

Chapter 7

Conclusions and Future Work

This chapter concludes the dissertation. The topics and findings discussed throughout this document will here be summarised.

7.1 Research Questions

The first four research questions were answered in Chapter 2 in the Literature Review. These questions were:

- What methods are there for object recognition already?
- What sorts of tags exist for object recognition?
- How do tags work?
- What methods for sorting objects already exist in the robotic world?

It was here that three types of visual fiducial tags were discussed: ARToolkit, ARTags, and AprilTags. It was found that AprilTags work through a graph-based segmentation method analysing the payload in the centre of the tag. It is this payload that allows for the pose of an object to be calculated.

The other four research questions were:

- How does depth affect tag recognition?

- How does occlusion affect tag recognition?
- How does the size of the tag affect detection?
- How does the object shape affect tag detection?

Through the analysis that was conducted, it was found that as the distance between the tag and the camera increased, the tag was less recognised and so, the detection accuracy decreased. It was also found that the tags cannot handle any occlusion of the payload which confirms what was stated in Wang & Olson (2016). In that paper, they had stated that they removed the ability for the tag to handle occlusion so that there were fewer false positives and so it decreased computation time. The accuracy of detection was affected by the tag size – it decreased as the tag decreased in size. The affect of tag size was also closely linked with the distance between the tag and camera. This was demonstrated by observing how the range of distances that would accurately detect the tag decreased as the tag became smaller. It was also learnt that object shape did not have much impact on the accuracy of detection.

Hence, through the testing and Literature Review, all the research questions were answered.

7.2 Project Objectives

The following Project Objectives were achieved:

1. **A verification of the functionality of artificial tagging through various tests determining how shape, size, camera angle, camera distance, lighting, tag size, and occlusion affect the function:** This was achieved through the testing and answering of the research questions. It was found that for a 25mm tag, the tag can be accurately detected in the range of 10-20cm at a 90 degree angle, with limited occlusion and with consistent lighting. The flat and curved surface had similar results
2. **The utilisation of the OpenMV camera as a potential low-cost machine vision system to accurately detect the AprilTags:** This was achieved in correspondance with the first objective as passing depended on the percentage accuracy

being greater than 80% as defined in Chapter 3. It was found that some of the data attained an accuracy above 80%. As a result, the data does not rule out the OpenMV camera as a potential camera but the data does show that there are some limitations to its use.

3. **The development of a combined machine vision and robotic arm system in order to autonomously detect and locate tags for autonomous sorting:** This objective was only partially achieved by the camera being attached to the end effector of Dexter HDI. Further work needs to be conducted here.

The fourth objective was not achieved as the whole system was not coordinated to pick up different medication packages to sort a box of them.

7.3 Conclusions from Analysis

Through the testing it was learnt that:

- The optimal range for a 25mm tag was 10-20cm
- A 45 degree angle can be used when the height above the tag is between 10-15cm
- A curved surface does not seem to affect the detection accuracy in the range of 10-20cm above the tag
- Sporadic changes in lighting cause the detection accuracy to significantly decrease

From these learnings, it can be concluded that there is still potential to use AprilTags for a pharmacy application. However, the use of small tags (less than 25mm) does not look promising from the data analysed. Needing the camera to be less than 10cm away before the tag can be detected is not useful in object localisation, and pick and place applications. Ideally, the camera should be able to detect the tag, and hence the object, from at least 20cm away so that there is plenty of space for the arm to move into the required position. But the data from the 25mm tag is reasonable, and this size tag could potentially be used on medication packaging. It is suggested, however, that more testing is completed to verify the suitability of the tags in this application as discussed in the next section.

7.4 Future Work

As specified in the methodology, there were more testing stages planned. However, due to the lack of time and impacts made by COVID-19, these stages were not attained.

The third stage was planned to be an advancement in autonomy from the previous stage. The step up would have been from using the dialog box to writing a script that would control the arm's movements. Ideally, it would be controlled by the camera so that it wouldn't move before 100 seconds in each position. This would create a more robust, less error prone testing. The positions of the robotic arm would be pre-defined like with the dialog box but the positions would not change before the timer from the camera script had been completed. The other advancement to the testing was to use medication packaging as the objects of testing. The key variable that would have been examined was positioning of tag on the package to determine whether things like bottle neck curvature, which is generally concave, or busyness of labelling would affect the tag recognition. The hypothesis is that recognition and detection accuracy would not be affected by these things. This stage would have also inspected more closely the accuracy of the translation coordinates that the AprilTags provide.

The final stage endeavoured to pick and place medication packaging, using the tags to give the object position. This stage would have investigated connecting the arm and camera to communicate in real-time so that the camera could control where the arm moved to. At first, this stage would have sought to detect the object when in motion before moving to pick it up and move it to a specific location. The difficulties here would be knowing how to move the robot arm before the camera has detected the tag and then using the coordinates from the camera to accurately and precisely move the arm to the object. Much work would need to be done to convert the coordinates and ensure that the coordinates were repeatable as there was some inconsistency in the data as mentioned in Chapter 6. After that, the goal would have been to move multiple objects, one at a time, to a given location. The difficulty here would have been in programming the camera and robot to know which item to select first.

Both Stage 3 and Stage 4 could be completed as future work. It would assist in further understanding the likelihood of this system being used for a pharmacy application.

Further verification of the tags could be undertaken by doing a study of the affects of

pritning resolution. A few different printer types could be examined like the basic home printer, the larger office printer, and then laser printing to determine whether there is an affect on the accuracy of detection. It would be particularly helpful to determine this for smaller tags so that it could assist in the viability for the Pharmacy application.

Another study could be undertaken on the OpenMV camera, testing the different lens to determine how the resolution of the lens improves the quality and accuracy of detection whilst still being a low-cost system.

For other future tests, it would be suggested to use the dialog box in Stage 1 rather than the 'Path and Play' program. Whilst it is a useful program, it does not help in achieving control and repeatability in robot positioning. There is the ability with this program to record the locations so that it is then repeatable but it is suggested to simply use the dialog box to attain this control. For Stage 2, it is suggested that a script is written in DDE to create jobs that control the positioning. The camera and arm systems can still be controlled separately in this instance. It is also suggested to have a lux metre so that variances in light can be recorded. This will assist in seeing whether light does have an affect on the tag detection and accuracy.

References

Abbood, W. T., Abdullah, O. I. & Khalid, E. A. (2019), 'A real-time automated sorting of robotic vision system based on the interactive design approach', *International journal on interactive design and manufacturing* **14**(1), 201–209.

Agyeman, K. (2020), 'About', `https://openmv.io/pages/about`. [Online; accessed September-2020].

April Robotics Laboratory (2010), 'AprilTag', `https://april.eecs.umich.edu/software/apriltag.html`. [Online; accessed April-2020].

Cheein, F. A. A., Lopez, N., Soria, C. M., di Sciascio, F. A., Pereira, F. L. & Carelli, R. (2010), 'Slam algorithm applied to robotics assistance for navigation in unknown environments', *Journal of neuroengineering and rehabilitation* **7**(1), 10–10.

Cognex (n.d.), 'WHAT IS MACHINE VISION', `https://www.cognex.com/en-au/what-is/machine-vision/what-is-machine-vision`. [Online; accessed March-2020].

Colyer, S. L., Evans, M., Cosker, D. P. & Salo, A. I. T. (2018), 'A review of the evolution of vision-based motion analysis and the integration of advanced computer vision methods towards developing a markerless system', *Sports medicine - open* **4**(1), 1–15.

Corke, P. (2017), *Robotics, Vision and Control: Fundamental Algorithms in MATLAB® Second, Completely Revised, Extended and Updated Edition*, Springer International Publishing AG.

Davies, E. (2005), *Machine Vision: Theory Algorithms Practicalities*, Elsevier.

Fiala, M. (2005*a*), Artag, a fiducial marker system using digital techniques, Vol. 2, IEEE, pp. 590–596 vol. 2.

Fiala, M. (2005*b*), Comparing artag and artoolkit plus fiducial marker systems, IEEE, pp. 6 pp.–.

Haddington Dynamics (2020*a*), 'Dexter Development Environment', `https://www.hdrobotic.com/software`. [Online; accessed September-2020].

Haddington Dynamics (2020*b*), 'Dexter HDI', `https://www.hdrobotic.com/dexter`. [Online; accessed May-2020].

Haddington Dynamics (2020*c*), 'Getting Started', `https://www.hdrobotic.com/software`. [Online; accessed September-2020].

Haddington Dynamics (2020*d*), 'Introducing dexter hdi', `https://www.youtube.com/watch?v=t7lnbrI4B5Q&feature=emb_logo`. Accessed Sept. 28, 2020.

iAuditor (2019), 'Risk Assessment Template Checklist', `https://public-library.safetyculture.io/products/risk-assessment-template-fETAU`. [Online; accessed May-2020].

Koehrsen, W. (2018), 'Beyond Accuracy: Precision and Recall', `https://towardsdatascience.com/beyond-accuracy-precision-and-recall-3da06bea9f6c`. [Online; accessed May-2020].

Krogius, M., Haggenmiller, A. & Olson, E. (2019), Flexible layouts for fiducial tags, *in* '2019 IEEE/RSJ International Conference on Intelligent Robots and Systems (IROS)', pp. 1898–1903.

Mada Sanjaya, W. S., Anggraeni, D., Munawwaroh, M., Nurasyidiek, M. Y. S., Rahayu, D. S., Samsudin, A., Santika, I. P. & Palupi, E. K. (2018), Colored object sorting using 5 dof robot arm based artificial neural network (ann) method, Vol. 1090, pp. 12070–.

Newton, J. (2020), 'Dexter gateware', `https://github.com/HaddingtonDynamics/Dexter/wiki/Gateware`. Accessed Sept. 28, 2020.

Nissler, C., Buttner, S., Marton, Z.-C., Beckmann, L. & Thomasy, U. (2016), Evaluation and improvement of global pose estimation with multiple AprilTags for industrial manipulators, Vol. 2016-.

Olson, E. (2011), Apriltag: A robust and flexible visual fiducial system, IEEE, pp. 3400–3407.

OpenMV (2020*a*), `https://openmv.io/`. [Online; accessed May-2020].

OpenMV (2020*b*), 'Download', `https://openmv.io/pages/download`. [Online; accessed September-2020].

OpenMV (2020*c*), 'OpenMV Cam H7', `https://openmv.io/collections/products/products/openmv-cam-h7`. [Online; accessed September-2020].

Raut, N. (2018), 'What is Hamming Distance?', `https://www.tutorialspoint.com/what-is-hamming-distance`. [Online; accessed May-2020].

Rodriguez-Gonzalez, C. G., Herranz-Alonso, A., Escudero-Vilaplana, V., Ais-Larisgoitia, M. A., Iglesias-Peinado, I. & Sanjurjo-Saez, M. (2019), 'Robotic dispensing improves patient safety, inventory management, and staff satisfaction in an outpatient hospital pharmacy', *Journal of Evaluation in Clinical Practice* **25**(1), 28–35.

Sakhare, K. V., Tewari, T. & Vyas, V. (2019), 'Review of vehicle detection systems in advanced driver assistant systems', *Archives of computational methods in engineering* **27**(2), 591–610.

Sanchez, A. & Martinez, J. (2000), Robot-arm pick and place behavior programming system using visual perception, Vol. 4, IEEE, pp. 507–510 vol.4.

TensorFlow (2020), 'Pose Estimation', `https://www.tensorflow.org/lite/models/pose_estimation/overview`. [Online; accessed May-2020].

Wang, J. & Olson, E. (2016), Apriltag 2: Efficient and robust fiducial detection, *in* '2016 IEEE/RSJ International Conference on Intelligent Robots and Systems (IROS)', pp. 4193–4198.

Appendix A

Project Specification

ENG 4111/2 (or ENG8002) Research Project

Project Specification

For:	**Cassandra Moore**
Topic:	Sorting medication packaging using a multi-axis robotic arm, machine vision and artificial tagging
Major:	Mechatronic Engineering
Supervisors:	Dr Toby Low Ross Leamon, Downey Engineering Ben Leamon, DCISIV Technologies
Sponsorship:	Downey Engineering DCISIV Technologies
Enrolment:	ENG4111 - ONC S1 2020 ENG4112 - ONC S2 2020
Project Aim:	To investigate the functionality and usability of artifical tagging through rigourously testing the tags by experimenting with different sized, shaped, and textured objects to achieve a method of sorting a box of medication packages.

Program: Version 2, 7 May 2020

1. Research the background information on machine vision techniques and the theory of and types artifical tagging.
2. Examine the differences in tagging methods and choose most appropriate method for this project.
3. Design experiments for a plane surface testing the accuracy of the tags through using different sized, shaped, and textured objects.
4. Analyse and compare the detection accuracy for the different objects.
5. Design and test an experiment detecting medication packaging for a pharmaceutical application.
6. Sort the same objects from a plane surface using the robotic arm.
7. Sort different objects from a plane surface using the robotic arm.

   As time and resources permit:
8. Sort a box of medication packages using artificial tagging and the robotic arm.
9. Analyse accuracy and efficiency of the sorting and the plausibility of the application.

Appendix B

Risk Assessment

Table B.1: Risk Matrix to Identify Levels of Risk (iAuditor 2019)

Risk Matrix

Likelihood		Very Likely	Likely	Unlikely	Highly Unlikely
Consequences	Fatality	High	High	High	Medium
	Major Injuries	High	High	Medium	Medium
	Minor Injuries	High	Medium	Medium	Low
	Negligible Injuries	Medium	Medium	Low	Low

Table B.2: Risk Evalutation and Management

Task	Hazard	Risk Level	Reduction measures	Final risk
1D	Injury from tool use (saw) Injury from loose material (wood flying up)	Medium	1) Ensure wood is properly secured before cutting to size 2) Ensure hands are kept out of line from saw cutting direction 3) Wear PPE	Low
3A	Injury from robotic arm Low levels of wattage	Medium	1) Double check coordinates in program before running robot 2) Keep clear of robot whilst running 3) Have clear access to power source to disconnect in case of damage 4) Keep work area free of food and drink	Low
3B	Injury from robotic arm Low levels of wattage	Medium	1) Double check coordinates in program before running robot 2) Keep clear of robot whilst running 3) Have clear access to power source to disconnect in case of damage 4) Keep work area free of food and drink	Low
3C	Injury from robotic arm Low levels of wattage	Medium	1) Double check coordinates in program before running robot 2) Keep clear of robot whilst running 3) Have clear access to power source to disconnect in case of damage 4) Keep work area free of food and drink	Low
3D	Injury from robotic arm Low levels of wattage	Medium	1) Double check coordinates in program before running robot 2) Keep clear of robot whilst running 3) Have clear access to power source to disconnect in case of damage 4) Keep work area free of food and drink	Low

Appendix C

Excerpts of data

Tag Family	Tag ID	Rotation	Tx	Ty	Tz	Rx	Ry	Rz	Clock
Tag Family TAG36H11	Tag ID 0	rotation 4.268902 (degrees)	Tx: 1.117145	Ty 0.018661	Tz -7.308357	Rx 179.427671	Ry 1.193642	Rz 4.268902	13.88889
Tag Family TAG36H11	Tag ID 0	rotation 4.444316 (degrees)	Tx: 1.116425	Ty 0.016555	Tz -7.317622	Rx 180.150118	Ry 0.176409	Rz 4.444316	15.38462
Tag Family TAG36H11	Tag ID 0	rotation 4.304762 (degrees)	Tx: 1.115658	Ty 0.020070	Tz -7.314345	Rx 179.165449	Ry 0.179445	Rz 4.304762	15.70681
Tag Family TAG36H11	Tag ID 0	rotation 4.210965 (degrees)	Tx: 1.119393	Ty 0.019046	Tz -7.301265	Rx 179.582348	Ry 1.576151	Rz 4.210965	15.26718
Tag Family TAG36H11	Tag ID 0	rotation 4.363432 (degrees)	Tx: 1.118234	Ty 0.016993	Tz -7.308860	Rx 179.972959	Ry 1.003849	Rz 4.363432	15.4321
Tag Family TAG36H11	Tag ID 0	rotation 4.437767 (degrees)	Tx: 1.116938	Ty 0.016578	Tz -7.318756	Rx 180.220547	Ry 359.842134	Rz 4.437767	14.52784
Tag Family TAG36H11	Tag ID 0	rotation 4.190148 (degrees)	Tx: 1.119833	Ty 0.019705	Tz -7.300487	Rx 179.162765	Ry 1.565163	Rz 4.190148	14.67505
Tag Family TAG36H11	Tag ID 0	rotation 4.401927 (degrees)	Tx: 1.118956	Ty 0.016810	Tz -7.301490	Rx 180.019388	Ry 1.514466	Rz 4.401927	14.8423
Tag Family TAG36H11	Tag ID 0	rotation 4.517715 (degrees)	Tx: 1.120362	Ty 0.015339	Tz -7.312765	Rx 180.081387	Ry 0.114425	Rz 4.517715	15.05017
Tag Family TAG36H11	Tag ID 0	rotation 4.477428 (degrees)	Tx: 1.121446	Ty 0.016362	Tz -7.323379	Rx 179.955292	Ry 359.934402	Rz 4.477428	15.45595
Tag Family TAG36H11	Tag ID 0	rotation 4.355206 (degrees)	Tx: 1.120410	Ty 0.016940	Tz -7.307423	Rx 179.944839	Ry 1.033316	Rz 4.355206	15.58074
Tag Family TAG36H11	Tag ID 0	rotation 4.336468 (degrees)	Tx: 1.120837	Ty 0.017263	Tz -7.308296	Rx 179.695368	Ry 1.034252	Rz 4.336468	15.40437
Tag Family TAG36H11	Tag ID 0	rotation 4.319039 (degrees)	Tx: 1.119908	Ty 0.017911	Tz -7.299761	Rx 179.156852	Ry 1.467534	Rz 4.319039	15.60624
Tag Family TAG36H11	Tag ID 0	rotation 4.380266 (degrees)	Tx: 1.120866	Ty 0.015486	Tz -7.302121	Rx 179.906583	Ry 1.461075	Rz 4.380266	15.64246
Tag Family TAG36H11	Tag ID 0	rotation 4.315925 (degrees)	Tx: 1.120516	Ty 0.018355	Tz -7.306441	Rx 178.874445	Ry 1.142145	Rz 4.315925	15.49587
Tag Family TAG36H11	Tag ID 0	rotation 4.373402 (degrees)	Tx: 1.122678	Ty 0.016590	Tz -7.316772	Rx 179.133725	Ry 0.662686	Rz 4.373402	15.68627
Tag Family TAG36H11	Tag ID 0	rotation 4.398996 (degrees)	Tx: 1.122036	Ty 0.016082	Tz -7.314815	Rx 179.386101	Ry 0.636704	Rz 4.398996	15.78459
Tag Family TAG36H11	Tag ID 0	rotation 4.354931 (degrees)	Tx: 1.122434	Ty 0.017090	Tz -7.308479	Rx 179.277525	Ry 1.272868	Rz 4.354931	15.625
Tag Family TAG36H11	Tag ID 0	rotation 4.357836 (degrees)	Tx: 1.122284	Ty 0.014495	Tz -7.307508	Rx 180.156622	Ry 1.207599	Rz 4.357836	15.58655
Tag Family TAG36H11	Tag ID 0	rotation 4.325732 (degrees)	Tx: 1.120344	Ty 0.017089	Tz -7.305016	Rx 179.289222	Ry 1.383937	Rz 4.325732	15.67398
Tag Family TAG36H11	Tag ID 0	rotation 4.334869 (degrees)	Tx: 1.120823	Ty 0.017240	Tz -7.307828	Rx 178.970361	Ry 1.145123	Rz 4.334869	15.625
Tag Family TAG36H11	Tag ID 0	rotation 4.284037 (degrees)	Tx: 1.120396	Ty 0.017281	Tz -7.306621	Rx 178.764153	Ry 1.182310	Rz 4.284037	15.61391
Tag Family TAG36H11	Tag ID 0	rotation 4.381705 (degrees)	Tx: 1.120478	Ty 0.016376	Tz -7.314428	Rx 179.050112	Ry 0.647131	Rz 4.381705	15.34356
Tag Family TAG36H11	Tag ID 0	rotation 4.377205 (degrees)	Tx: 1.121984	Ty 0.015754	Tz -7.315218	Rx 179.114604	Ry 0.696099	Rz 4.377205	15.27689
Tag Family TAG36H11	Tag ID 0	rotation 4.378701 (degrees)	Tx: 1.121641	Ty 0.015589	Tz -7.313752	Rx 179.228601	Ry 0.788397	Rz 4.378701	15.006
Tag Family TAG36H11	Tag ID 0	rotation 4.370171 (degrees)	Tx: 1.122348	Ty 0.014752	Tz -7.320684	Rx 179.150333	Ry 0.382556	Rz 4.370171	14.96834

1 2 3 4 5 6 7 8 9 10

Figure C.1: Test 2, Trial 1

C.1 Introduction to this Appendix

In this Appendix, some excerpts of data are included. All the data has not been included due to the size and number of data files that were collected during this project.

C.2 Potential Discrepancies in the Position Estimation of Pose Estimation

In Chapter 6, it was mentioned that there were some discrepancies in the Tx and Ty values within one test. This was particularly found during Stage 1 in using 'Path and Play'. Ten excerpts, from one test, are included here to demonstrate how the Tx and Ty values (columns four and five respectively) varied across trials even though the camera was not moved during these trials.

It was identified that there was better control within tests in Stage 2 when Dexter HDI was moved to specific locations.

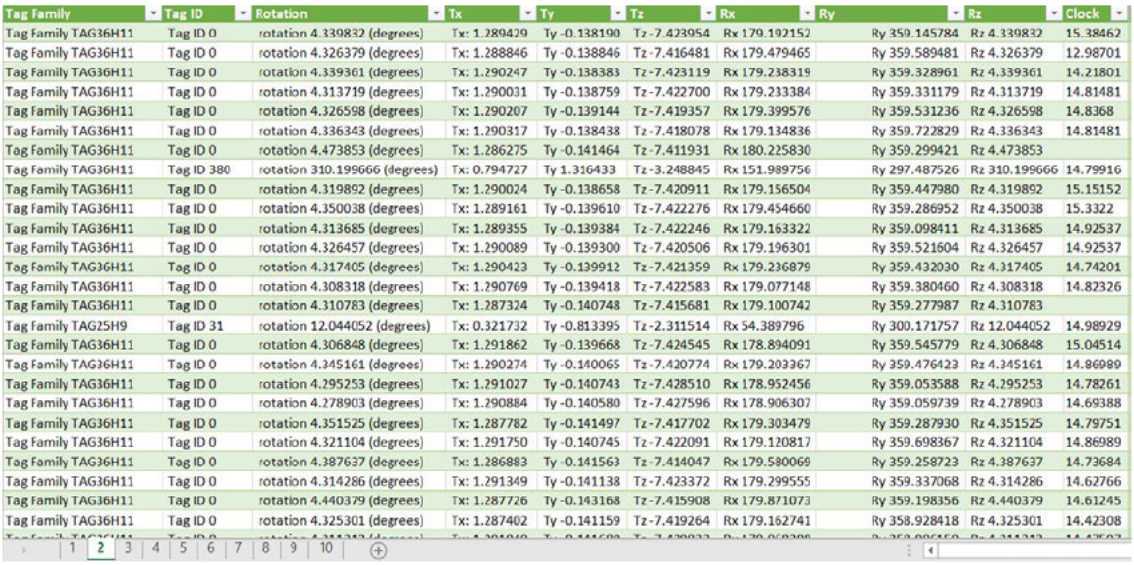

Tag Family	Tag ID	Rotation	Tx	Ty	Tz	Rx	Ry	Rz	Clock
Tag Family TAG36H11	Tag ID 0	rotation 4.339832 (degrees)	Tx: 1.289429	Ty -0.138190	Tz -7.423954	Rx 179.192152	Ry 359.145784	Rz 4.339832	15.38462
Tag Family TAG36H11	Tag ID 0	rotation 4.326379 (degrees)	Tx: 1.288846	Ty -0.138846	Tz -7.416481	Rx 179.479465	Ry 359.589481	Rz 4.326379	12.98701
Tag Family TAG36H11	Tag ID 0	rotation 4.339361 (degrees)	Tx: 1.290247	Ty -0.138383	Tz -7.423119	Rx 179.238319	Ry 359.328961	Rz 4.339361	14.21801
Tag Family TAG36H11	Tag ID 0	rotation 4.313719 (degrees)	Tx: 1.290031	Ty -0.138759	Tz -7.422700	Rx 179.233384	Ry 359.331179	Rz 4.313719	14.81481
Tag Family TAG36H11	Tag ID 0	rotation 4.326598 (degrees)	Tx: 1.290207	Ty -0.139144	Tz -7.419357	Rx 179.399576	Ry 359.531236	Rz 4.326598	14.8368
Tag Family TAG36H11	Tag ID 0	rotation 4.336343 (degrees)	Tx: 1.290317	Ty -0.138438	Tz -7.418078	Rx 179.134836	Ry 359.722829	Rz 4.336343	14.81481
Tag Family TAG36H11	Tag ID 0	rotation 4.473853 (degrees)	Tx: 1.286275	Ty -0.141464	Tz -7.411931	Rx 180.225830	Ry 359.299421	Rz 4.473853	
Tag Family TAG36H11	Tag ID 380	rotation 310.199666 (degrees)	Tx: 0.794727	Ty 1.316433	Tz -3.248845	Rx 151.989756	Ry 297.487526	Rz 310.199666	14.79916
Tag Family TAG36H11	Tag ID 0	rotation 4.319892 (degrees)	Tx: 1.290024	Ty -0.138658	Tz -7.420911	Rx 179.156504	Ry 359.447980	Rz 4.319892	15.15152
Tag Family TAG36H11	Tag ID 0	rotation 4.350038 (degrees)	Tx: 1.289161	Ty -0.139610	Tz -7.422276	Rx 179.454660	Ry 359.286952	Rz 4.350038	15.3322
Tag Family TAG36H11	Tag ID 0	rotation 4.313685 (degrees)	Tx: 1.289355	Ty -0.139384	Tz -7.422246	Rx 179.163322	Ry 359.098411	Rz 4.313685	14.92537
Tag Family TAG36H11	Tag ID 0	rotation 4.326457 (degrees)	Tx: 1.290089	Ty -0.139300	Tz -7.420506	Rx 179.196301	Ry 359.521604	Rz 4.326457	14.92537
Tag Family TAG36H11	Tag ID 0	rotation 4.317405 (degrees)	Tx: 1.290423	Ty -0.139912	Tz -7.421359	Rx 179.236879	Ry 359.432030	Rz 4.317405	14.74201
Tag Family TAG36H11	Tag ID 0	rotation 4.308318 (degrees)	Tx: 1.290769	Ty -0.139418	Tz -7.422583	Rx 179.077148	Ry 359.380460	Rz 4.308318	14.82326
Tag Family TAG36H11	Tag ID 0	rotation 4.310783 (degrees)	Tx: 1.287324	Ty -0.140748	Tz -7.415681	Rx 179.100742	Ry 359.277987	Rz 4.310783	
Tag Family TAG25H9	Tag ID 31	rotation 12.044052 (degrees)	Tx: 0.321732	Ty -0.813395	Tz -2.311514	Rx 54.389796	Ry 300.171757	Rz 12.044052	14.98929
Tag Family TAG36H11	Tag ID 0	rotation 4.306848 (degrees)	Tx: 1.291862	Ty -0.139668	Tz -7.424545	Rx 178.894091	Ry 359.545779	Rz 4.306848	15.04514
Tag Family TAG36H11	Tag ID 0	rotation 4.345161 (degrees)	Tx: 1.290274	Ty -0.140065	Tz -7.420774	Rx 179.203367	Ry 359.476423	Rz 4.345161	14.86989
Tag Family TAG36H11	Tag ID 0	rotation 4.295253 (degrees)	Tx: 1.291027	Ty -0.140743	Tz -7.428510	Rx 178.952456	Ry 359.053588	Rz 4.295253	14.78261
Tag Family TAG36H11	Tag ID 0	rotation 4.278903 (degrees)	Tx: 1.290884	Ty -0.140580	Tz -7.427596	Rx 178.906307	Ry 359.059739	Rz 4.278903	14.69388
Tag Family TAG36H11	Tag ID 0	rotation 4.351525 (degrees)	Tx: 1.287782	Ty -0.141497	Tz -7.417702	Rx 179.303479	Ry 359.287930	Rz 4.351525	14.79751
Tag Family TAG36H11	Tag ID 0	rotation 4.321104 (degrees)	Tx: 1.291750	Ty -0.140745	Tz -7.422091	Rx 179.120817	Ry 359.698367	Rz 4.321104	14.86989
Tag Family TAG36H11	Tag ID 0	rotation 4.387637 (degrees)	Tx: 1.286883	Ty -0.141563	Tz -7.414047	Rx 179.580069	Ry 359.258723	Rz 4.387637	14.73684
Tag Family TAG36H11	Tag ID 0	rotation 4.314286 (degrees)	Tx: 1.291349	Ty -0.141138	Tz -7.423372	Rx 179.299555	Ry 359.337068	Rz 4.314286	14.62766
Tag Family TAG36H11	Tag ID 0	rotation 4.440379 (degrees)	Tx: 1.287726	Ty -0.143168	Tz -7.415908	Rx 179.871073	Ry 359.198356	Rz 4.440379	14.61245
Tag Family TAG36H11	Tag ID 0	rotation 4.325301 (degrees)	Tx: 1.287402	Ty -0.141159	Tz -7.419264	Rx 179.162741	Ry 358.928418	Rz 4.325301	14.42308

Figure C.2: Test 2, Trial 2

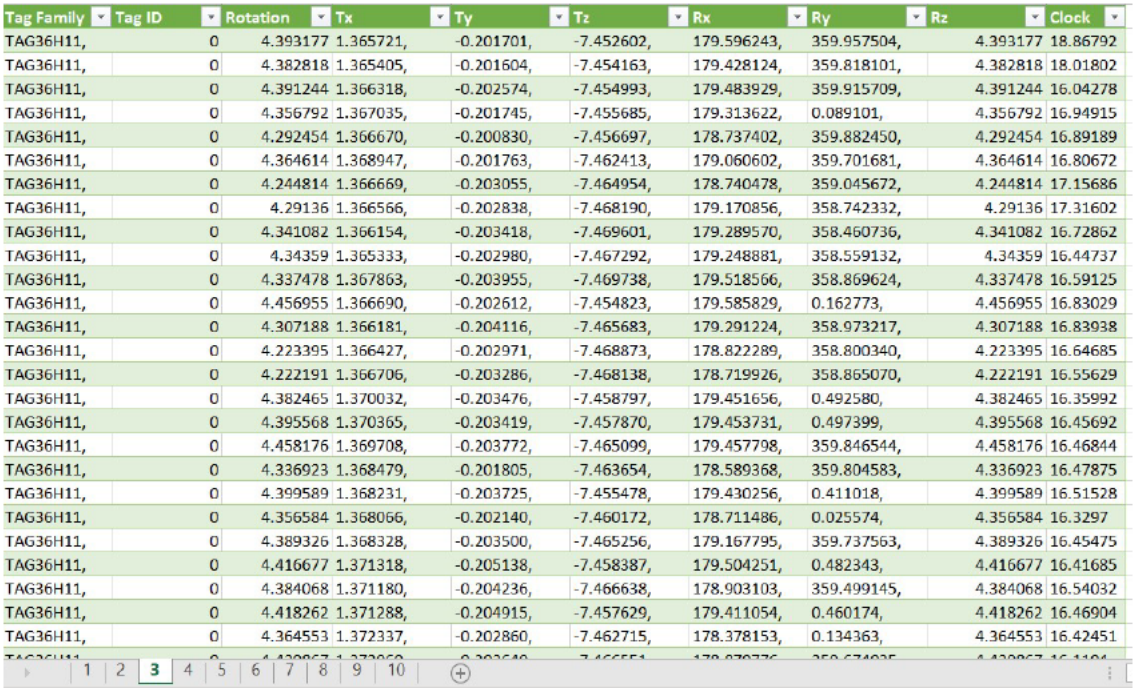

Tag Family	Tag ID	Rotation	Tx	Ty	Tz	Rx	Ry	Rz	Clock
TAG36H11,	0	4.393177	1.365721,	-0.201701,	-7.452602,	179.596243,	359.957504,	4.393177	18.86792
TAG36H11,	0	4.382818	1.365405,	-0.201604,	-7.454163,	179.428124,	359.818101,	4.382818	18.01802
TAG36H11,	0	4.391244	1.366318,	-0.202574,	-7.454993,	179.483929,	359.915709,	4.391244	16.04278
TAG36H11,	0	4.356792	1.367035,	-0.201745,	-7.455685,	179.313622,	0.089101,	4.356792	16.94915
TAG36H11,	0	4.292454	1.366670,	-0.200830,	-7.456697,	178.737402,	359.882450,	4.292454	16.89189
TAG36H11,	0	4.364614	1.368947,	-0.201763,	-7.462413,	179.060602,	359.701681,	4.364614	16.80672
TAG36H11,	0	4.244814	1.366669,	-0.203055,	-7.464954,	178.740478,	359.045672,	4.244814	17.15686
TAG36H11,	0	4.29136	1.366566,	-0.202838,	-7.468190,	179.170856,	358.742332,	4.29136	17.31602
TAG36H11,	0	4.341082	1.366154,	-0.203418,	-7.469601,	179.289570,	358.460736,	4.341082	16.72862
TAG36H11,	0	4.34359	1.365333,	-0.202980,	-7.467292,	179.248881,	358.559132,	4.34359	16.44737
TAG36H11,	0	4.337478	1.367863,	-0.203955,	-7.469738,	179.518566,	358.869624,	4.337478	16.59125
TAG36H11,	0	4.456955	1.366690,	-0.202612,	-7.454823,	179.585829,	0.162773,	4.456955	16.83029
TAG36H11,	0	4.307188	1.366181,	-0.204116,	-7.465683,	179.291224,	358.973217,	4.307188	16.83938
TAG36H11,	0	4.223395	1.366427,	-0.202971,	-7.468873,	178.822289,	358.800340,	4.223395	16.64685
TAG36H11,	0	4.222191	1.366706,	-0.203286,	-7.468138,	178.719926,	358.865070,	4.222191	16.55629
TAG36H11,	0	4.382465	1.370032,	-0.203476,	-7.458797,	179.451656,	0.492580,	4.382465	16.35992
TAG36H11,	0	4.395568	1.370365,	-0.203419,	-7.457870,	179.453731,	0.497399,	4.395568	16.45692
TAG36H11,	0	4.458176	1.369708,	-0.203772,	-7.465099,	179.457798,	359.846544,	4.458176	16.46844
TAG36H11,	0	4.336923	1.368479,	-0.201805,	-7.463654,	178.589368,	359.804583,	4.336923	16.47875
TAG36H11,	0	4.399589	1.368231,	-0.203725,	-7.455478,	179.430256,	0.411018,	4.399589	16.51528
TAG36H11,	0	4.356584	1.368066,	-0.202140,	-7.460172,	178.711486,	0.025574,	4.356584	16.3297
TAG36H11,	0	4.389326	1.368328,	-0.203500,	-7.465256,	179.167795,	359.737563,	4.389326	16.45475
TAG36H11,	0	4.416677	1.371318,	-0.205138,	-7.458387,	179.504251,	0.482343,	4.416677	16.41685
TAG36H11,	0	4.384068	1.371180,	-0.204236,	-7.466638,	178.903103,	359.499145,	4.384068	16.54032
TAG36H11,	0	4.418262	1.371288,	-0.204915,	-7.457629,	179.411054,	0.460174,	4.418262	16.46904
TAG36H11,	0	4.364553	1.372337,	-0.202860,	-7.462715,	178.378153,	0.134363,	4.364553	16.42451

Figure C.3: Test 2, Trial 3

Tag Family	Tag ID	Rotation	Tx	Column1.13	Column1.15	Rx	Ry	Rz	Clock
TAG36H11,	0	4.437203	1.439293,	-0.262689,	-7.474101,	179.874697,	0.886380,	4.437203	15.15152
TAG36H11,	0	4.413481	1.439398,	-0.264440,	-7.479803,	180.055027,	0.565586,	4.413481	16.94915
TAG36H11,	0	4.49182	1.439507,	-0.264154,	-7.473589,	180.212002,	0.821078,	4.49182	16.57459
TAG36H11,	0	4.399468	1.439447,	-0.263307,	-7.483929,	179.592180,	0.450509,	4.399468	
TAG25H9,	21	274.402666	1.439447,	-0.263307,	-7.483929,	179.549479,	359.592175,	274.402666	16.32653
TAG36H11,	0	4.415631	1.438690,	-0.263864,	-7.483019,	179.546795,	0.294188,	4.415631	
TAG25H9,	31	90.448837	0.820283,	-0.298346,	-3.155554,	185.576324,	304.583549,	90.448837	16.18123
TAG36H11,	0	4.556484	1.441120,	-0.265317,	-7.487433,	180.254765,	0.495049,	4.556484	15.58442
TAG36H11,	0	4.497065	1.440666,	-0.264507,	-7.481482,	180.180025,	0.499442,	4.497065	15.90909
TAG36H11,	0	4.411496	1.439459,	-0.264868,	-7.482535,	179.735994,	0.355611,	4.411496	16.26016
TAG36H11,	0	4.4407	1.439659,	-0.265123,	-7.483710,	179.935646,	0.256629,	4.4407	16.15799
TAG36H11,	0	4.443145	1.439830,	-0.265217,	-7.483843,	179.827499,	0.201433,	4.443145	16.26016
TAG36H11,	0	4.419489	1.439513,	-0.264947,	-7.485664,	179.547405,	0.112649,	4.419489	15.85014
TAG36H11,	0	4.442295	1.440334,	-0.264918,	-7.484428,	179.700937,	0.172063,	4.442295	15.72739
TAG36H11,	0	4.484426	1.441402,	-0.265765,	-7.488916,	179.777203,	359.966731,	4.484426	15.70048
TAG36H11,	0	4.442133	1.440649,	-0.263743,	-7.490008,	179.016471,	359.898543,	4.442133	15.65996
TAG36H11,	0	4.416833	1.441337,	-0.265262,	-7.484157,	179.685211,	0.378752,	4.416833	15.69038
TAG36H11,	0	4.466866	1.442575,	-0.263603,	-7.487544,	178.931475,	0.377527,	4.466866	15.59454
TAG36H11,	0	4.476984	1.442664,	-0.263622,	-7.486624,	179.003048,	0.472847,	4.476984	15.68266
TAG36H11,	0	4.472619	1.443365,	-0.263060,	-7.489918,	178.759766,	0.315872,	4.472619	15.69311
TAG36H11,	0	4.400154	1.442196,	-0.264294,	-7.485074,	179.013577,	0.436985,	4.400154	15.68951
TAG36H11,	0	4.400338	1.442305,	-0.263885,	-7.486253,	178.986740,	0.414578,	4.400338	15.74803
TAG36H11,	0	4.423917	1.442539,	-0.265444,	-7.483345,	179.650440,	0.630876,	4.423917	15.74213
TAG36H11,	0	4.485178	1.442411,	-0.266558,	-7.490213,	179.677477,	359.925723,	4.485178	15.75931
TAG36H11,	0	4.555899	1.444876,	-0.266846,	-7.486424,	180.143147,	0.330477,	4.555899	15.81843
TAG36H11,	0	4.596902	1.449151,	-0.268002,	-7.496919,	180.376673,	0.297647,	4.596902	15.89404

1 | 2 | 3 | 4 | 5 | 6 | 7 | 8 | 9 | 10

Figure C.4: Test 2, Trial 4

Tag Family	Tag ID	Rotation	Tx	Ty	Tz	Rx	Ry	Rz	Clock
Tag Family TAG36H11	Tag ID 0	rotation 4.544286 (degrees)	Tx: 1.520504	Ty -0.341560	Tz -7.534569	Rx 180.412903	Ry 0.693566	Rz 4.544286	16.39344
Tag Family TAG36H11	Tag ID 0	rotation 4.518853 (degrees)	Tx: 1.520566	Ty -0.341790	Tz -7.535885	Rx 179.874015	Ry 0.630597	Rz 4.518853	14.92537
Tag Family TAG36H11	Tag ID 0	rotation 4.605337 (degrees)	Tx: 1.518913	Ty -0.344676	Tz -7.531726	Rx 181.242924	Ry 0.575829	Rz 4.605337	14.63415
Tag Family TAG36H11	Tag ID 0	rotation 4.593910 (degrees)	Tx: 1.519969	Ty -0.346558	Tz -7.537349	Rx 181.091738	Ry 0.382822	Rz 4.593910	13.98601
Tag Family TAG36H11	Tag ID 0	rotation 4.608939 (degrees)	Tx: 1.519416	Ty -0.344767	Tz -7.536091	Rx 181.067228	Ry 0.519741	Rz 4.608939	14.28571
Tag Family TAG36H11	Tag ID 0	rotation 4.594098 (degrees)	Tx: 1.520642	Ty -0.345509	Tz -7.536767	Rx 180.525293	Ry 0.512706	Rz 4.594098	14.66993
Tag Family TAG36H11	Tag ID 0	rotation 4.582942 (degrees)	Tx: 1.520477	Ty -0.345747	Tz -7.536989	Rx 180.843496	Ry 0.629946	Rz 4.582942	15.15152
Tag Family TAG36H11	Tag ID 0	rotation 4.603646 (degrees)	Tx: 1.519370	Ty -0.345735	Tz -7.536088	Rx 180.950928	Ry 0.477704	Rz 4.603646	15.12287
Tag Family TAG36H11	Tag ID 0	rotation 4.623603 (degrees)	Tx: 1.519433	Ty -0.345556	Tz -7.526477	Rx 181.100101	Ry 1.156312	Rz 4.623603	14.92537
Tag Family TAG36H11	Tag ID 0	rotation 4.606201 (degrees)	Tx: 1.519604	Ty -0.346751	Tz -7.535817	Rx 181.284094	Ry 0.453694	Rz 4.606201	14.94768
Tag Family TAG36H11	Tag ID 0	rotation 4.546309 (degrees)	Tx: 1.520051	Ty -0.344504	Tz -7.535540	Rx 180.175209	Ry 0.626112	Rz 4.546309	14.70588
Tag Family TAG36H11	Tag ID 0	rotation 4.575081 (degrees)	Tx: 1.520506	Ty -0.345951	Tz -7.533996	Rx 180.630407	Ry 0.610071	Rz 4.575081	14.65201
Tag Family TAG36H11	Tag ID 0	rotation 4.642325 (degrees)	Tx: 1.520689	Ty -0.345968	Tz -7.531251	Rx 181.146221	Ry 1.163592	Rz 4.642325	14.92537
Tag Family TAG36H11	Tag ID 0	rotation 4.571250 (degrees)	Tx: 1.521930	Ty -0.344757	Tz -7.539018	Rx 180.073500	Ry 0.581541	Rz 4.571250	14.87779
Tag Family TAG36H11	Tag ID 0	rotation 4.582825 (degrees)	Tx: 1.522306	Ty -0.346494	Tz -7.536735	Rx 180.574980	Ry 0.700776	Rz 4.582825	15.01502
Tag Family TAG36H11	Tag ID 0	rotation 4.559445 (degrees)	Tx: 1.521172	Ty -0.344916	Tz -7.540018	Rx 180.254326	Ry 0.283355	Rz 4.559445	14.82854
Tag Family TAG36H11	Tag ID 0	rotation 4.642957 (degrees)	Tx: 1.521508	Ty -0.345185	Tz -7.543427	Rx 180.281878	Ry 359.688735	Rz 4.642957	14.83421
Tag Family TAG36H11	Tag ID 0	rotation 4.593767 (degrees)	Tx: 1.522075	Ty -0.346894	Tz -7.539989	Rx 180.555010	Ry 0.464695	Rz 4.593767	14.96259
Tag Family TAG36H11	Tag ID 0	rotation 4.576793 (degrees)	Tx: 1.521780	Ty -0.346613	Tz -7.534852	Rx 180.561495	Ry 0.568123	Rz 4.576793	14.92537
Tag Family TAG36H11	Tag ID 0	rotation 4.594383 (degrees)	Tx: 1.516080	Ty -0.344638	Tz -7.532376	Rx 180.296574	Ry 0.128791	Rz 4.594383	15.17451
Tag Family TAG36H11	Tag ID 0	rotation 4.538933 (degrees)	Tx: 1.516738	Ty -0.344739	Tz -7.531794	Rx 179.785275	Ry 0.261735	Rz 4.538933	15.10791
Tag Family TAG36H11	Tag ID 0	rotation 4.464671 (degrees)	Tx: 1.518113	Ty -0.344830	Tz -7.531875	Rx 179.681835	Ry 0.606710	Rz 4.464671	15.21439
Tag Family TAG36H11	Tag ID 0	rotation 4.553576 (degrees)	Tx: 1.518416	Ty -0.346543	Tz -7.540288	Rx 179.855680	Ry 359.627438	Rz 4.553576	15.24188
Tag Family TAG36H11	Tag ID 0	rotation 4.496660 (degrees)	Tx: 1.517918	Ty -0.345585	Tz -7.528164	Rx 180.097694	Ry 0.820442	Rz 4.496660	15.21877
Tag Family TAG36H11	Tag ID 0	rotation 4.515082 (degrees)	Tx: 1.519878	Ty -0.343369	Tz -7.538383	Rx 179.164400	Ry 0.062053	Rz 4.515082	15.14234
Tag Family TAG36H11	Tag ID 0	rotation 4.619955 (degrees)	Tx: 1.519789	Ty -0.345213	Tz -7.533124	Rx 180.373430	Ry 0.097505	Rz 4.619955	15.16035

1 | 2 | 3 | 4 | 5 | 6 | 7 | 8 | 9 | 10

Figure C.5: Test 2, Trial 5

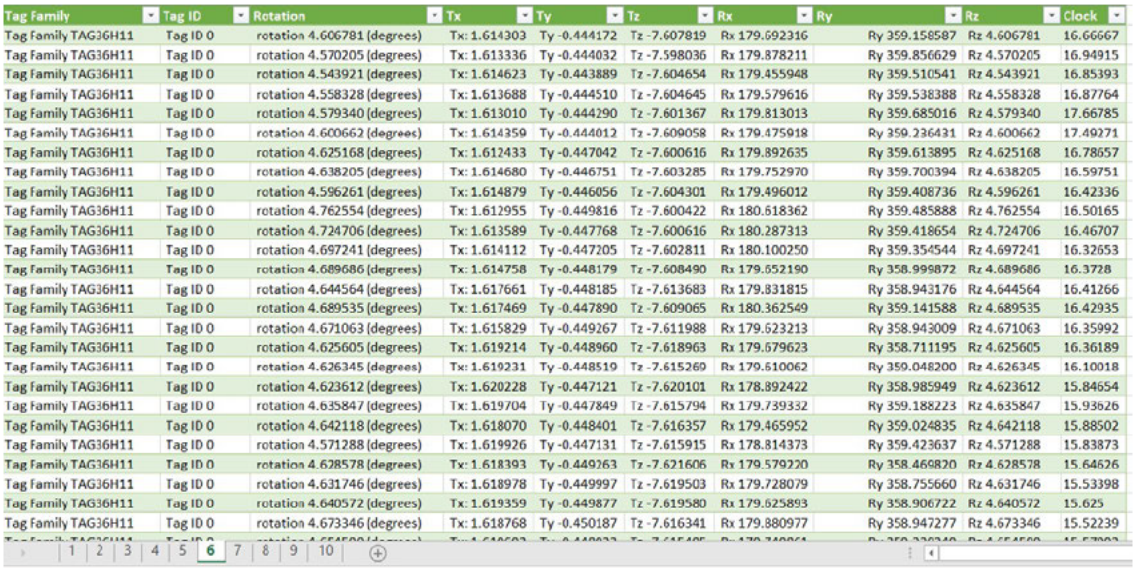

Tag Family	Tag ID	Rotation	Tx	Ty	Tz	Rx	Ry	Rz	Clock
Tag Family TAG36H11	Tag ID 0	rotation 4.606781 (degrees)	Tx: 1.614303	Ty -0.444172	Tz -7.607819	Rx 179.692316	Ry 359.158587	Rz 4.606781	16.66667
Tag Family TAG36H11	Tag ID 0	rotation 4.570205 (degrees)	Tx: 1.613336	Ty -0.444032	Tz -7.598036	Rx 179.878211	Ry 359.856629	Rz 4.570205	16.94915
Tag Family TAG36H11	Tag ID 0	rotation 4.543921 (degrees)	Tx: 1.614623	Ty -0.443889	Tz -7.604654	Rx 179.455948	Ry 359.510541	Rz 4.543921	16.85393
Tag Family TAG36H11	Tag ID 0	rotation 4.558328 (degrees)	Tx: 1.613688	Ty -0.444510	Tz -7.604645	Rx 179.579616	Ry 359.538388	Rz 4.558328	16.87764
Tag Family TAG36H11	Tag ID 0	rotation 4.579340 (degrees)	Tx: 1.613010	Ty -0.444290	Tz -7.601367	Rx 179.813013	Ry 359.685016	Rz 4.579340	17.66785
Tag Family TAG36H11	Tag ID 0	rotation 4.600662 (degrees)	Tx: 1.614359	Ty -0.444012	Tz -7.609058	Rx 179.475918	Ry 359.236431	Rz 4.600662	17.49271
Tag Family TAG36H11	Tag ID 0	rotation 4.625168 (degrees)	Tx: 1.612433	Ty -0.447042	Tz -7.600616	Rx 179.892635	Ry 359.613895	Rz 4.625168	16.78657
Tag Family TAG36H11	Tag ID 0	rotation 4.638205 (degrees)	Tx: 1.614680	Ty -0.446751	Tz -7.603285	Rx 179.752970	Ry 359.700394	Rz 4.638205	16.59751
Tag Family TAG36H11	Tag ID 0	rotation 4.596261 (degrees)	Tx: 1.614879	Ty -0.446056	Tz -7.604301	Rx 179.496012	Ry 359.408736	Rz 4.596261	16.42336
Tag Family TAG36H11	Tag ID 0	rotation 4.762554 (degrees)	Tx: 1.612955	Ty -0.449816	Tz -7.600422	Rx 180.618362	Ry 359.485888	Rz 4.762554	16.50165
Tag Family TAG36H11	Tag ID 0	rotation 4.724706 (degrees)	Tx: 1.613589	Ty -0.447768	Tz -7.600616	Rx 180.287313	Ry 359.418654	Rz 4.724706	16.46707
Tag Family TAG36H11	Tag ID 0	rotation 4.697241 (degrees)	Tx: 1.614112	Ty -0.447205	Tz -7.602811	Rx 180.100250	Ry 359.354544	Rz 4.697241	16.32653
Tag Family TAG36H11	Tag ID 0	rotation 4.689686 (degrees)	Tx: 1.614758	Ty -0.448179	Tz -7.608490	Rx 179.652190	Ry 358.999872	Rz 4.689686	16.3728
Tag Family TAG36H11	Tag ID 0	rotation 4.644564 (degrees)	Tx: 1.617661	Ty -0.448185	Tz -7.613683	Rx 179.831815	Ry 358.943176	Rz 4.644564	16.41266
Tag Family TAG36H11	Tag ID 0	rotation 4.689535 (degrees)	Tx: 1.617469	Ty -0.447890	Tz -7.609065	Rx 180.362549	Ry 359.141588	Rz 4.689535	16.42935
Tag Family TAG36H11	Tag ID 0	rotation 4.671063 (degrees)	Tx: 1.615829	Ty -0.449267	Tz -7.611988	Rx 179.523213	Ry 358.943009	Rz 4.671063	16.35992
Tag Family TAG36H11	Tag ID 0	rotation 4.625605 (degrees)	Tx: 1.619214	Ty -0.448960	Tz -7.618963	Rx 179.679623	Ry 358.711195	Rz 4.625605	16.36189
Tag Family TAG36H11	Tag ID 0	rotation 4.626345 (degrees)	Tx: 1.619231	Ty -0.448510	Tz -7.615269	Rx 179.610062	Ry 359.048200	Rz 4.626345	16.10018
Tag Family TAG36H11	Tag ID 0	rotation 4.623612 (degrees)	Tx: 1.620228	Ty -0.447121	Tz -7.620101	Rx 178.892422	Ry 358.985949	Rz 4.623612	15.84654
Tag Family TAG36H11	Tag ID 0	rotation 4.635847 (degrees)	Tx: 1.619704	Ty -0.447849	Tz -7.615794	Rx 179.739332	Ry 359.188223	Rz 4.635847	15.93626
Tag Family TAG36H11	Tag ID 0	rotation 4.642118 (degrees)	Tx: 1.618070	Ty -0.448401	Tz -7.616357	Rx 179.465952	Ry 359.024835	Rz 4.642118	15.88502
Tag Family TAG36H11	Tag ID 0	rotation 4.571288 (degrees)	Tx: 1.619926	Ty -0.447131	Tz -7.615915	Rx 178.814373	Ry 359.423637	Rz 4.571288	15.83873
Tag Family TAG36H11	Tag ID 0	rotation 4.628578 (degrees)	Tx: 1.618393	Ty -0.449263	Tz -7.621606	Rx 179.579220	Ry 358.469820	Rz 4.628578	15.64626
Tag Family TAG36H11	Tag ID 0	rotation 4.631746 (degrees)	Tx: 1.618978	Ty -0.449997	Tz -7.619503	Rx 179.728079	Ry 358.755660	Rz 4.631746	15.53398
Tag Family TAG36H11	Tag ID 0	rotation 4.640572 (degrees)	Tx: 1.619359	Ty -0.449877	Tz -7.619580	Rx 179.625893	Ry 358.906722	Rz 4.640572	15.625
Tag Family TAG36H11	Tag ID 0	rotation 4.673346 (degrees)	Tx: 1.618768	Ty -0.450187	Tz -7.616341	Rx 179.880977	Ry 358.947277	Rz 4.673346	15.52239

1 2 3 4 5 6 7 8 9 10

Figure C.6: Test 2, Trial 6

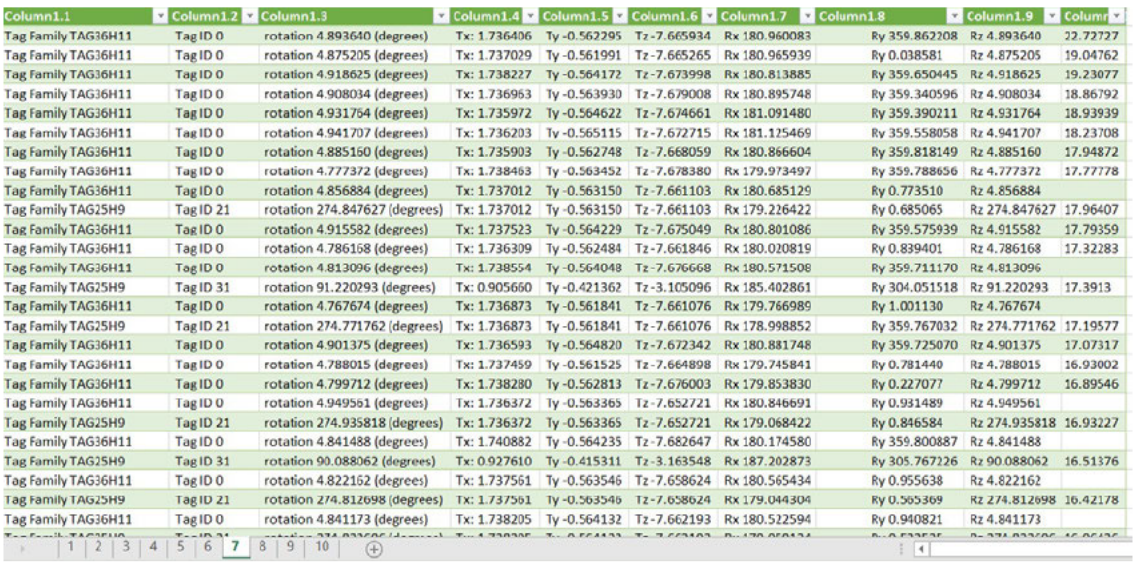

Column1.1	Column1.2	Column1.3	Column1.4	Column1.5	Column1.6	Column1.7	Column1.8	Column1.9	Column
Tag Family TAG36H11	Tag ID 0	rotation 4.893640 (degrees)	Tx: 1.736406	Ty -0.562295	Tz -7.665934	Rx 180.960083	Ry 359.862208	Rz 4.893640	22.72727
Tag Family TAG36H11	Tag ID 0	rotation 4.875205 (degrees)	Tx: 1.737029	Ty -0.561991	Tz -7.665265	Rx 180.965939	Ry 0.038581	Rz 4.875205	19.04762
Tag Family TAG36H11	Tag ID 0	rotation 4.918625 (degrees)	Tx: 1.738227	Ty -0.564172	Tz -7.673998	Rx 180.813885	Ry 359.650445	Rz 4.918625	19.23077
Tag Family TAG36H11	Tag ID 0	rotation 4.908034 (degrees)	Tx: 1.736963	Ty -0.563930	Tz -7.679008	Rx 180.895748	Ry 359.340596	Rz 4.908034	18.86792
Tag Family TAG36H11	Tag ID 0	rotation 4.931764 (degrees)	Tx: 1.735972	Ty -0.564622	Tz -7.674661	Rx 181.091480	Ry 359.390211	Rz 4.931764	18.93939
Tag Family TAG36H11	Tag ID 0	rotation 4.941707 (degrees)	Tx: 1.736203	Ty -0.565115	Tz -7.672715	Rx 181.125469	Ry 359.558058	Rz 4.941707	18.23708
Tag Family TAG36H11	Tag ID 0	rotation 4.885160 (degrees)	Tx: 1.735903	Ty -0.562748	Tz -7.668059	Rx 180.866604	Ry 359.818149	Rz 4.885160	17.94872
Tag Family TAG36H11	Tag ID 0	rotation 4.777372 (degrees)	Tx: 1.738463	Ty -0.563452	Tz -7.678380	Rx 179.973497	Ry 359.788656	Rz 4.777372	17.77778
Tag Family TAG36H11	Tag ID 0	rotation 4.856884 (degrees)	Tx: 1.737012	Ty -0.563150	Tz -7.661103	Rx 180.685129	Ry 0.773510	Rz 4.856884	
Tag Family TAG25H9	Tag ID 21	rotation 274.847627 (degrees)	Tx: 1.737012	Ty -0.563150	Tz -7.661103	Rx 179.226422	Ry 0.685065	Rz 274.847627	17.96407
Tag Family TAG36H11	Tag ID 0	rotation 4.915582 (degrees)	Tx: 1.737523	Ty -0.564229	Tz -7.675049	Rx 180.801086	Ry 359.575939	Rz 4.915582	17.79359
Tag Family TAG36H11	Tag ID 0	rotation 4.786168 (degrees)	Tx: 1.736309	Ty -0.562484	Tz -7.661846	Rx 180.020819	Ry 0.839401	Rz 4.786168	17.32283
Tag Family TAG36H11	Tag ID 0	rotation 4.813096 (degrees)	Tx: 1.738554	Ty -0.564048	Tz -7.676668	Rx 180.571508	Ry 359.711170	Rz 4.813096	
Tag Family TAG25H9	Tag ID 31	rotation 91.220293 (degrees)	Tx: 0.905660	Ty -0.421362	Tz -3.105096	Rx 185.402861	Ry 304.051518	Rz 91.220293	17.3913
Tag Family TAG36H11	Tag ID 0	rotation 4.767674 (degrees)	Tx: 1.736873	Ty -0.561841	Tz -7.661076	Rx 179.766989	Ry 1.001130	Rz 4.767674	
Tag Family TAG25H9	Tag ID 21	rotation 274.771762 (degrees)	Tx: 1.736873	Ty -0.561841	Tz -7.661076	Rx 178.998852	Ry 359.767032	Rz 274.771762	17.19577
Tag Family TAG36H11	Tag ID 0	rotation 4.901375 (degrees)	Tx: 1.736593	Ty -0.564820	Tz -7.672342	Rx 180.881748	Ry 359.725070	Rz 4.901375	17.07317
Tag Family TAG36H11	Tag ID 0	rotation 4.788015 (degrees)	Tx: 1.737459	Ty -0.561525	Tz -7.664898	Rx 179.745841	Ry 0.781440	Rz 4.788015	16.93002
Tag Family TAG36H11	Tag ID 0	rotation 4.799712 (degrees)	Tx: 1.738280	Ty -0.562813	Tz -7.676003	Rx 179.853830	Ry 0.227077	Rz 4.799712	16.89546
Tag Family TAG36H11	Tag ID 0	rotation 4.949561 (degrees)	Tx: 1.736372	Ty -0.563365	Tz -7.652721	Rx 180.846691	Ry 0.931489	Rz 4.949561	
Tag Family TAG25H9	Tag ID 21	rotation 274.935818 (degrees)	Tx: 1.736372	Ty -0.563365	Tz -7.652721	Rx 179.068422	Ry 0.846584	Rz 274.935818	16.93227
Tag Family TAG36H11	Tag ID 0	rotation 4.841488 (degrees)	Tx: 1.740882	Ty -0.564235	Tz -7.682647	Rx 180.174580	Ry 359.800887	Rz 4.841488	
Tag Family TAG25H9	Tag ID 31	rotation 90.088062 (degrees)	Tx: 0.927610	Ty -0.415311	Tz -3.163548	Rx 187.202873	Ry 305.767226	Rz 90.088062	16.51376
Tag Family TAG36H11	Tag ID 0	rotation 4.822162 (degrees)	Tx: 1.737561	Ty -0.563546	Tz -7.658624	Rx 180.565434	Ry 0.955638	Rz 4.822162	
Tag Family TAG25H9	Tag ID 21	rotation 274.812698 (degrees)	Tx: 1.737561	Ty -0.563546	Tz -7.658624	Rx 179.044304	Ry 0.565369	Rz 274.812698	16.42178
Tag Family TAG36H11	Tag ID 0	rotation 4.841173 (degrees)	Tx: 1.738205	Ty -0.564132	Tz -7.662193	Rx 180.522594	Ry 0.940821	Rz 4.841173	

1 2 3 4 5 6 7 8 9 10

Figure C.7: Test 2, Trial 7

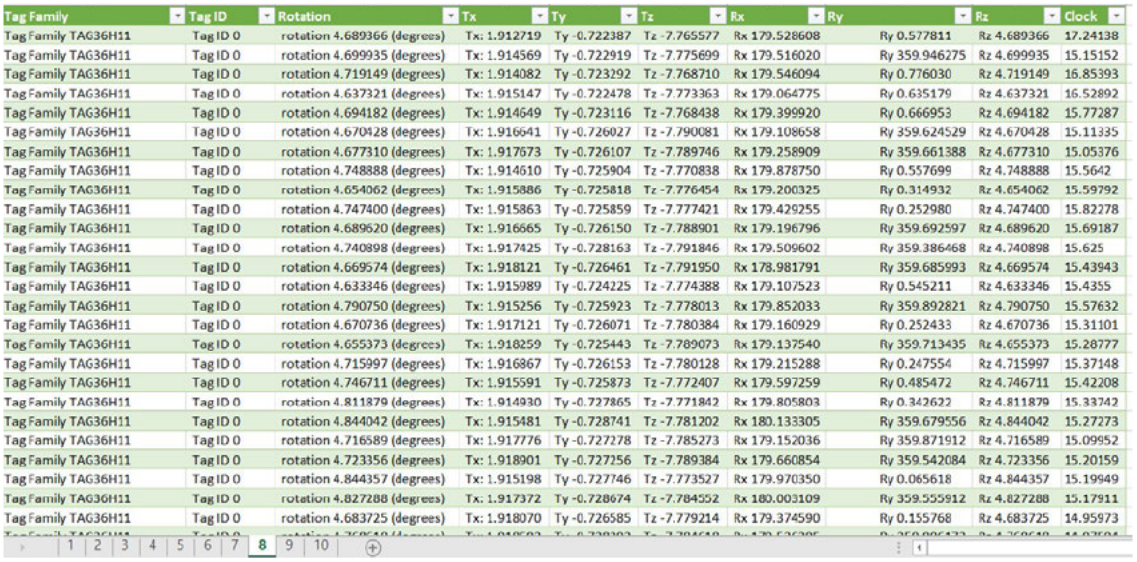

Tag Family	Tag ID	Rotation	Tx	Ty	Tz	Rx	Ry	Rz	Clock
Tag Family TAG36H11	Tag ID 0	rotation 4.689366 (degrees)	Tx: 1.912719	Ty -0.722387	Tz -7.765577	Rx 179.528608	Ry 0.577811	Rz 4.689366	17.24138
Tag Family TAG36H11	Tag ID 0	rotation 4.699935 (degrees)	Tx: 1.914569	Ty -0.722919	Tz -7.775699	Rx 179.516020	Ry 359.946275	Rz 4.699935	15.15152
Tag Family TAG36H11	Tag ID 0	rotation 4.719149 (degrees)	Tx: 1.914082	Ty -0.723292	Tz -7.768710	Rx 179.546094	Ry 0.776030	Rz 4.719149	16.85393
Tag Family TAG36H11	Tag ID 0	rotation 4.637321 (degrees)	Tx: 1.915147	Ty -0.722478	Tz -7.773363	Rx 179.064775	Ry 0.635179	Rz 4.637321	16.52892
Tag Family TAG36H11	Tag ID 0	rotation 4.694182 (degrees)	Tx: 1.914649	Ty -0.723116	Tz -7.768438	Rx 179.399920	Ry 0.666953	Rz 4.694182	15.77287
Tag Family TAG36H11	Tag ID 0	rotation 4.670428 (degrees)	Tx: 1.916641	Ty -0.726027	Tz -7.790081	Rx 179.108658	Ry 359.624529	Rz 4.670428	15.11335
Tag Family TAG36H11	Tag ID 0	rotation 4.677310 (degrees)	Tx: 1.917673	Ty -0.726107	Tz -7.789746	Rx 179.258909	Ry 359.661388	Rz 4.677310	15.05376
Tag Family TAG36H11	Tag ID 0	rotation 4.748888 (degrees)	Tx: 1.914610	Ty -0.725904	Tz -7.770838	Rx 179.878750	Ry 0.557699	Rz 4.748888	15.5642
Tag Family TAG36H11	Tag ID 0	rotation 4.654062 (degrees)	Tx: 1.915886	Ty -0.725818	Tz -7.776454	Rx 179.200325	Ry 0.314932	Rz 4.654062	15.59792
Tag Family TAG36H11	Tag ID 0	rotation 4.747400 (degrees)	Tx: 1.915863	Ty -0.725859	Tz -7.777421	Rx 179.429255	Ry 0.252980	Rz 4.747400	15.82278
Tag Family TAG36H11	Tag ID 0	rotation 4.689620 (degrees)	Tx: 1.916665	Ty -0.726150	Tz -7.788901	Rx 179.196796	Ry 359.692597	Rz 4.689620	15.69187
Tag Family TAG36H11	Tag ID 0	rotation 4.740898 (degrees)	Tx: 1.917425	Ty -0.728163	Tz -7.791846	Rx 179.509602	Ry 359.386468	Rz 4.740898	15.625
Tag Family TAG36H11	Tag ID 0	rotation 4.669574 (degrees)	Tx: 1.918121	Ty -0.726461	Tz -7.791950	Rx 178.981791	Ry 359.685993	Rz 4.669574	15.43943
Tag Family TAG36H11	Tag ID 0	rotation 4.633346 (degrees)	Tx: 1.915989	Ty -0.724225	Tz -7.774388	Rx 179.107523	Ry 0.545211	Rz 4.633346	15.4355
Tag Family TAG36H11	Tag ID 0	rotation 4.790750 (degrees)	Tx: 1.915256	Ty -0.725923	Tz -7.778013	Rx 179.852033	Ry 359.892821	Rz 4.790750	15.57632
Tag Family TAG36H11	Tag ID 0	rotation 4.670736 (degrees)	Tx: 1.917121	Ty -0.726071	Tz -7.780384	Rx 179.160929	Ry 0.252433	Rz 4.670736	15.31101
Tag Family TAG36H11	Tag ID 0	rotation 4.655373 (degrees)	Tx: 1.918259	Ty -0.725443	Tz -7.789073	Rx 179.137540	Ry 359.713435	Rz 4.655373	15.28777
Tag Family TAG36H11	Tag ID 0	rotation 4.715997 (degrees)	Tx: 1.916867	Ty -0.726153	Tz -7.780128	Rx 179.215288	Ry 0.247554	Rz 4.715997	15.37148
Tag Family TAG36H11	Tag ID 0	rotation 4.746711 (degrees)	Tx: 1.915591	Ty -0.725873	Tz -7.772407	Rx 179.597259	Ry 0.485472	Rz 4.746711	15.42208
Tag Family TAG36H11	Tag ID 0	rotation 4.811879 (degrees)	Tx: 1.914930	Ty -0.727865	Tz -7.771842	Rx 179.805803	Ry 0.342622	Rz 4.811879	15.33742
Tag Family TAG36H11	Tag ID 0	rotation 4.844042 (degrees)	Tx: 1.915481	Ty -0.728741	Tz -7.781202	Rx 180.133305	Ry 359.679556	Rz 4.844042	15.27273
Tag Family TAG36H11	Tag ID 0	rotation 4.716589 (degrees)	Tx: 1.917776	Ty -0.727278	Tz -7.785273	Rx 179.152036	Ry 359.871912	Rz 4.716589	15.09952
Tag Family TAG36H11	Tag ID 0	rotation 4.723356 (degrees)	Tx: 1.918901	Ty -0.727256	Tz -7.789384	Rx 179.660854	Ry 359.542084	Rz 4.723356	15.20159
Tag Family TAG36H11	Tag ID 0	rotation 4.844357 (degrees)	Tx: 1.915198	Ty -0.727746	Tz -7.773527	Rx 179.970350	Ry 0.065618	Rz 4.844357	15.19949
Tag Family TAG36H11	Tag ID 0	rotation 4.827288 (degrees)	Tx: 1.917372	Ty -0.728674	Tz -7.784552	Rx 180.003109	Ry 359.555912	Rz 4.827288	15.17911
Tag Family TAG36H11	Tag ID 0	rotation 4.683725 (degrees)	Tx: 1.918070	Ty -0.726585	Tz -7.779214	Rx 179.374590	Ry 0.155768	Rz 4.683725	14.95973

Figure C.8: Test 2, Trial 8

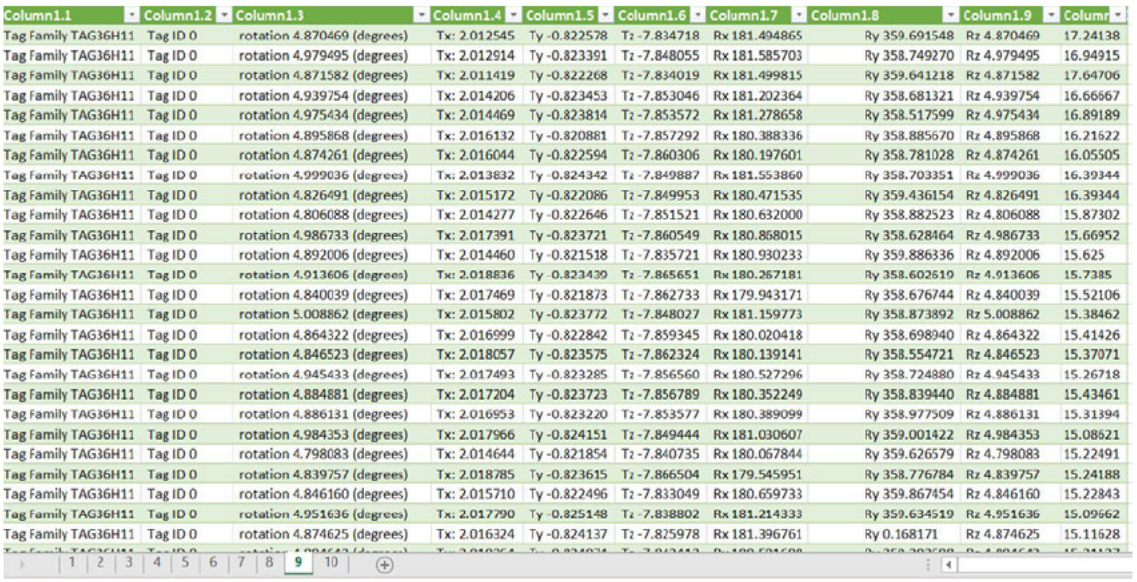

Column1.1	Column1.2	Column1.3	Column1.4	Column1.5	Column1.6	Column1.7	Column1.8	Column1.9	Column
Tag Family TAG36H11	Tag ID 0	rotation 4.870469 (degrees)	Tx: 2.012545	Ty -0.822578	Tz -7.834718	Rx 181.494865	Ry 359.691548	Rz 4.870469	17.24138
Tag Family TAG36H11	Tag ID 0	rotation 4.979495 (degrees)	Tx: 2.012914	Ty -0.823391	Tz -7.848055	Rx 181.585703	Ry 358.749270	Rz 4.979495	16.94915
Tag Family TAG36H11	Tag ID 0	rotation 4.871582 (degrees)	Tx: 2.011419	Ty -0.822268	Tz -7.834019	Rx 181.499815	Ry 359.641218	Rz 4.871582	17.64706
Tag Family TAG36H11	Tag ID 0	rotation 4.939754 (degrees)	Tx: 2.014206	Ty -0.823453	Tz -7.853046	Rx 181.202364	Ry 358.681321	Rz 4.939754	16.66667
Tag Family TAG36H11	Tag ID 0	rotation 4.975434 (degrees)	Tx: 2.014469	Ty -0.823814	Tz -7.853572	Rx 181.278658	Ry 358.517599	Rz 4.975434	16.89189
Tag Family TAG36H11	Tag ID 0	rotation 4.895868 (degrees)	Tx: 2.016132	Ty -0.820881	Tz -7.857292	Rx 180.388336	Ry 358.885670	Rz 4.895868	16.21622
Tag Family TAG36H11	Tag ID 0	rotation 4.874261 (degrees)	Tx: 2.016044	Ty -0.822594	Tz -7.860306	Rx 180.197601	Ry 358.781028	Rz 4.874261	16.05505
Tag Family TAG36H11	Tag ID 0	rotation 4.999036 (degrees)	Tx: 2.013832	Ty -0.824342	Tz -7.849887	Rx 181.553860	Ry 358.703351	Rz 4.999036	16.39344
Tag Family TAG36H11	Tag ID 0	rotation 4.826491 (degrees)	Tx: 2.015172	Ty -0.822086	Tz -7.849953	Rx 180.471535	Ry 359.436154	Rz 4.826491	16.39344
Tag Family TAG36H11	Tag ID 0	rotation 4.806088 (degrees)	Tx: 2.014277	Ty -0.822646	Tz -7.851521	Rx 180.632000	Ry 358.882523	Rz 4.806088	15.87302
Tag Family TAG36H11	Tag ID 0	rotation 4.986733 (degrees)	Tx: 2.017391	Ty -0.823721	Tz -7.860549	Rx 180.868015	Ry 358.628464	Rz 4.986733	15.66952
Tag Family TAG36H11	Tag ID 0	rotation 4.892006 (degrees)	Tx: 2.014460	Ty -0.821518	Tz -7.835721	Rx 180.930233	Ry 359.886336	Rz 4.892006	15.625
Tag Family TAG36H11	Tag ID 0	rotation 4.913606 (degrees)	Tx: 2.018836	Ty -0.823439	Tz -7.865651	Rx 180.267181	Ry 358.602610	Rz 4.913606	15.7385
Tag Family TAG36H11	Tag ID 0	rotation 4.840039 (degrees)	Tx: 2.017469	Ty -0.821873	Tz -7.862733	Rx 179.943171	Ry 358.676744	Rz 4.840039	15.52106
Tag Family TAG36H11	Tag ID 0	rotation 5.008862 (degrees)	Tx: 2.015802	Ty -0.823772	Tz -7.848027	Rx 181.159773	Ry 358.873892	Rz 5.008862	15.38462
Tag Family TAG36H11	Tag ID 0	rotation 4.864322 (degrees)	Tx: 2.016999	Ty -0.822842	Tz -7.859345	Rx 180.020418	Ry 358.698940	Rz 4.864322	15.41426
Tag Family TAG36H11	Tag ID 0	rotation 4.846523 (degrees)	Tx: 2.018057	Ty -0.823575	Tz -7.862324	Rx 180.139141	Ry 358.554721	Rz 4.846523	15.37071
Tag Family TAG36H11	Tag ID 0	rotation 4.945433 (degrees)	Tx: 2.017493	Ty -0.823285	Tz -7.856560	Rx 180.527296	Ry 358.724880	Rz 4.945433	15.26718
Tag Family TAG36H11	Tag ID 0	rotation 4.884881 (degrees)	Tx: 2.017204	Ty -0.823723	Tz -7.856789	Rx 180.352249	Ry 358.839440	Rz 4.884881	15.43461
Tag Family TAG36H11	Tag ID 0	rotation 4.886131 (degrees)	Tx: 2.016953	Ty -0.823220	Tz -7.853577	Rx 180.389099	Ry 358.977509	Rz 4.886131	15.31394
Tag Family TAG36H11	Tag ID 0	rotation 4.984353 (degrees)	Tx: 2.017966	Ty -0.824151	Tz -7.849444	Rx 181.030607	Ry 359.001422	Rz 4.984353	15.08621
Tag Family TAG36H11	Tag ID 0	rotation 4.798083 (degrees)	Tx: 2.014644	Ty -0.821854	Tz -7.840735	Rx 180.067844	Ry 359.626579	Rz 4.798083	15.22491
Tag Family TAG36H11	Tag ID 0	rotation 4.839757 (degrees)	Tx: 2.018785	Ty -0.823615	Tz -7.866504	Rx 179.545951	Ry 358.776784	Rz 4.839757	15.24188
Tag Family TAG36H11	Tag ID 0	rotation 4.846160 (degrees)	Tx: 2.015710	Ty -0.822496	Tz -7.833049	Rx 180.659733	Ry 359.867454	Rz 4.846160	15.22843
Tag Family TAG36H11	Tag ID 0	rotation 4.951636 (degrees)	Tx: 2.017790	Ty -0.825148	Tz -7.838802	Rx 181.214333	Ry 359.634519	Rz 4.951636	15.09662
Tag Family TAG36H11	Tag ID 0	rotation 4.874625 (degrees)	Tx: 2.016324	Ty -0.824137	Tz -7.825978	Rx 181.396761	Ry 0.168171	Rz 4.874625	15.11628

Figure C.9: Test 2, Trial 9

Tag Family	Tag ID	rotation	Tx	Ty	Tz	Rx	Ry	Rz	Clock
Tag Family TAG36H11	Tag ID 0	rotation 4.895632 (degrees)	Tx: 2.100122	Ty -0.902390	Tz -7.916378	Rx 179.611692	Ry 358.623338	Rz 4.895632	13.88889
Tag Family TAG36H11	Tag ID 0	rotation 4.863741 (degrees)	Tx: 2.100470	Ty -0.903405	Tz -7.916450	Rx 179.516878	Ry 358.664298	Rz 4.863741	15.26718
Tag Family TAG36H11	Tag ID 0	rotation 4.945400 (degrees)	Tx: 2.099619	Ty -0.902855	Tz -7.914702	Rx 179.934921	Ry 358.624387	Rz 4.945400	15.70681
Tag Family TAG36H11	Tag ID 0	rotation 4.964086 (degrees)	Tx: 2.099413	Ty -0.905429	Tz -7.907964	Rx 180.347824	Ry 358.634996	Rz 4.964086	15.26718
Tag Family TAG36H11	Tag ID 0	rotation 4.925958 (degrees)	Tx: 2.099963	Ty -0.902708	Tz -7.911035	Rx 179.751492	Ry 358.830094	Rz 4.925958	15.29052
Tag Family TAG36H11	Tag ID 0	rotation 4.925132 (degrees)	Tx: 2.101321	Ty -0.904687	Tz -7.916326	Rx 179.851222	Ry 358.534694	Rz 4.925132	15.0
Tag Family TAG36H11	Tag ID 0	rotation 4.934660 (degrees)	Tx: 2.099376	Ty -0.904073	Tz -7.903966	Rx 180.321074	Ry 358.975315	Rz 4.934660	
Tag Family TAG25H9	Tag ID 22	rotation 280.532551 (degrees)	Tx: 1.032200	Ty -0.539095	Tz -3.227043	Rx 5.413934	Ry 53.318667	Rz 280.532551	14.95727
Tag Family TAG36H11	Tag ID 0	rotation 4.906937 (degrees)	Tx: 2.098111	Ty -0.902084	Tz -7.893870	Rx 180.335340	Ry 359.535670	Rz 4.906937	15.12287
Tag Family TAG36H11	Tag ID 0	rotation 4.844124 (degrees)	Tx: 2.097595	Ty -0.902070	Tz -7.893061	Rx 180.206890	Ry 359.408474	Rz 4.844124	15.15152
Tag Family TAG36H11	Tag ID 0	rotation 4.912746 (degrees)	Tx: 2.100525	Ty -0.903021	Tz -7.905053	Rx 179.999781	Ry 359.091902	Rz 4.912746	15.36098
Tag Family TAG36H11	Tag ID 0	rotation 4.955682 (degrees)	Tx: 2.097904	Ty -0.903020	Tz -7.890463	Rx 180.719395	Ry 359.762931	Rz 4.955682	15.5587
Tag Family TAG36H11	Tag ID 0	rotation 4.929307 (degrees)	Tx: 2.096845	Ty -0.903477	Tz -7.886373	Rx 181.161957	Ry 359.500456	Rz 4.929307	15.64537
Tag Family TAG36H11	Tag ID 0	rotation 4.910106 (degrees)	Tx: 2.095236	Ty -0.901238	Tz -7.876674	Rx 181.007185	Ry 359.920311	Rz 4.910106	15.58753
Tag Family TAG36H11	Tag ID 0	rotation 4.771199 (degrees)	Tx: 2.099505	Ty -0.902973	Tz -7.899861	Rx 179.808817	Ry 359.601545	Rz 4.771199	15.69507
Tag Family TAG36H11	Tag ID 0	rotation 4.797577 (degrees)	Tx: 2.097810	Ty -0.901487	Tz -7.885978	Rx 180.273762	Ry 359.847927	Rz 4.797577	15.27495
Tag Family TAG36H11	Tag ID 0	rotation 4.801707 (degrees)	Tx: 2.097331	Ty -0.901590	Tz -7.885343	Rx 180.271444	Ry 359.852123	Rz 4.801707	15.19468
Tag Family TAG36H11	Tag ID 0	rotation 4.768701 (degrees)	Tx: 2.099130	Ty -0.902263	Tz -7.895811	Rx 180.031586	Ry 359.475112	Rz 4.768701	15.23298
Tag Family TAG36H11	Tag ID 0	rotation 4.899153 (degrees)	Tx: 2.097896	Ty -0.903911	Tz -7.890674	Rx 180.594149	Ry 359.672117	Rz 4.899153	15.17707
Tag Family TAG36H11	Tag ID 0	rotation 4.798243 (degrees)	Tx: 2.100487	Ty -0.903792	Tz -7.893952	Rx 180.206699	Ry 359.900141	Rz 4.798243	15.15152
Tag Family TAG36H11	Tag ID 0	rotation 4.880601 (degrees)	Tx: 2.102764	Ty -0.904083	Tz -7.907813	Rx 179.927135	Ry 359.070969	Rz 4.880601	15.10574
Tag Family TAG36H11	Tag ID 0	rotation 4.856851 (degrees)	Tx: 2.102650	Ty -0.904423	Tz -7.898122	Rx 180.280418	Ry 359.291530	Rz 4.856851	15.10791
Tag Family TAG36H11	Tag ID 0	rotation 5.164915 (degrees)	Tx: 2.101603	Ty -0.906972	Tz -7.891432	Rx 181.730137	Ry 359.147859	Rz 5.164915	15.19337
Tag Family TAG36H11	Tag ID 0	rotation 4.921655 (degrees)	Tx: 2.103740	Ty -0.905707	Tz -7.903275	Rx 180.388336	Ry 359.025478	Rz 4.921655	15.13158
Tag Family TAG36H11	Tag ID 0	rotation 4.773297 (degrees)	Tx: 2.101198	Ty -0.903496	Tz -7.885838	Rx 180.071259	Ry 0.366681	Rz 4.773297	15.11335
Tag Family TAG36H11	Tag ID 0	rotation 4.875296 (degrees)	Tx: 2.102948	Ty -0.905532	Tz -7.891079	Rx 180.634394	Ry 359.979343	Rz 4.875296	15.1607

1 2 3 4 5 6 7 8 9 10

Figure C.10: Test 2, Trial 10

Appendix D

OpenMV H7 Data Sheet

OpenMV-H7 A Python programmable machine vision camera.

1 Features

- 32-Bit Arm Cortex-M7 operating at 400MHz.
- High bandwidth 1MB SRAM / 2MB FLASH.
- Double-precision Floating Point Unit (FPU).
- Full DSP instructions, hardware JPEG encoding.
- 2 UARTs, 2 I2C, 1 SPI, 1 CAN, 3 TIM/PWM.
- 1 USB full speed (FS) for programming.
- 1 RGB LED and 2 IR LEDS on board.
- 1 uSD Card socket (supports up to 64GBs).
- High efficiency switching regulator (1A out).
- Low noise LDO for sensor analog supply.
- LiPo battery connector.
- Less than 150-mA power consumption.
- Modular sensor design supports multiple sensors:
  - OV7725 640x480.
  - MT9V034 (Global Shutter Sensor).
  - FLIR 1,2 and 3 thermal imaging sensors.

2 Description

The OpenMV cameras are low-power, Python3 programmable machine vision cameras that support an extensive set of image processing functions and neural networks. OpenMV cameras are programmed using a cross-platform IDE which allows viewing the camera's frame buffer, accessing sensor controls, uploading scripts to the camera via serial over USB (or WiFi/BLE if available).
The OpenMV-H7 camera base board is based on the STM32H7 Arm Cortex-M7 MCU operating at 400MHz, and featuring 1MB SRAM, 2MB FLASH, FPU, DSP and a hardware JPEG encoder. The base board has a modular sensor design, decoupling the sensor from the camera. The modular sensor design enables the camera to support multiple sensors including OV7725, MT9V03x global shutter sensor and FLIR Lepton 1, 2 and 3 thermal sensors.

Device Information

PART NUMBER	BODY SIZE (NOM)
OPENMV-H7	1.4 in × 1.75 in

3 Applications

- Home automation.
- Robot guidance.
- Industrial Applications.
- Surveillance Applications.
- Object detection and tracking.

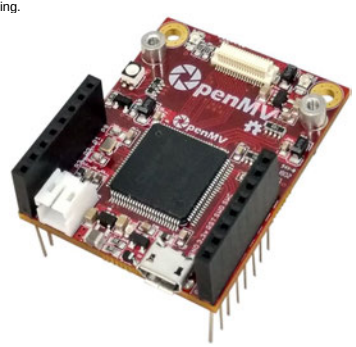

Table of Contents

4 Pin Configurations and Functions

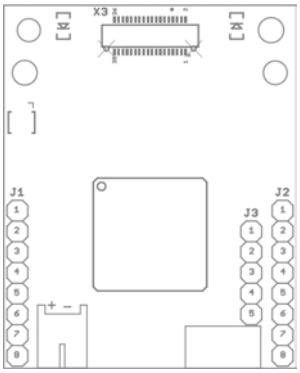

Pin Functions

Pin			Description
Header	No	Name	
J1 Pin Configuration			
J1	1	P0	UART1 RX – TM1 CH3N – SPI 2 MOSI
	2	P1	UART1 TX – TM1 CH2N – SPI 2 MISO
	3	P2	CAN2 TX – TM1 CH1N – SPI 2 SCLK
	4	P3	CAN2 RX – SPI 2 SS
	5	P4	TIM2 CH3 – I2C 2 SCL – UART 3 TX
	6	P5	TIM2 CH4 – I2C 2 SDA – UART3 RX
	7	P6	TIM2 CH1 – DAC – ADC
	8	3.3	3.3V Rail (250 mA Supply MAX).
J2 Pin Configuration			
J2	1	RST	Reset (Connect to GND to reset).
	2	BOOT	Boot 0 (Connect to 3.3V for DFU mode).
	3	SYN	Frame synchronization pin (Use to frame sync cams).
	4	P9	Servo3 – TIM4 CH3
	5	P8	Servo2 – TIM4 CH2 – I2C4 SDA
	6	P7	Servo1 – TIM4 CH1 – I2C4 SCL
	7	VIN	VIN (3.6V – 5V).
	8	GND	GND Rail
J3 Pin Configuration			
J3	1	SWC	Serial wire debug clock.
	2	SWD	Serial wire debug data.
	3	RST	Reset (active low).
	4	3.3V	3.3V rail (500 mA Supply MAX)
	5	GND	GND rail

5 Electrical Characteristics

5.1 Absolute Maximum Ratings[1]

SYMBOL	RATINGS	MIN	MAX	UNIT
V_{IN}	External input supply voltage range.	3.6	5.5	V
V_{OUT}	External output supply voltage range.		3.3	
V_{IO}	Input voltage range on ADC/DAC pins.	-0.3	4.0	
	Input voltage range on any other pins.	-0.3	7.3	
I_{OUT}	External output supply current range.		600	mA
I_{IO}	Output current sunk by any I/O and control pin		20	
	Output current sourced by any I/O and control pin		-20	
ΣI_{IO}	Total output current sunk by all I/Os and control pins		140	mA
	Total output current sourced by all I/Os and control pins		140	
T	Junction temperature.		125	°C
T_{stg}	Storage temperature.	-65	150	

5.2 Recommended Operating Conditions

SYMBOL	RATINGS	MIN	MAX	UNIT
V_{IN}	External input supply voltage range.	3.6	5.0	V
V_{OUT}	External output supply voltage range.		3.3	
V_{IO}	Input voltage range on ADC/DAC pins.	-0.3	3.6	
	Input voltage range on any other pins.	-0.3	5.0	
I_{OUT}	External output supply current range.		500	mA
T	Junction temperature.	-40	125	°C

(1) Stresses beyond those listed under *Absolute Maximum Ratings* may cause permanent damage to the device. These are stress ratings only, which do not imply functional operation of the device at these or any other conditions beyond those indicated under *Recommended Operating Conditions*. Exposure to absolute-maximum-rated conditions for extended periods may affect device reliability.

6 Mechanical Information

The following information is the most current data available for the designated device. This data is subject to change without notice and without revision of this document.